Anglia Ruskin University

FACULTY OF SCIENCE AND TECHNOLOGY

THE DESIGN OF A NON-PYROTECHNIC ACTIVE BONNET ACTUATOR TO MITIGATE PEDESTRIAN HEAD INJURY

SIMON HOFFMAN

Supervisor: Dr Mehrdad Asadi

A Thesis in partial fulfilment of the requirements of Anglia Ruskin University for the degree of Master of Philosophy

Submitted: August 2019

Dedication

I dedicate this thesis to my family. In particular a special thank you to my parents Jacobus and Theronda Hoffman, for their continuous encouragement and support throughout my education. If not for this, my academic achievements and this thesis would not have been possible.

Acknowledgements

This thesis and project was conducted at Anglia Ruskin University under the supervision of Dr Mehrdad Asadi, to whom I would like to express my gratitude for his advice and encouragement throughout the project, also to Dan Jackson for his assistance during the manufacturing and practical testing throughout the project.

ANGLIA RUSKIN UNIVERSITY

Over the previous years, the requirements for future vehicle generations relating to pedestrian protection have been especially reviewed by automobile groups. These discussions brought forward new government regulations, which propose various testing methods which verify pedestrian protection on vehicles. In order for vehicles to comply with the head impact tests, the bonnet is required to have certain stiffness characteristics along with sufficient clearance between the bonnet and the engine components. However, if by design the vehicle has limited clearance optimal head protection can also be achieved by lifting the bonnet. This method consists of a sensory system which can identify a pedestrian impact, and an actuator system which can lift the bonnet into position during deployment.

This project introduces a new active bonnet actuator, which is a fully resettable and reusable device which utilises a standard compression spring to store the energy required to lift the bonnet. The proposed design offers a simplified release mechanism compared to existing designs, which in addition offers a reduction in weight, and manufacturing cost whilst meeting current industry performance criteria. Finite Element will be used to verify the designs performance and insure structural integrity. While the new design is only verified through simulation, further testing and development would be required for the design to transition into usable product, this study does indicate that the new design has potential as an alternative lifting device for pedestrian protection.

FACULTY OF SCIENCE AND TECHNOLOGY

MASTER OF PHILOSOPHY

The Design of a Non-Pyrotechnic Active Bonnet Actuator to Mitigate Pedestrian Head Injury

SIMON HOFFMAN

August 2019

Supervisor: Dr Mehrdad Asadi

Keywords: Active Bonnet, Pop-Up Bonnet, Actuator, Resettable, Pedestrian Protection, FEA, Ansys

Table of Contents

Abbreviations

AAAM – Association for the Advancement of Automotive Medicine

ACL – Anterior Cruciate Ligament

AIS – Abbreviated Injury Scale

CAD – Computer Aided Design

DAI – Diffuse Axonal Injury

EDH – Epi Dural Hematoma

EEVC – European Enhanced Vehicle-Safety Committee

Euro NCAP – European New Car Assessment Program

FEA – Finite Element Analysis

FEM – Finite Element Model

G – Acceleration due to gravity ($9.81ms^{-2}$)

GHO – Global Health Observatory

GSI – Gadd Severity Index

GTR – Global Technical Regulations

HBM – Human Body Models

HIC – Head Injury Criterion

HPC – Head Performance Criterion

ICH – Intracerebral hemorrhage

IHRA – International Harmonised Research Activities

KSI – Killed or Seriously Injured

LCL – Lateral Collateral Ligament

LOC – Loss of Consciousness

MCL – Medial Collateral Ligament

MGG – Micro Gas Generator

Nm – Newton-metre

PCL – Posterior Cruciate Ligament

PMHS – Post-Mortem Human Subjects

SMART – Shape Memory Alloy ReseTable

WAD – Wrap Around Distance

WSTC – Wayne State Tolerance Curve

List of Figures

List of Tables

List of Graphs

Chapter 1: Introduction

The expression pedestrian can be referred to as a person “afoot” according to New York State Law (2017), but generally implies a person who is running or walking.

Over the previous decade the population across the world has significantly increased (Tur, 2013). This rapid population growth has a direct influence on the demand for mobility which consequently has given rise to tremendous traffic volume. This increase has had an adverse effect on the number of road accidents involving pedestrians, who are either killed or seriously injured. In addition, the World Health Organization in their 2013 publication predicts that traffic injuries will globally become the 5th cause of mortality by 2030 (Pia, 2010). Even with the implementation of numerous safety countermeasures (World Health Organization, 2004). According to (Department for Transport, 2017) 25,160 people in the UK were seriously injured or killed in 2016, it was noted that this was an increase of 6 percent from the previous year. Although these figures gives a close representation, they often exclude injuries which occur in private roadways, particularly low severity injuries which are often not reported to the police, and as a result are not recorded (Karsch et al., 2012). In vehicle pedestrian impacts head injuries are the most frequently injury body region which can often lead to permanent disabilities or death (Hu and Klinich, 2012).

Vehicle testing began in 70’s when the European Enhanced Vehicle-Safety Committee (EEVC) was established and started developing testing standards and criteria to improve vehicle safety (EEVC, 2003). This subsequently has prompted car manufacturers over the years to improve and enhance the frontal parts of their vehicles; focusing primarily on the bonnet, bumper and headlamps. Since most serious injuries occur on the head and lower limbs of the impacted pedestrian (Ramesh et al., 2012). As research suggest the most likely area to be impacted by the pedestrians head is the vehicles bonnet. Various studies have shown that more than 50 percent of pedestrian fatalities were as a result of impact with the vehicles bonnet or the windscreen. As a result it is important for the bonnet to comply with pedestrian protection (Kalliske and Friesen, 2001). In order to avoid human fatalities during a vehicle-pedestrian collision, numerous safety concepts have been developed and proposed within the automotive safety industry. The active bonnet is one of the proposed methods used to increase the pedestrian protection offered by the vehicle as well as meet the safety regulations (Xu et al., 2010). The active bonnet system lifts the bonnet to a specific height within a predetermined time, when a vehicle pedestrian collision has occurred and must be fully deployed prior to the pedestrians head striking the bonnet. This provides a reasonable clearance between the bonnet and the ridged engine components. When the pedestrians

head strikes the deployed bonnet, the additional clearance allows the bonnet to deform and absorb more impact energy through structural deformation of the bonnet. Consequently the head impact severity can be reduced as a result. The active system is primarily composed of a detection sensor(s) and the lifting mechanism. The performance of the lifting mechanism directly effects the pedestrian protection offered by the active bonnet system (Shin et al., 2007). The lifting mechanism is used to transmit motion of the actuator to the vehicles bonnet. Currently there are a variety of methods which have been developed with varying degrees of success (Ye et al., 2011). One of the main challenges currently is to have a system which is resettable after deployment, which most of the current systems are not capable of.

1.1 Aims and Objectives of the Research

Recognising key operational and performance characteristics of current active systems is crucial in assessing the competing designs. Identification of limitations of these systems is therefore necessary in order to propose an alternative system.

The main objective of the research is to design an alternative lifting actuator to be used during a vehicle-pedestrian collision to provide the lifting force to elevate the bonnet. The study focuses on investigating various lifting methods which aim to be resettable and provide a cheaper alternative to current systems. The aim of the project is to establish a suitable lifting source to provide the force required to lift the bonnet, as well as a mechanism to release the system during deployment in a controlled manner whilst upholding performance criteria and resetability.

To define limitations for the research, the performance of existing systems are not published in the public domain instead the general industries expected performance criteria has to be used for comparison. The final proposed design will be validated through finite element simulation to evaluate the performance and integrity but will not be verified though physical testing.

The geometry of the modelled structure will be presented and given in a 3D graphical representation, summarised in detail. The stress distribution will be evaluated during operating conditions to evaluate structural integrity. Where the effect of the forces generated during deployment will be closely examined.

By modelling and simulating the proposed mechanism, the aim for this project is to demonstrate the structural integrity and performance characteristics of an alternative lifting mechanism.

1.2 Purpose of Research

In comparison to other active bonnet actuators, the new design offers many advantages. Despite the satisfactory performance of other actuators, such as the Mercedes's system which is quite large and poses constraints with regards to placement within the engine compartment. The proposed design, on the other hand offers a reduced overall weight in addition to having greater freedom with positioning within the engine compartment. Moreover, it has the added benefit of being resettable and reusable which many current systems do not offer.

Due to the simple design, the system has low manufacturing costs, this is largely due to the design requiring minimal machining and most components are off the shelf and can easily be procured. This has the added benefit of being mass produced, broadening the potential for the system to be used on lower spec vehicles as well as being easily adoptable in a variety of other countries where active systems are currently not used.

This thesis is compiled of six chapters. Where, chapter 1 outlines the project and the intended objectives. Chapter 2 consists of Injury distribution and the anatomy of frequently injured body parts. This is compiled by using detailed accident data and various other literature resources. As the research suggests, typically the pedestrian's head and legs are the most frequently injured regions. Chapter 2 also covers the anatomy of these frequently injured body regions and also covers the injury mechanism as well as the injury criteria. Chapter 3 focusses on a detailed study on the types of pedestrian injury devices, the different regulations and test procedures proposed by various organisations to aid in the reduction of injury severity. Chapter 4 presents a number of methods specifically developed to reduce head injuries, such as energy absorbing bonnets, collapsible hinges and latches as well as different active systems and concepts. Finally, the Aims of the study are presented in chapter 5. And lastly a conclusion of the study will be presented in chapter 6.

Chapter 2: Injury Distribution and Anatomy of Frequently Injured Body Parts

2.1 Injury Patterns

In 2013 there were approximately 1.25 million road deaths globally (GHO, 2017). On the other hand the sum of pedestrians surviving vehicle collisions far outweighs the total amount of fatalities. Figure 1 shows, that in Europe, pedestrians account for the second highest amount of fatalities after occupants in passenger cars.

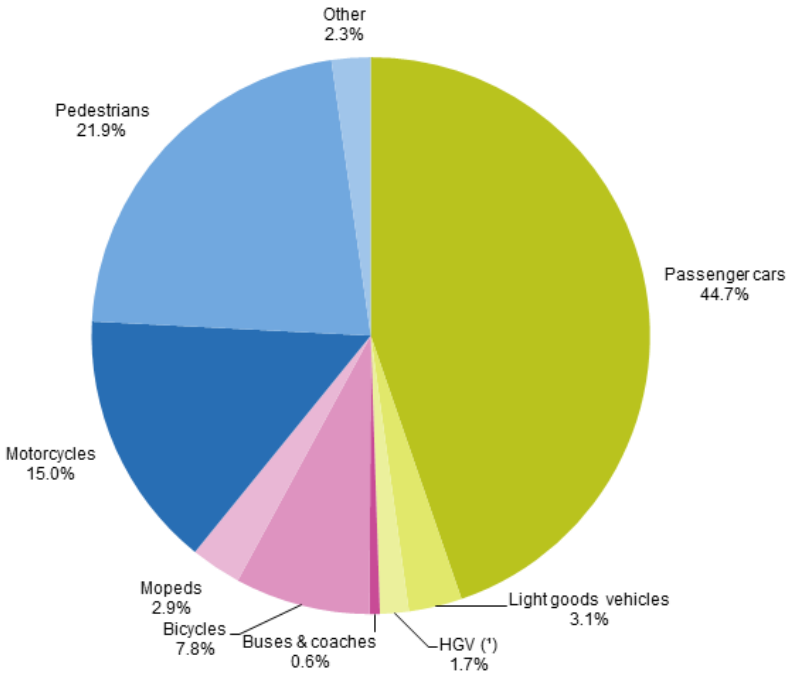

Figure 1. Fatality distribution depending on type of road user (Eurostat, 2016)

In 2016, there were 5,480 pedestrians Killed or Seriously Injured (KSI) and 18,300 slightly injured in the UK (Department for Transport, 2017). In 2015 5,376 pedestrians lost their lives and approximately 70,000 suffered injuries in the US. And according to (NHTSA, 2017), a pedestrian was injured every 7.5 minutes and killed every 1.6 hours in traffic collisions. Pedestrian fatalities comprise of 11 percent of all road deaths in the US (CDPH Public Health , 2017). In other regions such as Japan, pedestrian fatalities account for more than 30 percent of all traffic related deaths, which is significantly higher than the US and Europe (2-Chome and Chuo-ku, 2006).

The most widely used method for defining injury severity in road related injuries is referred to as the Abbreviated Injury Scale (AIS). AIS, is a global severity ranking classification, which

categorises individual body regions in accordance to its relative severity. The severity of the injury is ranked using a 6 points scale where 1 is very minor and 6 for maximum severity (unsurvivable) (AAAM, 2017). The distribution of AIS 1+ to AIS 4+ in Figure 2 shows that the head and lower extremities occur most frequent. Although head injuries often lead to death, hence they are deemed the most severe. But lower limb injuries are also very significant due to the high probability of long term disabilities which will result in elevated social cost (Gupta, 2014).

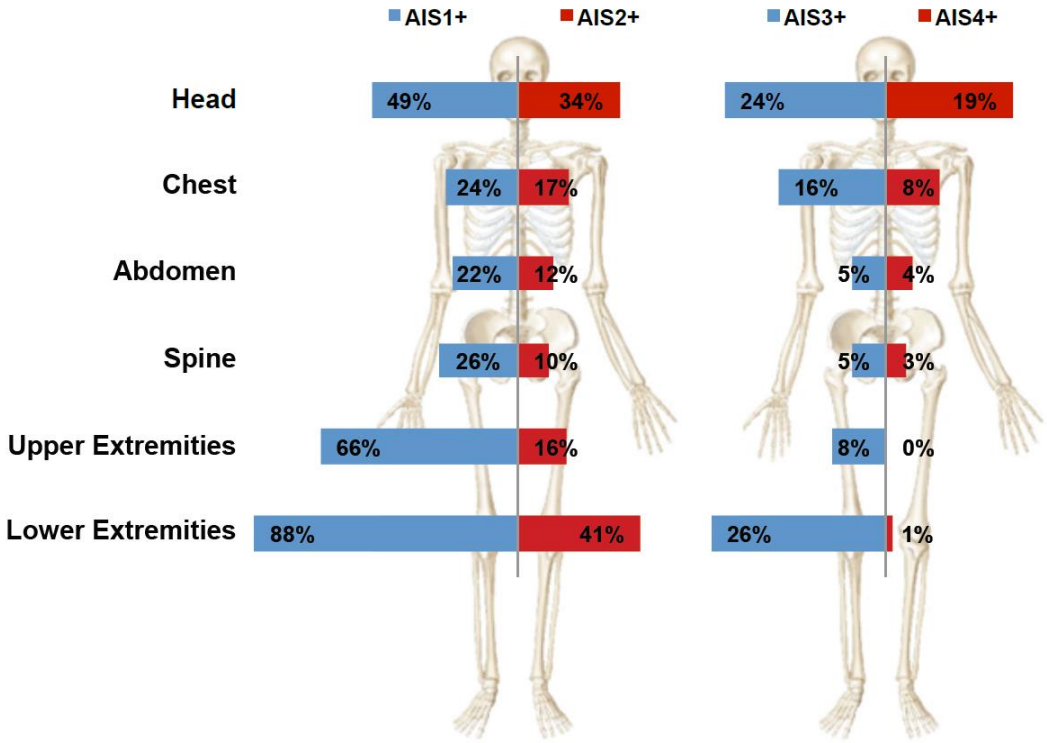

Figure 2. Probability and injury severity for each body region (Helmer et al., 2010)

2.2 Head Anatomy and Injuries

To better understand the head injury mechanism, a concise summary of head injury types and their relation to the anatomy of the human head is reviewed. The human head is made of skull, scalp and brain. The brain directs the body by receiving signals, evaluating and then organising the information and sends signals to the rest of the body to respond accordingly.

The central nervous system consists of the spinal cord and the brain. The brain consists of four key elements: diencephalon, cerebrum, cerebellum as well as the brain stem, as illustrated in Figure 3. The longest part of the brain is the cerebrum which is located above

the cerebellum and diencephalon. The cerebrum comprises of dual hemispheres which are attached to one another by the corpus callosum and is divided by the falx cerebri. The four hemispheres can be categorised by the different lobes: temporal, frontal, occipital and parietal seen in Figure 4. At the different hemispheres or lobes unique motor and sensory functions are controlled. The outer portion of the cerebrum consists of grey matter, underneath this the white matter is found and in the center the deep grey matter. The second largest portion of the brain is the cerebellum, where the primary function is the control of muscle movements. The diencephalon is positioned lower in relation to the cerebrum, which consists of hypothalamus, epithalamus and thalamus. The spinal cord is a continuation of the brain stem which comprises of pons, midbrain and medulla oblongata. The main role of the medulla oblongata is to relay information between the spinal cord and the brain. Many vital activities are controlled in this section, and injury can be fatal (Fahlstedt, 2015).

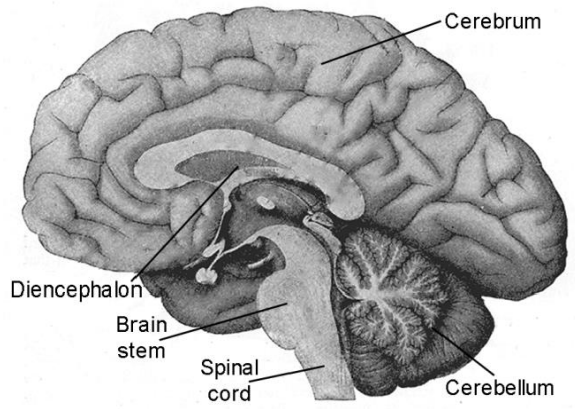

Figure 3. Brain anatomy (Fahlstedt, 2015)

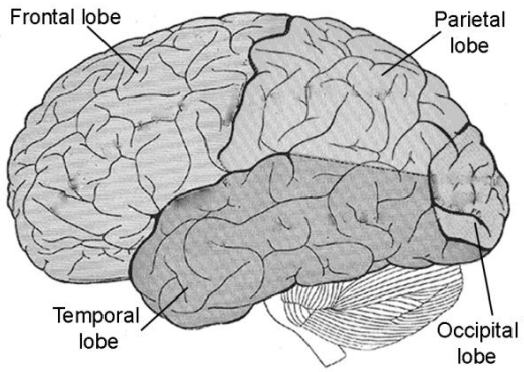

Figure 4. Main parts of brain (Fahlstedt, 2015)

Due to the important role of the brain it's not surprising that the skull and brain are the most important injury associated components within a vehicle-pedestrian collision. Scalp injuries which are frequent in automotive accidents include laceration and contusion. Head injuries are the result of skull fracture or soft tissue damage to the brain. The types of brain injuries that occur often and are of concern are diffuse axonal and concussions. Other injuries include hematoma and contusions which also occur frequently during vehicle-pedestrian accidents (Farkya and Cheng, 2015).

AIS		
1	Minor	Headache Scalp abrasion Mild concussion with no LOC
2	Moderate	Tiny contusion, EDH and ICH (cerebrum) Closed, simple vault fracture Cerebral concussion with LOC <1 hour
3	Serious	Small bruise (cerebrum) Base fracture Severe concussion with LOC 1-6 hour
4	Severe	Large contusion (cerebrum) Complex vault and base fracture Mild DAI with LOC 6-24 hours
5	Critical	Major penetrating injury to the skull Brain stem compression, contusion, infarction DAI with LOC > 24 hours
6	Unsurvivable	Crush injury Brain stem laceration, massive destruction, penetrating injury and transection

Table 1. Head injury examples with different AIS levels (AAAM, 2005)

2.3 Lower Leg Anatomy and Injury

The lower limb includes the ankle, foot, lower leg, thigh, knee, and pelvis. The pelvis links the spine to the lower extremities which consists of four bones, where the coccyx and the sacrum form the rear portion, while the hip bones form the frontal and side portions. The femur is the thighs long bone and is connected proximally via the hip, fixed to the pelvis and linked distally to the knee. The lower leg consists of the tibia and fibula between the knee and the ankle. The femur and lower leg are connected via the knee joint which consists of tendons, muscles menisci and ligaments. Lastly, the foot is connected to the lower leg and is made up of several bones. These bones can be subjected to large moments and forces during a collision with a vehicle (Schmitt et al., 2010).

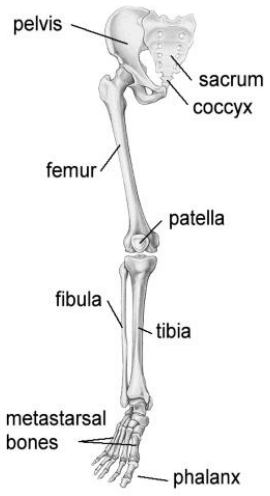

Figure 5. Anatomy of human lower extremities (Schmitt et al., 2010)

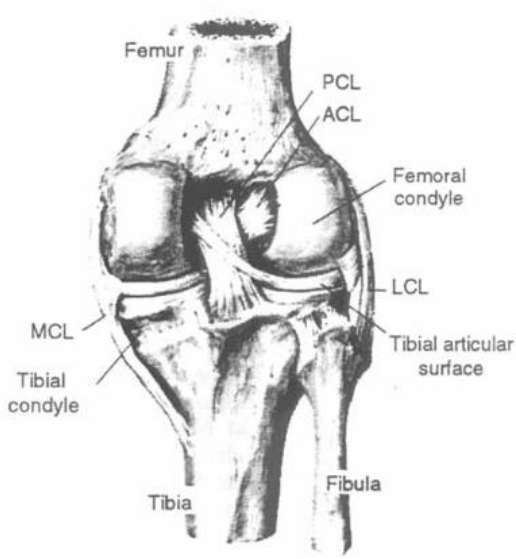

Figure 6. Ligaments of human knee (Schmitt et al., 2010)

During a collision the four knee ligaments which are frequently injured are posterior cruciate ligament (PCL), lateral collateral ligament (LCL), medial collateral ligament (MCL) and anterior cruciate ligament (ACL). Their injuries are usually the result of excessive forces in areas of restricted joint motion (Farkya and Cheng, 2015).

During a vehicle-pedestrian impact fractures of the fibula, tibia, knee-patella bones in the feet and the femur are common. Additionally, a knee ligament rupturing occurs often; in particular the collateral ligament (Schmitt et al., 2010). A reduced cross section results in fractures occurring more frequently amongst distal-third of the tibia and the mid-shaft region. A more serious tibia injury is a crack of the tibial plateau which occurs in the upper most section of the tibia (Farkya and Cheng, 2015).

In the case for the knee ligaments, the injury assessment criteria use the elongation of the knee ligaments. The elongation of the MCL is used to predict the bending angle of the knee, whereas the PCL and ACL are used for the shear displacement measurement of the knee. For the case of tibia fractures, the bending moment of the tibia is measured at different cross-sections. This is then used as injury criteria as this measurement is used in Human Body Models (HBM) and in the leg-form impactor (Farkya and Cheng, 2015).

2.4 Pedestrian Kinematics

Pedestrians involved in a traditional vehicle-pedestrian accident, the kinematics have been well documented in numerous studies such as in (Simms and Wood, 2009) based on pedestrian impact dummies as well as post-mortem human subjects (PMHS). Because of the importance of understanding the body kinematics in injury mitigation in vehicle-pedestrian accidents, a brief summary of typical body kinematics is reviewed in this section.

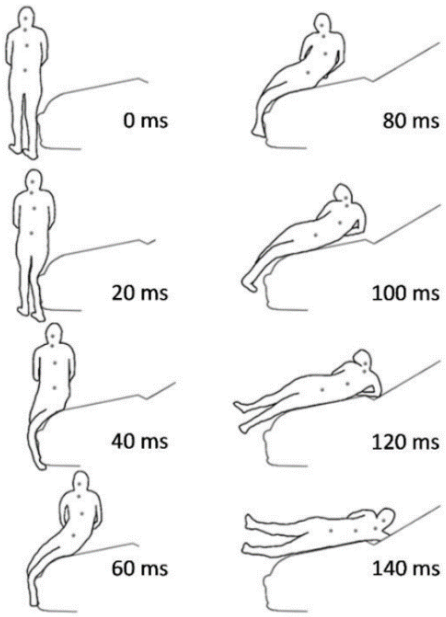

Figure 7. Human body kinematics during a 40 km/h collision (Paas et al., 2012)

As seen in Figure 7, in a typical scenario the initial contact with the vehicles front end profile begins with contact between the front bumper and the legs, this contact is the major cause of leg injuries for a pedestrian during a vehicle-pedestrian collision (Paas, 2015). In this stage, the rotation of the pedestrian's longitudinal axis is initiated. The amount of rotation and the direction is established by which leg is facing forward, since this dictates the orientation of the pelvis prior to impact (Forman et al., 2015).

A few milliseconds after vehicle-leg contact, the bonnet leading edge makes contact with the pelvic region in a typical case for a sedan car or in some cases the upper leg in lower sports cars, resulting in the bonnet leading edge being another main contributor to pedestrian leg injuries (Paas, 2015). Up until this impact, the inertia created keeps the head and upper torso remaining in the upright position. While the vehicle maintains its forward direction and partially pulling the pelvis, the torso will begin to pivot towards the vehicle as a result. The

arms of the pedestrian's however do not normally stick to this path due to the gravity and inertia keeping the arms in the vertical position (Ishikawa et al., 1993). This chain of events in certain instances can result in the vehicle impacting the person's shoulder, upper arm or even the elbow, this happens when the rotation of the upper body of the person around the longitudinal axis is small (Paas, 2015).

As in the case with the upper arm, the persons head doesn't instantly pursue the motion of the torso. As the torso descends to the car, the inertia created, causes the persons head to lag behind this motion, until the motion generated by the neck finally draws the head towards the car, which results in the head impacting against the car. After the initial of phase of vehicle-pedestrian contact, this is followed by head-vehicle contact this is referred to as the (primary impact), the body enters a second phase which is either the flight phase, where the pedestrian is carried on the vehicles bonnet, if not a phase of rolling or sliding off occurs (Simms and Wood, 2009). Which phase occurs depends largely on the vehicle shape, breaking and vehicle speed (Hamache et al., 2012). Followed by the pedestrian hitting the ground, which is subsequently followed by sliding and rolling until the body reaches the resting position.

The pedestrian's kinematics in the different phases illustrated by the motion with reference to the motional parameters of the centre of gravity of the body, where Figure 8, gives a representation of the Z-components Centre of gravity position, where the vertical lines illustrate the different impact phases.

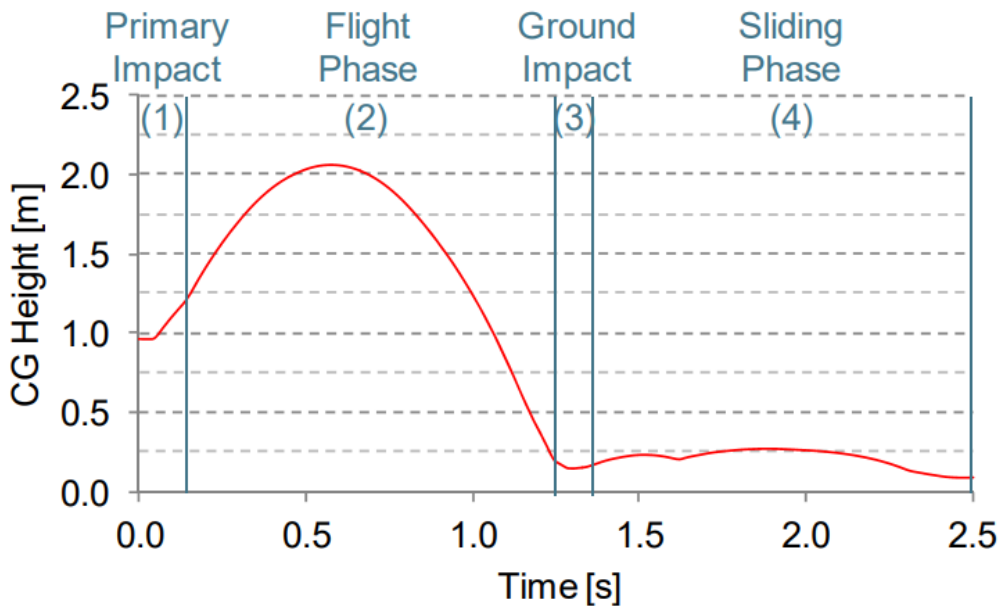

Figure 8. Pedestrians Centre of gravity during a 40 km/h impact at (Hamache et al., 2012)

2.5 Head Injury Criteria

Head injuries will most often lead to a pedestrian fatality, as a result of impact with a vehicle (Traumatic Brain Injury, 2001). Although the head injury mechanism is very complex, it has been the focus of considerable research, and has sparked much debate on whether angular or linear acceleration are the main determinant for brain injury (King et al., 2003). Other factors which influence the severity are frontal or sideways impacts, also the time interval of the deceleration and acceleration phase and the resultant movement of the person's brain in relation to the skull (Stevenson, 2006).

The Wayne State University tolerance curve, established from conducting tests on human cadavers, which defines the head injury level with respect to the time duration of the linear acceleration impulse, which is established from the probability of a skull fracture after a head impact (Gurdjian et al., 1966). Points above the curve would result in a high probability of death or brain injury.

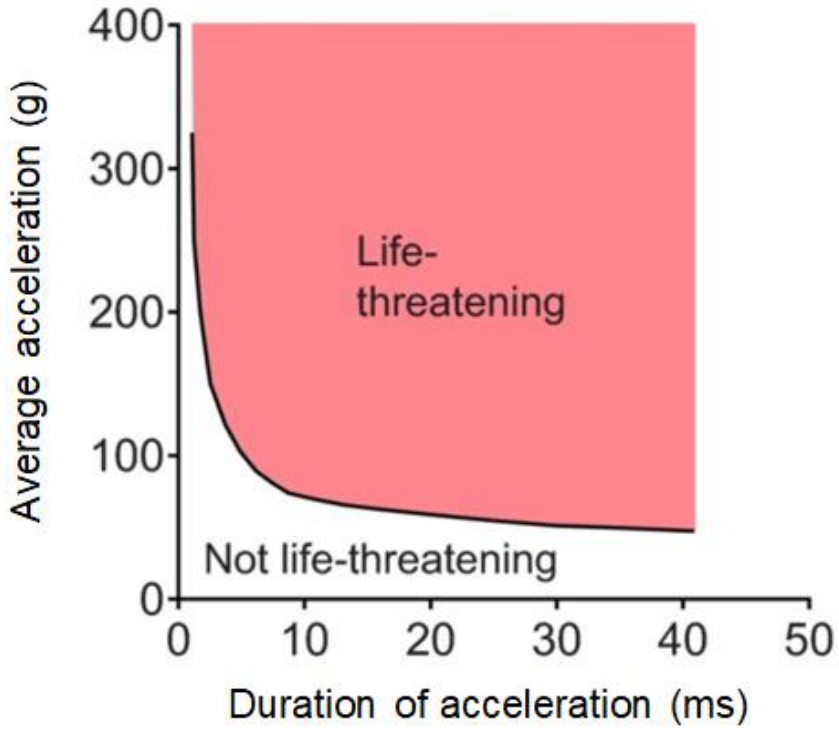

Figure 9. Wayne State Tolerance Curve (WSTC) (Namjoshi et al., 2013)

As the pursuit for a common criterion eventually led to the Gadd Severity Index (GSI) which evaluates the likelihood of head injury during crash testing by proposing a weighted impulse criterion to account for the shape of the acceleration pulses. The GSI originated from an integration of the Wayne State Tolerance curve, where the acceleration component is biased by using an exponent of 2.5. Where the value of 2.5 correspond to the gradient of the

(WSTC), if it were to be plotted logarithmically with the time intervals of 2.5 and 50 millisecond (Gadd, 1966).

$$GSI = \int_{t_1}^{t_2} a^{2.5} dt \qquad \text{Equation 1}$$

Where a symbolises the average linear acceleration, and the initial t_1, and t_2 for the end time, time intervals respectively. Gadd suggests that the threshold value of 1000 GSI for concussions in frontal impacts should be considered (Gadd, 1966).

This later lead to the progression of The Head Injury Criterion (HIC) developed by Versace (1971) (Eppinger et al., 1999).

$$\text{HIC} = \max\left\{\left[\frac{1}{t_2 - t_1}\int_{t_1}^{t_2} a(t)dt\right]^{2.5}(t_2 - t_1)\right\} \qquad \text{Equation 3}$$

Where $a(t)$ is the subsequent head acceleration measured in g's which is gauged from the centre of gravity of the head. And t_1, and t_2 are the time intervals between the initial and end time (measured in seconds), during this period the HIC reaches a maximum value, which should not exceed 1000, and the time intervals (t_2 - t_1) significantly influence the HIC calculations. Within the automotive industry the value of 36ms was deemed appropriate for HIC values. However, this time window is gradually being replaced by a much smaller time window of 15ms to limit the use to hard impacts only, and the HIC threshold to 700 (Gupta, 2014).

Limitations of HIC as an injury criterion are (Stevenson, 2006):

- It does not take into account the angular accelerations
- It is only used for hard contacts
- The anterior-posterior acceleration is the only source for the original data

2.6 Discussion

As the literature suggests pedestrians account for the second highest fatalities of all road users and in some countries this figure can be up to 30 percent. Typically the lower extremities are injured most frequently due to the kinematics of a typical pedestrian-vehicle collision and head injuries result in the most loss of life. Although head injuries such as diffuse axonal and concussions which result in the most fatalities tends to be the main area of focuses. However, often overlooked are lower limb injuries which often result in long term damage and permanent disability which can results in a high social cost.

Due to the large amount of injuries and fatalities caused as a result of vehicle-pedestrian collisions, this has led to an increase in demand for injury assessment methods to determine which factors influence the severity of brain injury. With the WSTC being established in the 60's through testing human cadavers, however this initial method was fairly crude and was subjected to large amounts of criticism (McHenry, 2008). Which as a result later led to the development of the GSI in the 70's to better account for the acceleration impulses, and finally the HIC was then proposed by NHTSA as a replacement for the GSI. Although the HIC still has limitations it is still the most accepted method for assessing head injury in automotive impact conditions (Mellander, 1986).

Chapter 3: Evaluation Protocols and Safety Assessments

In aid of research and regulatory assessment work for pedestrian safety, the use of physical and numerical testing methods is used (Fredriksson, 2011) .

One of the physical test substitutes was to use a whole Post Mortem Human Subject's body (PMHS). The test subject would impact a car in order to reconstruct the kinematics experienced during a vehicle-pedestrian collision, and to some extent assessed the injuries sustained. However it was difficult to evaluate modifications to the vehicles frontal structures using this method. Alternative physical testing devices were to use local impactors (headform and legform), which are currently used in the Global Technical Regulations (GTR) and European New Car Assessment Program (Euro NCAP). The use of local impactors is successful in assessing the outcome of vehicle front profile structural changes to prevent pedestrian injuries on local body regions, although these local impactors are effective they cannot be used to realistically reconstruct the kinematics of a whole pedestrian (Gupta, 2014). As a result, in the early 2000's the development of full size child and adults pedestrian dummies had been developed by Autoliv and Chalmers University, but was limited to assessing impact dynamics only, then later Honda and Gesac developed the Polar dummy which was more advanced which could asses both injuries and kinematics (Fredriksson, 2011).

3.1 Local Impactors

The lower legform impactor is referred to as the TRL-LFI, which was designed and developed by EEVC WG17 to be used as an injury assessment tool whilst carrying out legform impacts to assess pedestrian kinematics (Gupta, 2014). In the TRL-LFI, the knee element is made up of a shear spring; a bending plate and the skin consist of confor^{TM} foam and Neoprene. Once a physical test has been carried out, the bending plate and the confor^{TM} foam have to be replaced and the confor^{TM} is also very sensitive to humidity (Konosu, 2008). The design is aimed to partially replicate the human's leg characteristics, where the femur is fixed at the furthest point by the knee and the closest end by the hip, this configuration allowed the impactor to bend freely in the middle. Strain gauges which are situated in the middle to determine the maximum bending moment, and load cells are located on the upper and lower supports of the legform. The measurements taken are to identify possible risk of injury which are knee bending angle, tibia acceleration and knee

shear displacement. The impactor however doesn't take any measurements in the fibula or tibia region. A few of the restrictions of the TRL-LFI are the variation of long bone stiffness of the human and the impactor, and therefore the kinematics are not reflected accurately, resulting in an insufficient assessment capability using the TRL-LFI legform (Konosu, 2008).

Due to the insufficient assessment capabilities of the TRL-LFI legform, in 2000 JAMA-JARI began to design and develop a more suitable legform impactor known as the Flex-PLI which offered better injury assessment due to the more accurately modeled kinematics. The new impactor has a more human like flexible long bones (tibia and femur), and benefits from an incorporated knee restraint system (GTR9-C-04, 2011). During physical tests the flesh consists of synthetic rubber and neoprene sheets which can be reused. Further development came in 2006 with the flex-GT and the final version in 2009, which offered a significant improvement on previous versions due to the vast amount of data which can be collected, it had the ability to record the bending moment in the femur in three separate locations where as the Flex-PLI cannot and showed significant improvements on the impact kinematics compared to TRL-LFI legform (Konosu, 2008) .

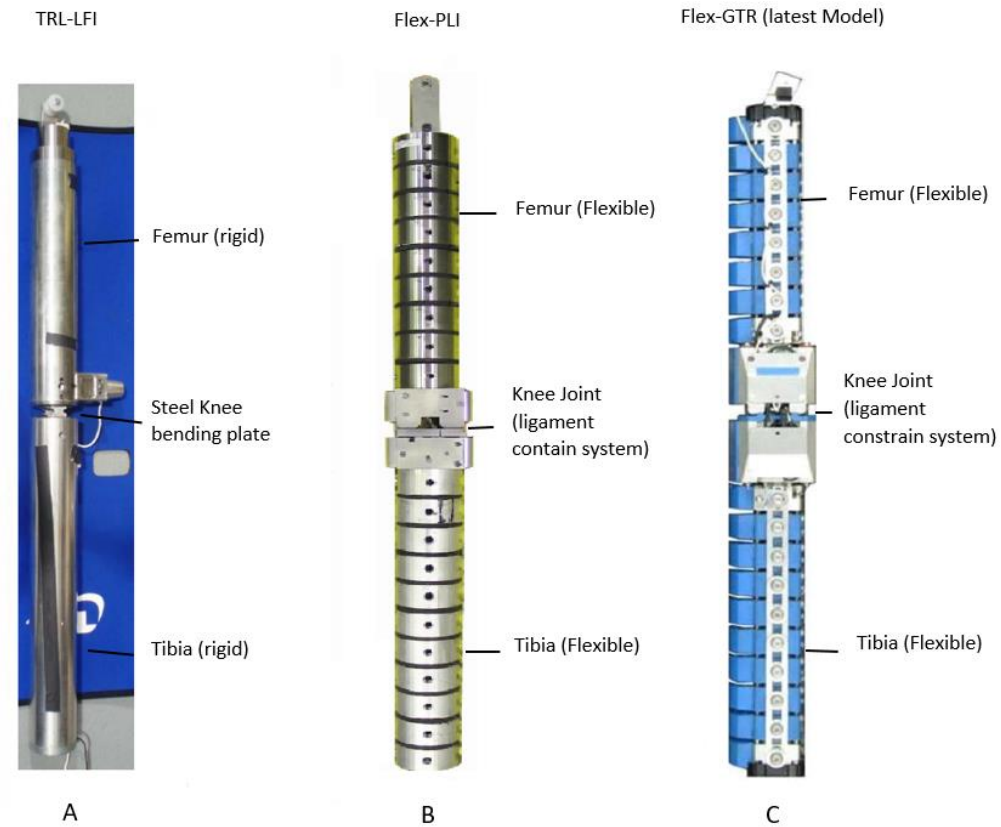

Figure 10. Legform Impactors (TRL-LFI), (Flex-PLI), (Flex-GTR) (Konosu, 2008)

The headform impactors represent the human head of an adult and child pedestrian. The earlier headforms had a mass of 4.8kg for adults and 2.5kg for a child. In the later models the mass of the adult was 4.5kg and the child 3.5kg (Anderson et al., 2008). The headform core consist of aluminum, where a steel plate is fixed to the surface of the core, this is to secure the impactor to the magnetic holding frame prior to any propulsion tests. Two m2 nylon screws are used in the European propulsion systems which are designed to fail in order to release the impactor during its propulsion. The impactor skin consists of polyvinyl chloride (PVC). Both impactors are fitted with three accelerometers situated close to the center of gravity of the impactor (Matsui et al., 2004). In order to check the impactor's biofidelity (Skin Stiffness) they are tested using a drop test (Matsui et al., 2003). The use of headform impactors is beneficial to assess vehicle front structures in the initial design phase to estimate the head acceleration and HIC values during the early phase. However due to the impactors being free flight, It cannot account for the real life kinematics experienced by the head and neck during an impact, therefore headform impactors should only be used as an injury prediction tool (Gupta, 2014).

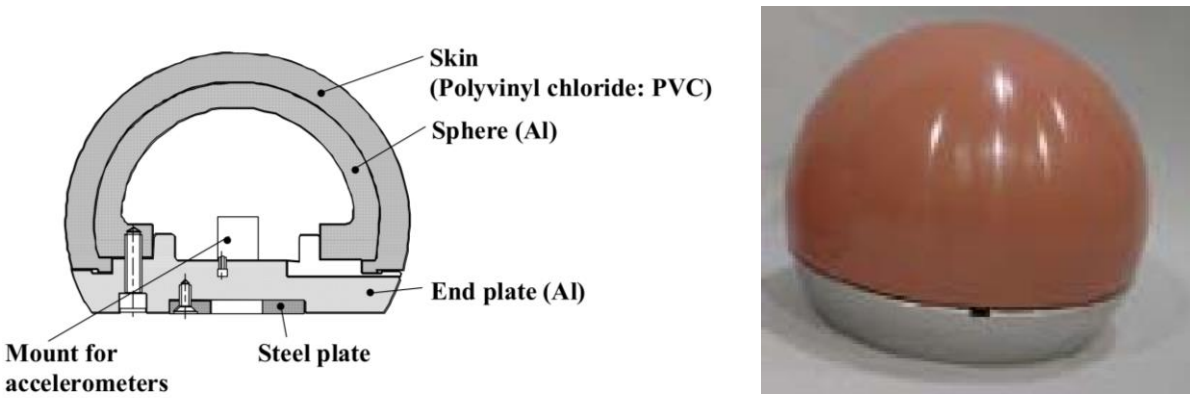

Figure 11. Adult Headform impactor design (left), assembled (right) (Matsui, et al., 2003)

Due to the complex kinematics which occurs during a vehicle-pedestrian impact, the use of local impactors is inadequate to evaluate comprehensively the degree of protection potentially offered by the safety countermeasures of the vehicle. One of the main limitations is the result of the lack of pre-deformation of the bonnet caused by the pedestrian torso prior to head impact (Chen, 2017). Consequently subsystem testing is not effective in assessing active safety systems such as active bonnets and pedestrian airbags. These safety countermeasures usually have complex detection devices and sensors which detect contact with a pedestrian that cannot be effectively evaluated using subsystem testing (Gupta, 2014).

3.2 Full-scale Pedestrian Test Dummies

In the initial stages testing with full-scale test dummies have not produced completely successful results. Some of the issues which occurred during the tests were, difficulty with evaluating the different phases of impact, potential of damage to test dummy, unclear repeatability and finally the kinematics observed were different from that observed from (PMHS) (Mizuno, 2003). In order to make full-scale test dummies a viable test method, a new more robust and repeatable pedestrian test dummy which can perform more human like needed to be developed (T.J et al., 1999).

A new pedestrian dummy was developed in joint collaboration of JARI, Honda R&D and GESAC. The first version was known as Polar I, this was a modified version of Thor the NHTSA frontal test dummy. The modifications were specifically aimed to improve the kinematic response throughout lateral impacts at a variety of impact speeds. The later dummy was known as the Polar II, which included a more human-like representation of the knee, a more compliant shoulder and a flexible tibia. However, pedestrian dummies have a variety of disadvantages for use in test regulations intended for pedestrian protection. The most significant disadvantage is the necessity for a whole family of test dummies to account for all forms of real life physiques. Consequently the sub-system test method is preferred (Mizuno, 2003).

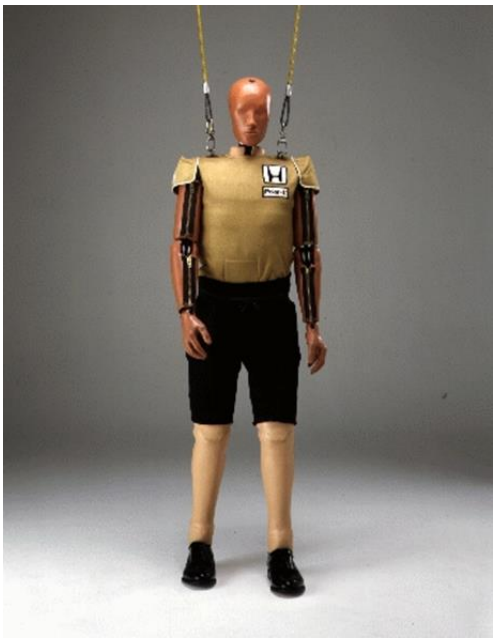

Figure 12. Frontal view of polar test dummy (Mizuno, 2003)

3.3 Development of Test Procedures for Pedestrian Safety

Four main groups are currently, or have previously been involved in developing procedural tests for evaluating the degree of protection provided by vehicles for pedestrians. The four groups consist of, the International Standards Organisation (ISO), United States National Highway Traffic Safety Administration (NHTSA), European Experimental Vehicles Committee (EEVC), and International Harmonised Research Activities (IHRA). Each group undertook the task by developing sub testing methods or components, as opposed to full size test dummies (Mc Lean, 2005). This was due as mentioned before problems with repeatability, it requires a whole family of test dummies, and issues with it behaving human-like.

During the 1980 the NHTSA was involved in developing pedestrian protection test methods, this work was later suspended in 1992. Currently the NHTSA are contributing to the work conducted by IHRA PS (International Harmonized Research Activity for Pedestrian Safety). The EEVC now renamed European Enhanced Vehicle-safety Committee, participated in the development of test procedures in favor of pedestrian safety throughout the WG7, 10 and also 17. ISO (International Standards Organisation) began conducting work for pedestrian safety, the ISO working group activity moved in the direction of the IHRA program in the 1990s. The IHRA program suggested to harmonise the pedestrian safety technical regulations in 1996 (Gupta, 2014).

The EEVC proposed various tests, the main three proposed by the EEVC are: Headform to bonnet test (where higher importance is given to the child headform test), upper legform to bumper test, and legform to bonnet leading edge (with a height of 500 mm if this is exceeded an optional alternative upper legform to bumper test can be conducted) (EEVC, 1998). The proposed impact speed by the EEVC is 40 km/h, using the EEVC adult headform with a mass of 4.8kg and the child 2.5kg. The proposed safety acceptance level calculated by the resultant acceleration of the accelerometer should not exceed 1000 HIC value for the adult and child headform and a maximum knee lateral shear displacement of 6mm, 15 degrees of lateral knee rotation, a maximum of 150 g’s for the top of the tibia of the lower leg legform impactor as well as the upper limit for the bending moment being 220 N.m for the upper legform (Janssen, 1996).

ISO pedestrian protection group is much like the EEVC, but has proposed a different adult and child headform impactor to the EEVC. Where the ISO adult headform is 4.5 kg and the child 3.5 kg (Mizuno, 2003). The headforms are the same diameter as the EEVC. The pedestrian test procedures created by IHRA also very closely resemble the EEVC test

procedures; however the headform specifications used are identical to the ISO's headform. The test procedures IHRA developed are used for a range of vehicle speeds between 30 – 50 km/h (Mizuno, 2005).

3.4 European Union Directive Regulation

The early proposal of the European Union Directive was for protection of a pedestrian during a collision with a vehicle, which was centered on the use of the EEVC test methods. The EU directive requirements are in two phases. In phase 1, the requirement is that a child headform test should be conducted with a mass of 3.5 kg and a diameter of 165 mm with an impactor speed for 35 km/h at an angle of 50°. Where the HIC value must not exceed 1000 over two thirds of the tested area, and the remaining third should have a HIC of 2000. Where beginning in 2005, all vehicles manufactured must conform to these two tests which measure the protection against leg and head injuries. The second set of tests in phase 2, the adult and child head are each impacted at 40 km/h at an angle of 65°, the child headform has a reduced mass of 2.5 kg compared to the 3.5 kg of phase 1 and the adult being a mass of 4.8 kg and the value of HIC should not exceed 1000 for both impactors on any location within the bonnet test area. Starting in 2010, four tougher tests are being introduced where two are regarding head injuries and two relating to leg injuries (Mc Lean, 2005).

3.5 Global Technical Regulations (GTR)

The GTR is based on International Harmonized Research Activity (IHRA) data, which is sourced from various countries. Due to the head impacts of adult/child comprising of above 30 percent of severe and fatal injuries. The GTR focusses on protecting these body areas specifically. As suggested in the GTR the maximum benefit for pedestrian safety would be if all vehicles comply with the technical requirements, but recognises that the application on heavier vehicles such as busses would be of limited value in their current form. This is because the test methods proposed in the GTR have been developed for current light vehicles, based on the pedestrian kinematics of when impacted by such vehicle. Therefore the scope of its function is restricted to be used on passenger vehicles, sports utility vehicles (SUV), as well as light trucks. Given that these vehicles are the vast majority of vehicles found on the road. Based on the data the GTR would focus to improve the safety by making it a requirement that vehicle bumpers and bonnets can absorb kinetic energy more

effectively if the vehicles is impacted at 40 km/h, at this speed a vehicle-pedestrian collisions accounts for more that 75 percent of accidents resulting in (AIS1+), as reported by IHRA (Global technical regulation No. 9, 2009).

The GTR is comprised of two sets of criteria to assess the performance, which applies to the front bumper along with the bonnet top and wings. The GTR developed specific test procedures for each area with the use of sub system impactors for the adult leg, and for child and adult head protection (Global technical regulation No. 9, 2009).

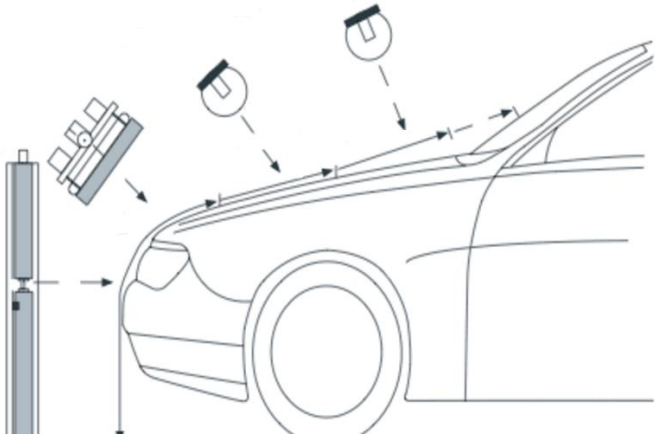

Figure 13. GTR Pedestrian Protection Test Procedures (Shape Corp, 2017)

3.5.1 (GTR) Test Procedures

Legform to bumper test: In order to assess the leg protection of the front bumper, the bumper requires being subject to a pedestrian lower impact forces. The test procedure specifies that the bumper to be impacted at speed 40 km/h with the legform impactor which represents the injury characteristics of an adult's leg. If the vehicle has a bumper which is lower than 425 mm it is tested with the lower legform impactor, if the vehicle has a lower bumper height above 500 mm they must be tested using an upper legform impactor. While vehicles which have a bumper height ranging between 425 mm and 500 mm can be tested by either upper or lower leg impactor depending on the manufacturer's preference. Since pedestrians typically wear shoes the base of the impactor must be 25 mm above the ground (Global technical regulation No. 9, 2009). These tests assess the acceleration of the tibia, shear of the knee joint, rotation between the tibia and the femur (Agrahari et al., 2009).

Child headform to bonnet test: the Wrap Around Distance (WAD) was selected mainly based on data provided by Europe, Australia, USA and Japan. The child headform is constrained to the vehicles front by a perimeter determined from the 1000 mm WAD, but is also constrained at the rear by a 1700 mm WAD. The wings/bonnet are impacted at a 35 km/h at an impact angle of 50° to the horizon (Global technical regulation No. 9, 2009) .

Adult headform to bonnet test: based on data gathered the headform test starts at the front where a 1700 mm WAD was determined, where the test area ends at the rear edge with a 2100 mm WAD. The wings/bonnet is impacted using an adult headform at 35 km/h at an impact angle of 65° to the horizon (Global technical regulation No. 9, 2009).

Impactor form	Injury Assessment Parameter	Threshold
Lower Legform	Knee Bending Angle	19 Degrees
	Knee Shear Displacement	6 mm
	Upper Tibia Acceleration	170 g's
Upper Legform	Sum of Impact Forces	7.5 KN
	Bending moment	510 Nm
Child Headform	HIC	Must not exceed 1000 over 2/3 of whole area for adult and child combined. The remaining HIC must not exceed 1700 for the remaining test area
Adult Headform	HIC	

Table 2. GTR injury criteria (Global technical regulation No. 9, 2009)

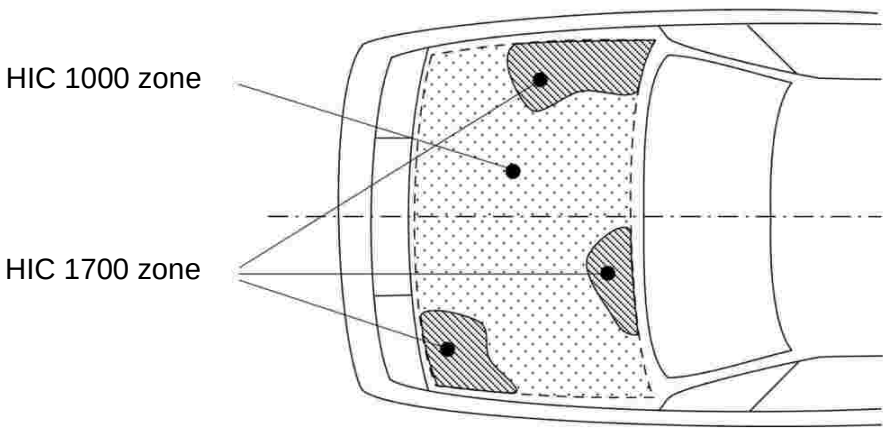

Figure 14. Indicating HIC 1700 and 1000 zones in GTR tests (Eur-Lex, 2009)

3.6 Pedestrian Safety Rating System Euro NCAP

The European New Car Assessment Programme (Euro NCAP) began in 1997, the program was aimed at providing consumers with a safety performance rating of the more common road cars sold in Europe. Prior to 2009, each individual vehicle was awarded using a three individual star ratings system which focuses on child, occupant safety as well as pedestrian protection. The three star rating system, was replaced in 2009 with a single 5 star overall rating system, the overall rating system combines the results of four key test areas: child protection, adult protection, pedestrian protection and a new section for safety assist technology (Ratingen et al., 2016). Euro NCAP conduct a sequence of impact tests which replicate impacts involving adult and child pedestrians at 40 km/h (Ward, 2014). Where the upper legform evaluates the bonnets leading edge, the lower legform evaluates the protection of the lower leg offered by the bumper, while the use of headforms are to impact the top of the bonnet to assess head injury potential (Gupta, 2014). Leg protection may be improved using a bumper which can deform if struck by the leg of the pedestrian. Leg protection is improved further if the impact occurs lower and further from the knee, as a result the forces are distributed around the longer length of the knee. Improvements to the bonnet leading edge can be achieved by removal of unnecessary rigid structures. In order to enhance the head protection the bonnet must be capable of deflecting, it's also crucial that adequate deformation space is provided between the bonnet and the rigid structures below (Ward, 2014).

Prior to testing, the test vehicle must be marked by keeping to the marking guidelines provided by (Euro NCAP, 2015). The marking lines which are used; bumper corners, bonnet leading edge reference line, bumper reference lines, bonnet side reference lines and bonnet top WAD lines. The test parameters for a child/small adult head test impact zone boundaries lay between 1000 mm and 1500 mm WAD lines and the adult head impact zones are between 1700 mm and 2100 mm. A head impact speed of 40 km/h, where a child headform impact occurs at 50°± 2° from the ground reference level, whereas the adult headform impact occurs at 65°± 2° (Euro NCAP, 2014).

Impactor form	Injury Assessment Parameter	Threshold
Lower Legform	Knee bending Angle	15 deg
	Knee shear displacement	6 mm
	Upper Tibia acceleration	150 g
Upper Legform	Sum of impact forces	5 KN
	Bending moment	300 Nm
Child/Adult Headform	HIC	1000

Table 3. EuroNCAP injury criteria (Euro NCAP, 2014)

The manufacturer of the vehicle is required to provide their test data which they predicted during head impact for all grid points tested and is required to be presented depending on the color scheme or alternatively the HIC values can be provided.

Green	HIC < 650	1.00 Point
Yellow	650 ≤ HIC < 100	0.75 Point
Orange	1000 ≤ HIC < 1350	0.50 Point
Brown	1350 ≤ HIC < 1700	0.25 Point
Red	1700 ≤ HIC	0.00 Point

Table 4. EuroNCAP scoring (Euro NCAP, 2015)

A limit of 24 point are achievable for the prescribed headform test zones, where an overall score for all the grid points are calculated as a percentage of the maximum attainable score (Euro NCAP, 2015).

3.7 Discussion

Since the development of pedestrian injury assessment criterions, physical and numerical testing has become vital to determine the injury mechanism and severity posed by a pedestrian-vehicle impact. During the initial stages full PMHS were used to assess the injury kinematics and severity but proved to be limited. This resulted in the development of full scale pedestrian test dummies to better assess the injuries sustained. Conversely, the use of full size dummies were eventually substituted for

local impactors due to the high cost of test dummies. These impactors are much more economical and provided a more repeatable test environment in compared to the test dummies, and are the most preferred method used in industry for safety testing protocols and adopted by safety testing groups such as ISO, NHTSA, EEVC and IHRA (Crandall, et al., 2002).

Chapter 4: Pedestrian Safety Offered by Vehicles

In the past, vehicle designs were primarily aimed at improving the protection and safety of the occupants, however in recent years numerous studies have proven that the same can be done for pedestrians. The approach used to enhance and develop the vehicles safety performance can be categorised in to the following; Passive approach for example of this can be altering the way the front wings, bonnet and windshield wipers assemblies are fixed whilst upholding its strength and performance but allowing deformation when impacted by a pedestrian. This can also be achieved by altering the material stiffness to enhance the energy absorption characteristics which also greatly enhance the safety during a vehicle-pedestrian impact (ROSPA, 2015). The second can be referred to as the active approach where the bonnet is lifted using actuators to increase the clearance between the bonnet surface and the rigid engine components, thus providing adequate space for the bonnet to deform (Takahashi et al., 2013).

4.1 Passive Safety Countermeasures

The design of a vehicles front-end assembly has an immense consequence on the level of resultant injuries sustained during a collision with a pedestrian (Gupta and Yang, 2013). Car frontal designs have changed tremendously over the years, one of the most obvious changes are smoother appearances to the frontal structure most recognisable is the smoother front bumpers where most pre 2000 cars had large protruding bumpers and resulted in a nearly rectangular front leading edges which pose a 79% higher risk to pedestrian leg injury (Otte and Haasper, 2005). Other less subtle changes which auto makers began to address in the initial stages were protruding bonnet ornaments, which were imbedded into the front grill or designed to collapse, and wing mirrors are now mounted on springs (Edmunds, 2009).

Based on the kinematics of a pedestrian during an impact, the bonnet is a critical element which can dictate the severity of the head trauma. Bonnet performance demands as mentioned before require two key principles, efficient energy absorption and adequate deformation space between the engine and the bonnet. Over time bonnets were optimised for better energy absorption during head impacts consequently lowering the HIC value. The main method of optimising was using various shapes and inner patters and materials (Krishnamoorthy, 2012). Although these bonnet optimisations prove to be very effective they

are limited by other structural factors such as oil canning; due to using very thin material on the outer skin to promote energy absorption (Bhanage et al., 2016), which are often not considered during the optimisation process. Figure 15, shows an inner panel where the local stiffness does not deviate considerably as in traditional bonnet inner panels. It was found that this is very beneficial to have the continuous stiffness distribution because of the ease of altering the bonnet to be more or less rigid overall merely by altering the cones geometry (Kerkeling et al., 2005).

Figure 15. Cadillac Seville bonnet inner structure (Kerkeling et al., 2005)

Christoph Kerkeling (2005), found that the closed multi-cone inner panel design increased the torsional stiffness of the bonnet. Additionally the single inner panel's stiffness is increased which allows for a reduced inner panel thickness. Consequently the local stiffness and the active mass are reduced, which enhances pedestrian head impact protection. The inner panel's outer frame primarily defines the bending stiffness of the bonnet and the bonnet reinforcements at the fixing points for the bump stops and the hinge latch. The inner frames outer structure of the inner panel is therefore kept and the multi cone usually only replaces the inner portion of the inner panel (Kerkeling et al., 2005).

Abolfazl Masoumi (2011), investigated different bonnet materials (aluminum, steel and composite) which have all been tested and assessed to meet structural requirements as well as pedestrian HIC. This is because there is a high demand for car manufacturers to continuously look at methods to reduce the weight of car components in order to reduce fuel consumption. The results suggest that by using aluminum without changing any of the bonnet configurations such as: style, ergonomics, aerodynamics and strength compared to the steel bonnet. When tested the aluminum bonnet resulted in lower HIC value and a 50% weight reduction, although it has a lower strength factor than the steel bonnet. And the composite offered further improvements on the HIC and torsional stiffness as well as

reduced weight but was found to be the most costly solution (Masoumi et al., 2011). In summary, that besides material change, modification and structural enhancement of the inner structure could offer lower displacement and could offer reduced HIC values as another solution (Cheng and Wang, 2002).

To lower the HIC, two key principles should be applied: provide low stiffness of impacted vehicle body panels and to provide sufficient deformation space to avoid making contact with rigid components. As seen in Graph 1, the acceleration which occurs within the initial few milliseconds is dictated by the active mass. Consequently the materials, their thickness and the amount of components impacted have a major effect. Whereas the second peak is defined by the structural stiffness which is effected by the components size and the type of mountings used. In order to obtain sufficient deformation space components under the bonnet should be packed following specified clearance criteria, components which penetrate the clearance space are considered critical and may need to be relocated or redesigned to comply with HIC targets (Kerkeling et al., 2005).

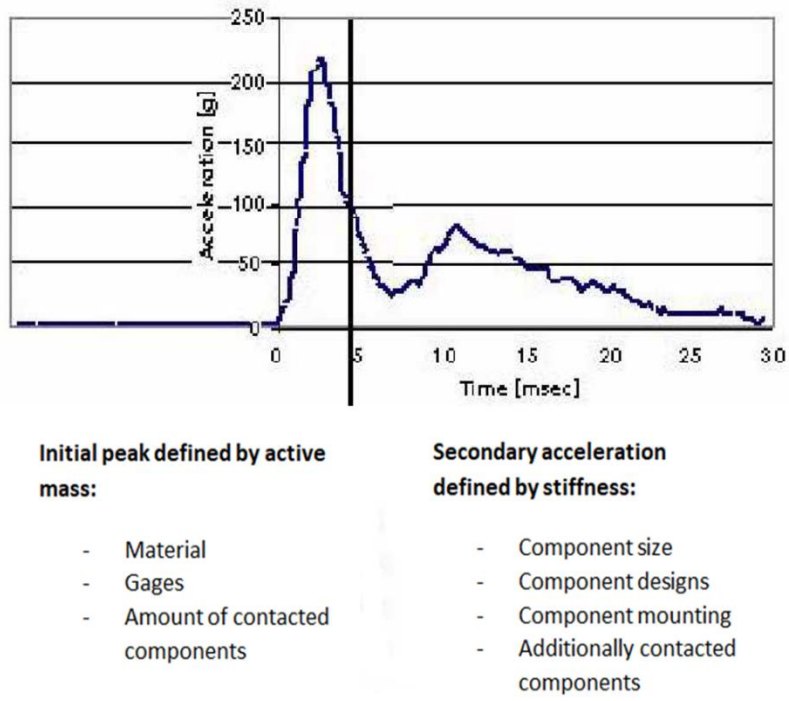

Graph 1. Influence of mass and stiffness on the acceleration (Kerkeling et al., 2005)

The next essential area of the bonnet required to comply with pedestrian protection are the latches, bump stops and the hinges fenders. These areas are typically the most difficult to comply with the impact criteria and pose the greatest challenge to auto manufactures, this area is also where most none deployable bonnets are the stiffest (Ames and Martin, 2015). The hinges are required to transfer forces from the vehicle to the bonnet and vice versa, the hinge mountings requirements are often conflicting with pedestrian protection and the

durability load cases. For the durability load tests, the mounting are required to be durable enough to not result in excessive movement during normal driving conditions. A person leaning on the bonnet when closed or open doesn't result in any plastic deformation, hinge movement needs to be minimal during low speed impact test to preserve the bonnet and fenders and the bonnet shouldn't intrude into the windscreen during high speed frontal crashes (Gupta, 2014).

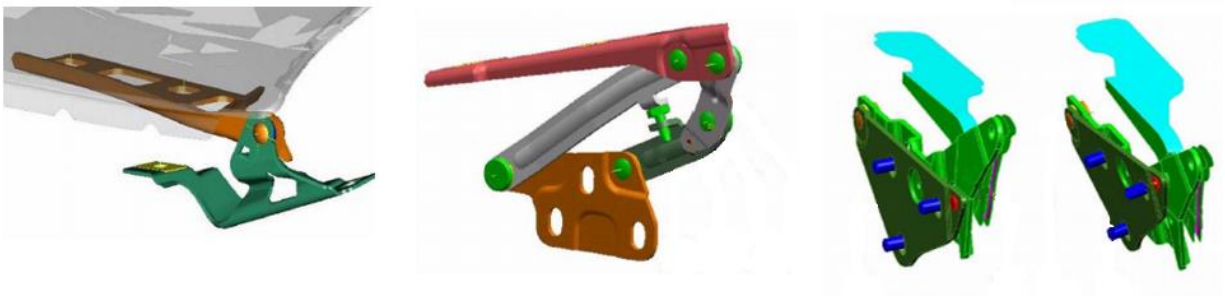

A - Single joint hinge

B - Multi joint hinge with deformable parts and collapsible

C - Single joint hinge with deformable parts and collapsing mechanism

Figure 16. Types of bonnet hinges modified from (Kerkeling et al., 2005)

The optimum acceleration and HIC are usually not achieved in the bonnet mounting areas. At the mounting points the resultant acceleration typically are longer lasting than other areas, which throughout the impact requires to be kept at a lower constant level. (Kerkeling et al., 2005), developed some conceptual designs which suggests that a single-joint hinge Figure 16A with incorporated deformable parts could be compliant with head impact requirements. The benefit of using this hinge is that it may allow the hinges pivot point to remain in the head impact zone. Its limitation is providing a constant reaction force caused by plastic deformation of the hinge during a head impact. Another solution is using a Multi-joint hinge Figure 16B which typically consists of two main parts one connected to the car body and the other to the bonnet, which are connected via two levers, depending on the assembly and the position of the levers when the bonnet is in the closed position, this arrangement could provide sufficient deformation space during a head impact. The two levers should be situated that they allow deformation in the lateral direction causing them to deform in the vertical direction during head impact loading.

Another approach to comply with HIC levels, as mentioned before the bonnet must be designed to be able to manage the impact energy generated by a pedestrian head impact. However the bonnets ability to absorb energy effectively is greatly influenced by the proximity and clearance of engine components and the bonnet, yet in many cases having a

large clearance can affect the driver's visibility, aerodynamics and styling which are not desirable. (Liu et al., 2015), created a "sandwich" bonnet to comply with pedestrian safety requirements. The bonnet design consisted of three aluminum substructures which are; the outer skin the rippled middle section and the support plate as the lower section.

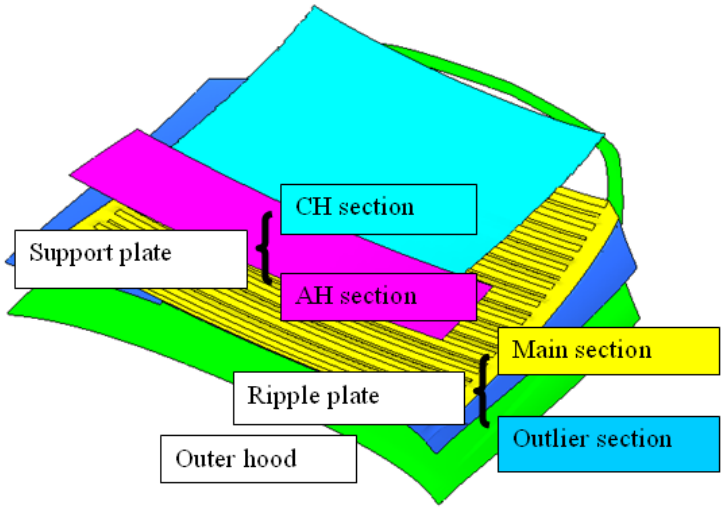

Figure 17. Exploded view of bonnet design (upside down view) (Liu et al., 2015)

As seen in figure 17, the outer bonnet is fixed to the ripple plate using glue strips on the higher ridges of the main section of ripple plate and glue spots in the outlier section of the ripple plates, whereas the support plate is bonded using either bolts, rivets or spot-welds (Liu et al., 2015).

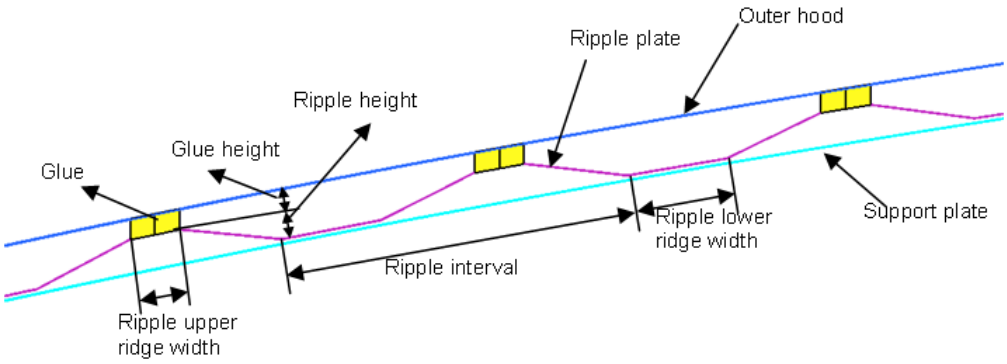

Figure 18. Enlarged cross-sectional view of sandwich bonnet assembly (Liu et al., 2015)

Most of the optimising and enhancement is aimed at improving the energy absorption of the bonnet and hinges to promote energy absorption, and the plastic components within the engine bay are often considered as very minor impact stiffness contributors. However (Boggess and Wong, 2003), Investigated focusing on the cowl region to examine the stiffness contribution and the effects on the HIC value.

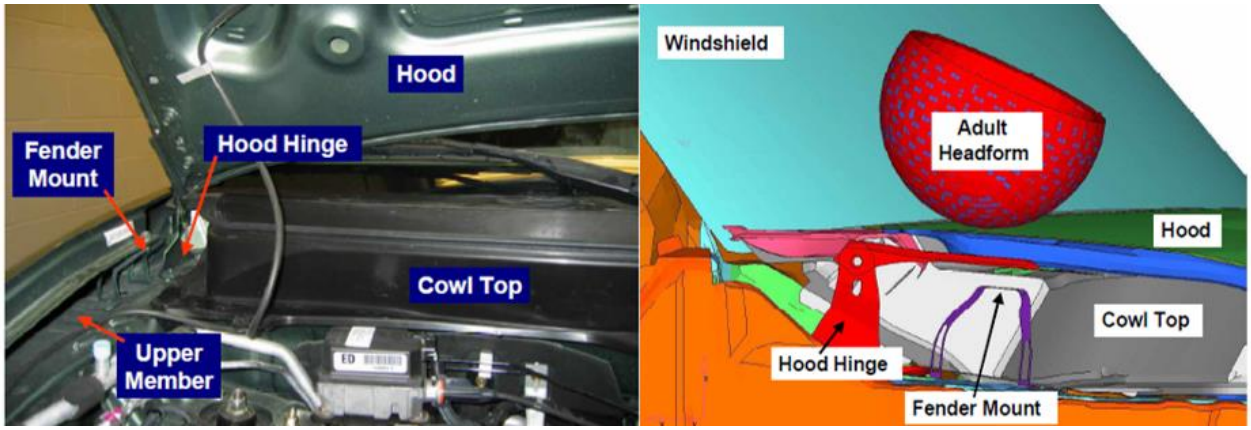

Figure 19. Headform impacting the bonnet at the fender seam (Boggess and Wong, 2003)

In the preliminary testing showed that the cowl top stiffness accounted for around 50% of the HIC value and 35% of the overall average stiffness. The geometry of the cowl was modified to aid in deformation and to reduce the overall stiffness contribution. The final results show a 75% reduction in the HIC and 65% reduction in the resultant head deceleration. The results demonstrate the importance of developing plastic components in all of the bonnet areas, and the most important areas are where the stiffness is added in conjunction with other stiff components such as fender mounting brackets, wiper assemblies and bonnet hinges (Boggess and Wong, 2003).

4.2 Active Safety Countermeasure

Due to automakers opting for sleeker vehicle geometry, as a result low bonnet profiles, which is more desirable for vehicle manufacturers for aerodynamic performance and styling. Conversely this may enhance the vehicle aerodynamically and enhance the vehicle visually but the low bonnet profiles have a negative effect on pedestrian head protection. The result is far less space between the rigid engine components, a clearance required for effective energy absorption (Ames and Martin, 2015). Although many car manufactures are able to comply with safety regulations and provide enough clearance, through structural changes and optimisations and component layout adjustments. However, improving the head protection of pedestrians through optimising the structure is becoming more limited with current and future safety regulations (Xu et al., 2010). There is another solution which lifts the bonnet during the event of a pedestrian vehicle impact (Lee et al., 2007). The motivation for the approach came from the main underlying issue of insufficient deformation space between the bonnet and underlying structures such as the engine components. At these locations the injury level tends to much higher. Therefore to reduce the injury level the

bonnet can be lifted increasing the deformation space and can mitigate injury levels (Shin et al., 2007). Also, a further benefit is adding the bonnet lifting mechanism to existing vehicles, designed for a market without strict pedestrian protect which will allow manufactures to sell in different market places without major styling and structural alterations. The positive potentials of the active bonnets have been shown by numerous studies (Nagatomi et al., 2005), (Fredriksson et al., 2006), (Takahashi et al., 2013).

The working principle behind the active bonnet deployment is that the vehicle is fitted with a control unit which initiates the bonnets deployment when the vehicle senses a pedestrian collision and the impact characteristics are within the predetermined threshold from which the ECU using a complex algorithm decides if deployment will be effective within the required time (Lee et al., 2007). The ECU unit receives input from sensors situated within the bumper, in the form of pressure tubes, resistive/capacitance sensors or accelerometers.

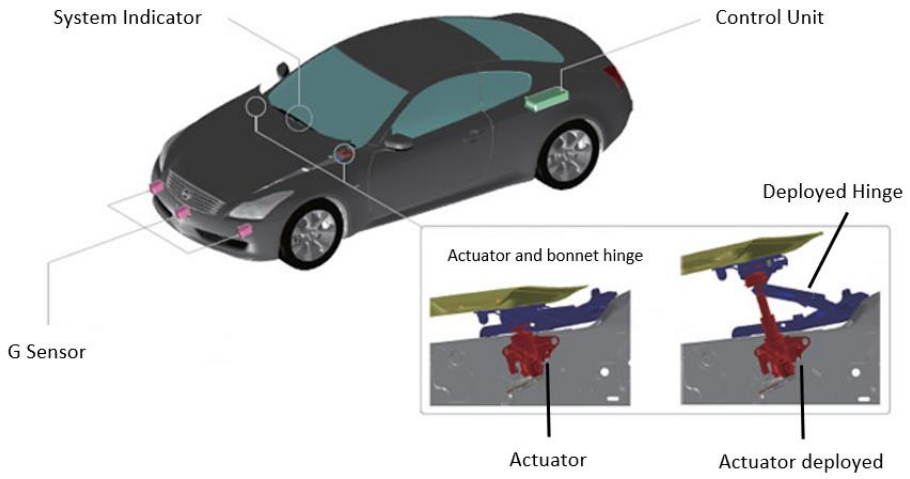

Figure 20. Nissan active bonnet system configuration (Nissan Motor Corporation, n.d.)

During a pedestrian collisions, the kinematics show that most often the legs of the pedestrian contacts the bumper first, followed by the upper body collapsing onto the bonnet. Oppose to a collision with a roadside pole where the system should not deploy through classification of the impact pulse.

Table 5. Deployment matrix example for active bonnet system (Lee et al., 2007)

	Target Objects
Must Fire	Adult Legform (13.6 kg)
	Thin Pole with Foam (Child Legform 3.7 kg)
Must not fire	Thick Rigid Pole (12.2 kg)
	Thin Rigid Pole (3.7 kg)
	Rough Road

As seen in table 5, for the “must fire” and “must not fire” cases, the difference between rigid pole and legform impactor is how the object being impacted distributes its stiffness. If the designed algorithm can differentiate among these conditions, this will cover most real world scenarios.

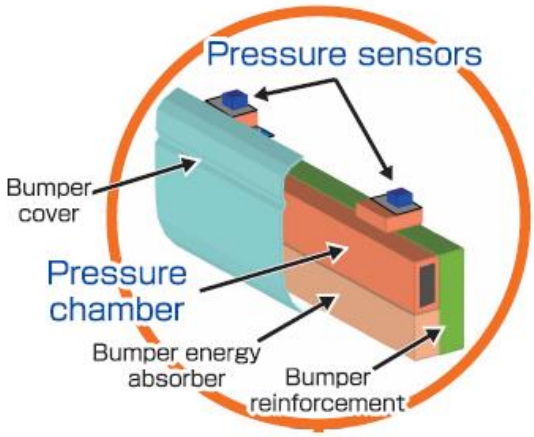

Figure 21. Active bonnet bumper sensor configuration (Takahashi et al., 2013)

Hiroyuki Takahashi, developed a pressure sensor method in order to detect a pedestrian impact. This method incorporates a pressure chamber and pressure sensors to establish the effective mass of the object during collision. This allows the systems to differentiate between a collision with a road side object and pedestrians. The use of this system allows for stable detection of pedestrians even with a variation of vehicle shape and collision position (Takahashi et al., 2013).

The use of fiber optic contact sensors have also been investigated by Oliver Scherf. It was noted that due to technological challenges it was not viable to use predictive (pre-crash) sensing methods for pedestrian detection, hence why most designs relied on the contact sensing method (Scherf, 2007).

Figure 22. Configuration of fiber optic sensors (Scherf, 2007)

The fiber optic sensor operating principle is based on micro bending of the optical fiber strands. Each fiber is concealed by a coating which is reflective, to reduce light loss during transfer. During the treatment process the coating is removed partially from the fiber, thus resulting in a reduction or amplification compared to the reference state (Scherf, 2007).

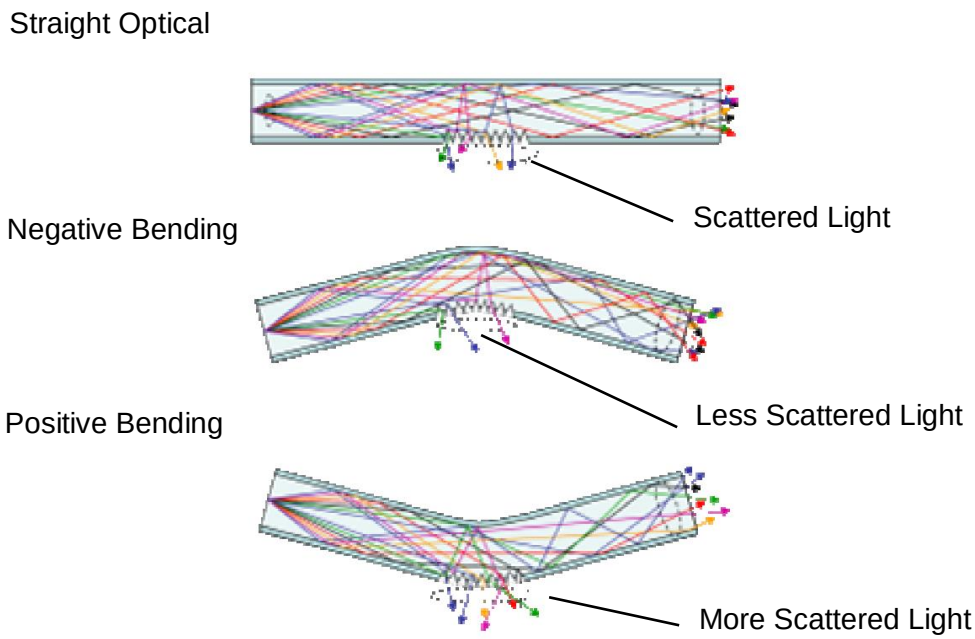

Figure 23. Demonstrating the micro bending principle (Scherf, 2007)

Light is lost continuously through the straight fibers, which increase during upward deflection and reduces during downwards deflection. The rate at which light is lost is directly associated to the flex direction of the fiber. The light intensity is then converted by an optoelectronic interface where the light signal is converted to a voltage (Scherf, 2007).

Piezoelectric technology has also been used for pedestrian sensing, where the piezoelectric effect can be used to measure the force, acceleration and strain. For the use of pedestrian protection one or more sensors can be integrated into the vehicles front profile. The sensors will identify the primary impact; the stress detected by the sensor from the impact is then turned to piezoelectricity and is analysed by the sensor circuit. By analysing the signal generated by the sensor, vital data from the signal can determine the dimensions and effective mass of the object. If the preset threshold is met a trigger signal will be sent to deploy the active system. Due to the fast response time of the piezoelectric sensor (15 ms), it has the ability to analyse and detect the impact shortly after the pedestrian strikes (Zanella et al., 2002).

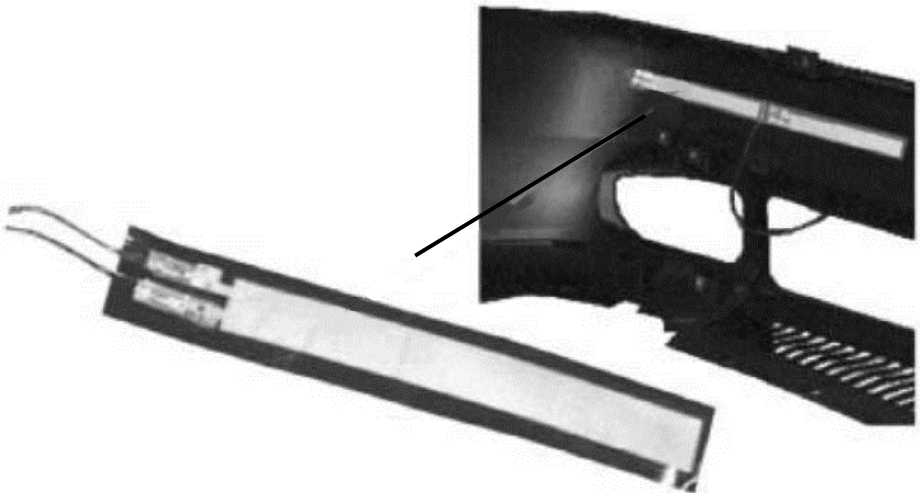

Figure 24. Sensor module incorporated into an Alfa Romeo bumper (Zanella et al., 2002)

The use of contact sensors presents some advantages. They offer high resistance to environmental factors, low cost and fast reaction time. However, because contact sensors can only react once an impact has occurred, the response time may be too high for use in certain safety systems. Further to this, the contact sensors are always on the bumper, or alternatively the impact signal is sometimes transferred through the bumper system. Because of the high level of temperature dependency of the foam stiffness within the bumper, the sensor output may be unstable during fluctuating temperatures (Huang, 2010) .

In order to provide clearance between the bonnet and the ridged components within the engine bay, it requires a lifting mechanism which can lift the bonnet to the desired height prior to the pedestrians head making contact with the bonnet, as well as withstand the force generated by the pedestrians head during impact whilst remaining deployed. The performance of the mechanism to lift the bonnet, directly affects the level of protection offered to the pedestrian (Ye et al., 2011).

In general the bonnet lift height can be defined by: (the clearance between the engine and the bonnet + lift height) must be greater than the vertical displacement when the bonnet is subject to loading. However, the lifting height can vary considerably between different vehicles due to the type of actuator used, the structural stiffness of the bonnet and the placement of under bonnet components (Zander, 2017).

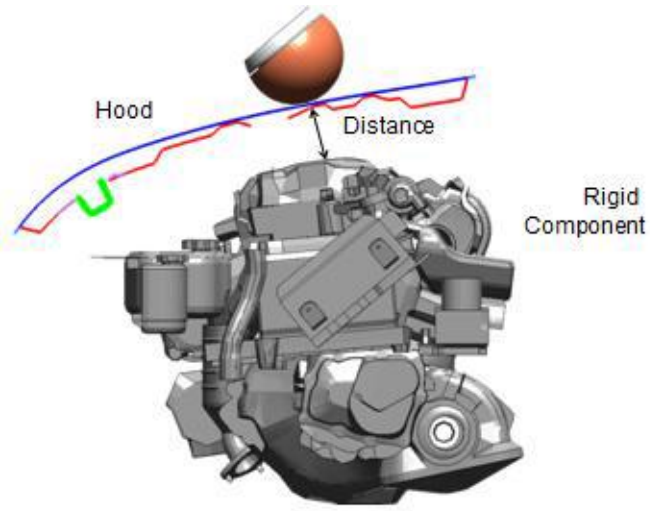

Figure 25. Illustration of clearance required to absorb the kinetic energy (Baleki and Ferreira, 2009)

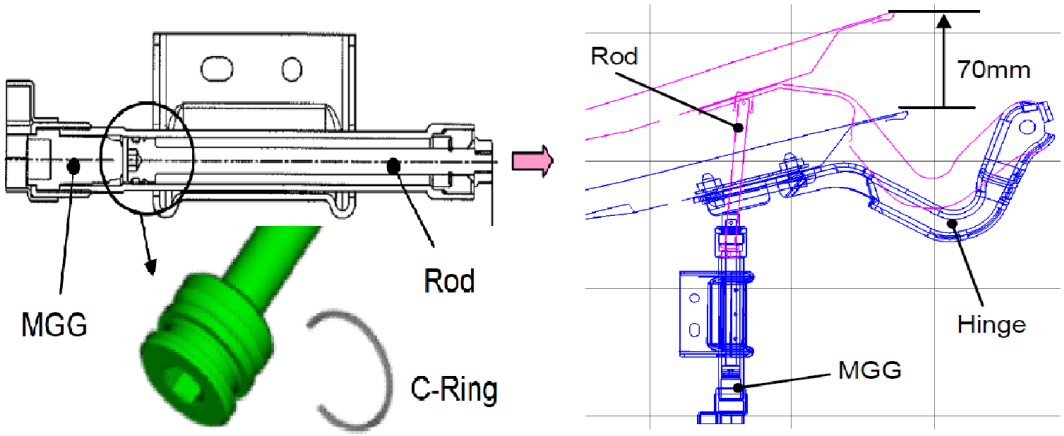

Figure 26. Actuator configuration and actuator activated (Takahashi et al., 2013)

In order to activate the push-rod, a micro gas generator (MGG) is used. This created a high pressure gas which in turn forces the rod into the upwards position typically between 20-30 ms. After deployment the bonnet can be semi reset, but the system would need replacement in order to be used again (Xu et al., 2010).

In the example illustrated in figure 26 the bonnet is raised by 70 mm, thus creating enough distance between the engine components and the bonnet, thereby reducing the severity of

the head injury of the pedestrians. As the pedestrian impacts the bonnet, the end of the rod is bent towards the rear of the bonnet; consequently the bonnet moves downwards further aiding to the energy absorption capabilities (Xu et al., 2010).

Although the primary lifting method is with the use of pyrotechnics, which are small and light weight, fast lifting and require only a small amount of energy to initiate. However, due to the nature of pyrotechnics they serve as a single use purpose, and cannot be reset after deployment, and in some cases they may deploy too fast and buckle the bonnet. Because of this fundamental draw backs, it has given rise to a different approach in the form of stored energy with the use of gas struts or springs. Which both have been proven to meet the reaction times required but require manual resetting after use. On the other hand (Barnes et al., 2008) developed a fully automated multi use lifting system the “SMART (Shape Memory Alloy ReseTable) Spring Lift”.

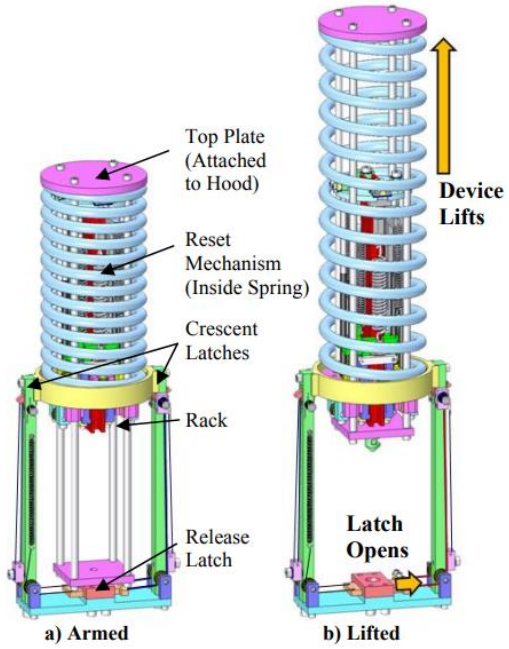

Figure 27. SMArt lift device armed and lifted states (Barnes et al., 2008)

In its normal state the Shape Memory Alloy ReseTable (SMART) is in the ready to fire state (armed), where the spring that’s lifts is compressed and held by the SMA release latch at the base. Upon detection of a pedestrian impact the deployment signal releases the latch and the spring which in turn lifts the bonnet. This system deployment response is comparable to that of pyrotechnics, but is fully resettable (Barnes et al., 2008).

Further extending on the energy stored approach (Luntz et al., 2007). The “Dual Chamber SMART lift” (Luntz et al., 2007), this features a pneumatic spring in conjunction with two

spaces which store compressed air at each side of the air cylinder, which can lift the bonnet rapidly by emptying the air from the upper chamber with the use of a fast acting Shape Memory Alloy (SMA) valve causing the air in the lower chamber to expand and create the lift required. The device can be re-armed by removing the air out of the lower chamber, and re pressurising both chambers.

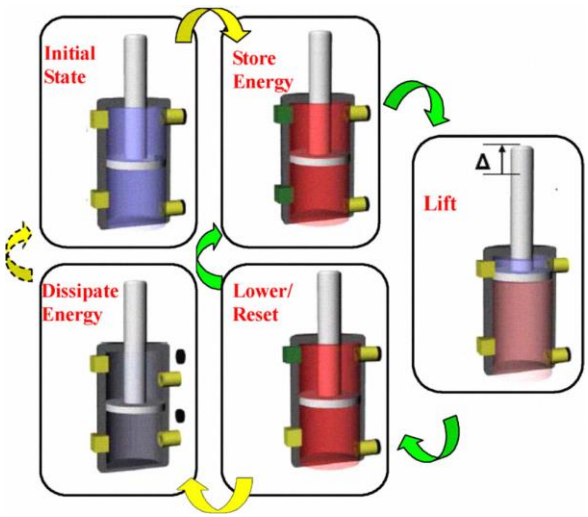

Figure 28. Duel chamber SMART device operating cycles (Luntz et al., 2007)

Seen in Figure 28, initially with no stored energy, it's then filled up to pre-determined pressure, thus storing the energy. To deploy the upper chamber is then vented triggering the device to lift (Luntz et al., 2007).

The above systems reviewed are all passive active lifting systems; they are activated after the initial impact with the bumper has occurred from a pedestrian. The main technical challenge faced with these designs are correct timing from initial contact with the front bumper and the head striking the bonnet, which occurs in approximately 60 ms. If the bonnet is not lifted in time it won't be in the correct position to provide optimal head protection. Because of the relatively large height the bonnet needs to achieve, the stored energy approach is employed: either with the use of springs or pyrotechnics. The majorities of devices currently used are non-reusable or resettable and are not able to alter their performance to keep the same velocity whilst adjusting to the extrinsic conditions for instance terrain changes, or fluctuations in temperatures (Xu et al., 2010).

4.3 Discussion

The effectiveness of active bonnets has raised a number of questions during the initial steps for pedestrian safety standards development. The main cause of concern was due to the high complexity of the system and the fine-tuning required for them to function correctly. The device must be triggered and then physically lift the bonnet to the upwards position, prior to the pedestrians head striking the bonnet, the lifting mechanism must be robust enough to not only withstand the forces generated from the initial lift but must be able to support the mass of the pedestrians head and torso. The timing for deploying the bonnet is very precise, and the sensors need to be calibrated to mitigate false deployment, the system must also be able to distinguish between a pedestrian and none-pedestrian. This was further complicated with the introduction of vehicles with active suspension, making matters worse (Lawrence et al., 2006).

Since 2010, vehicles with the active bonnet performed considerably better than conventional bonnets in the Euro NCAP headform tests with a score of 17.2 (out a maximum of 24) and conventional passive bonnets with 13.8 average score. Since the development of the active bonnet, the Skoda Octavia has been the only model which fitted the active bonnet technology as standard but later removed it. Active bonnets can also be fitted to vehicles not originally designed to use it, and pass the pedestrian protection requirements. One example of the was the Dodge Caravan which was not intended for a market with pedestrian protection, but by retro fitting the sensors and lifting actuators to the existing design rather than the lengthy and expensive redesign of the vehicles front profile, for use with none deployable bonnet, the vehicle was able to be brought to the European market. Due to the high number of active systems in production today, it is apparent that engineers have overcome the technical challenges presented in the initial stages, but testing standardisation has yet to be achieved. Active bonnets are now considered another technical advance in the field of automotive safety (Ames and Peter, 2015).

Chapter 5: Methodology

5.1 Feasibility Study of the Different Proposed Lifting Methods

Generally there are two methods to reduce the pedestrian head impact severity which can be either active or passive. Which route depends on the manufactures decision and the definition of head safety requirements based on the technology they can offer and the regulations. The passive approach is to decrease the stiffness of the bonnet structure to allow for a sufficient amount of deformation during a head impact. The energy required to deform the bonnet is gained form the kinetic energy produced by the pedestrians body. Resulting in, the kinetic energy being absorbed into the bonnet, reducing the injuries inflicted onto the persons head, but for this approach to work effectively it requires an area of clearance between the bonnet and the engine components. Most modern cars have very closely packed engine compartments and are almost completely filled. Enlargement or alterations to this area can have negative impacts on design characteristics, weight distribution and could increase aerodynamic drag, which in turn may increase fuel consumption. These fundamental disadvantages can be reduced by using active bonnets, which in the event of an accident lifts the rear portion of the bonnet to provide sufficient clearance between the engines.

The basis of the active bonnet lift system is to provide the driving force to allow the bonnet to pivot upwards. The driving force is produced with the use of springs, pyrotechnic cartridges, electro-mechanism, pneumatic or hydraulic units (Ševĉik et al., 2013). This must be incorporated into a suitable bonnet hinge which must function as a conventional hinge allowing the bonnet to be opened and closed upward and downward, but must also have the ability to be lifted at the rearwards portion during active system deployment (Evrard, 2011). Timing is the main technical challenge with only 60 ms from the initial contact with the front bumper, which after sensor processing leaving only a 25 – 50 ms time window (subject to sensor timing, car platform, etc) to lift the bonnet to the fully deployed position. However if the bonnet is lifted exceedingly fast, the generated bending moment may well be significant enough to buckle the bonnet under its own inertia. Therefore, between the bumper being impacted and the bonnet lifting there is a very narrow target range time to lift the bonnet. If the bonnet deploys during a none-pedestrian impact it is very desirable to have a system which can be repositioned, and allow the car occupant to drive away without the visibility being affected. To save the car owner repair costs, the actuator should be resettable by the vehicle user. Although the active approach is more complicated, due to the addition of sensors and actuators, it does however provide car designers with much more freedom

when it comes to the aerodynamics and packaging of engine components (Luntz and Johnson, 2015). The use of explosive (pyrotechnic) actuators are more commonly used, due to the compact size and light weight, but they are not reusable and the stored explosive energy can potentially be dangerous because it cannot be released prior to servicing. Also the high cost to the vehicle owner to replace actuators if false deployment has occurred.

Current investigation aims to focus on the stored energy approach by introducing alternative lifting methods, which is both reusable, resettable and potentially a cheaper alternative to the current designs used on the active bonnet systems.

5.1.1 CO_2 Cartridge Approach

The first proposed design will incorporate the use of compressed gas (CO_2) to provide the lifting force. This system features a separate pressurised gas cartridge which is rapidly discharged into the second cylinder illustrated in Figure 29, where a piston will be driven upwards to a pre-determined height. This lifting device will either be incorporated into the bonnet hinge or as a standalone system. The device is reset by evacuating the remaining gas from the lower chamber (below the piston). The device could be disarmed by removing the gas cylinder if required for safety or maintenance. The performance of the device can be tailored by altering the port size, size of gas cylinder and increasing/decreasing the pistons stroke length and bore size.

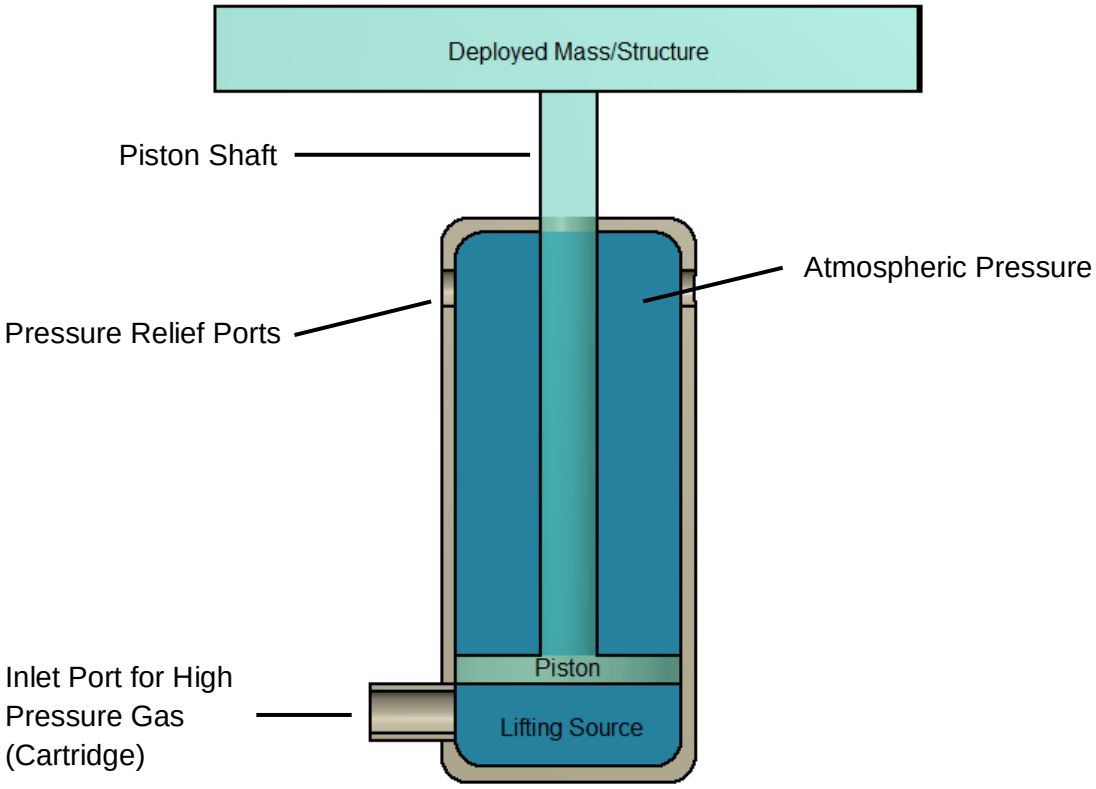

Figure 29. Lifting device architecture

Initially the device's stored energy is contained within a gas cylinder, when required the gas cartridge is pierced, thus releasing the pressured gas, basic operation is illustrated in Figure 30.

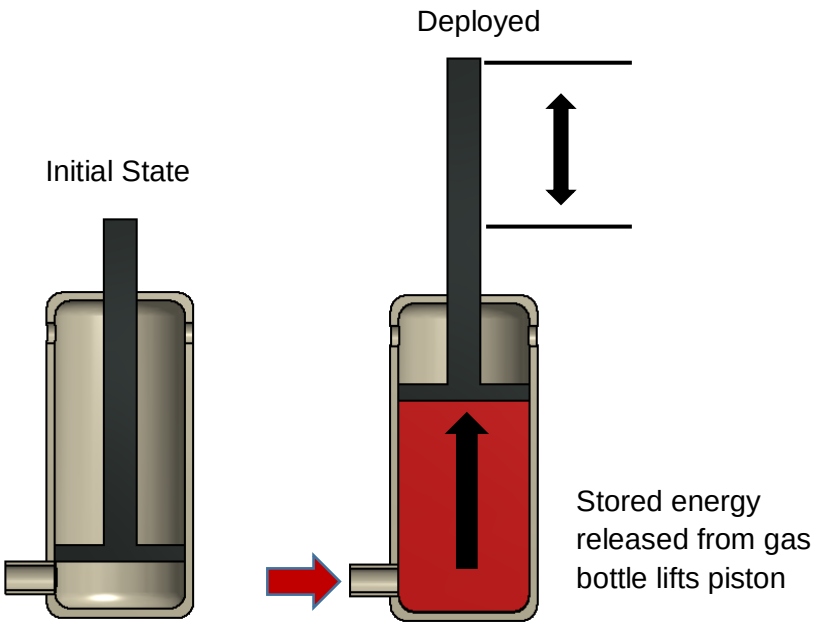

Figure 30. Illustration of gas lifting mechanism operational cycles

The use of CO_2 was opted for in this investigation due to the cost, and cartridges were easily obtainable and were available in a variety of sizes to scale up the experiments.

In the preliminary stage of the investigation a method for rapidly releasing the CO_2 from a 12g cartridge is explored. This will be done initially, by practically proving whether the concept is a viable method to peruse.

The first proposed design to release the CO_2

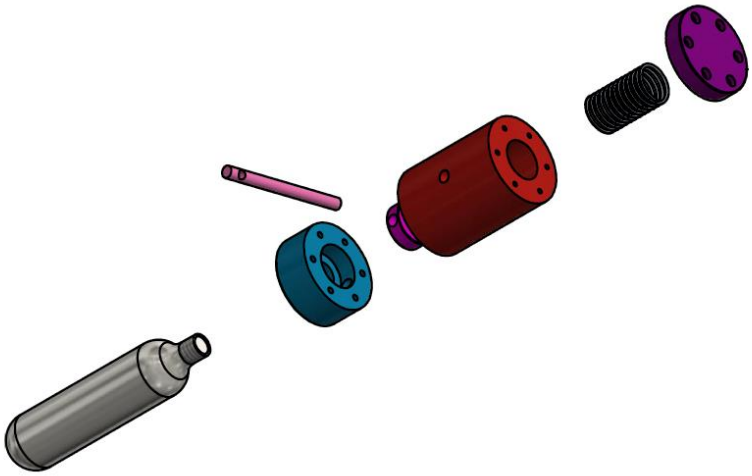

Figure 31. Exploded CAD view of CO2 piercer mechanism

The design featured a spring driven piercer, where upon the release mechanism being pulled, the piercer is driven into the CO_2 cartridge and the gas is released rapidly. The springs length was selected to generate enough force to create a sufficient hole in the CO_2 cartridge but was short enough that the piston would move freely just before impact, allowing the piston to be pushed back easily by the compressed gas, resulting in maximum gas flow.

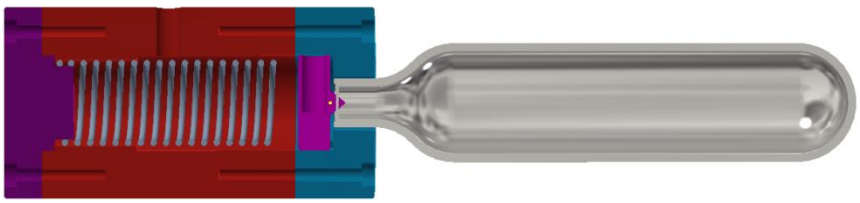

Figure 32. Internal view of CO_2 piercer mechanism

Testing the CO_2 discharge mechanism where Figure 33 shows the rapid discharge of the cartridge.

Figure 33. Operation of CO_2 release

Figure 34. Discharge cartridge showing pierced hole

The pierced orifice was very small and resulted in 2/3 releasing and the remainder freezing.

The next design incorporated a 12V DC solenoid valve where the CO_2 cartridge would be pre pierced and the line would be filled with CO_2 gas up until the solenoid valve seen in Figure 35. The advantage of this configuration is that there is a larger reservoir of pre-expanded liquid CO_2 to gas, whereas with the first iteration it was mainly in liquid sate within the cylinder. This should reduce the likelihood of the lines freezing as the overall pressure of the system has now also been reduced. To operate a simple 12V supply was connect with a switch. Once pressed the solenoid valve would open and the gas was rapidly released. In

comparison to the first design this improved the timing, and almost all of the CO_2 was discharged instantly, however freezing of the line did still occur and resulted in a small amount of dry ice remaining. The freezing is the result of reducing the working pressure, the difference in the high pressure inlet (cartridge) and the low pressure outlet (surrounding atmosphere), results in a temperature drop, this can be significant enough to cause the CO_2 to freeze and form dry ice (Harris Products Group, 2017) .The two main constraints of this design was that the lines used were of very small diameter, and the reservoir to pre-expand the CO_2 liquid into gas was limited consequently.

The second proposed design prototype to release the CO_2 using a solenoid controlled valve

Figure 35. Solenoid controlled CO_2 release mechanism

In summary, although the lifting capabilities of CO_2 were not fully investigated in this project, research by (Pappully et al., 2017) and (Luntz et al., 2007) suggests the use of pneumatic cylinders can potentially be a method of lifting a bonnet within the specified time frame. For this investigation CO_2 was deemed unsuitable as a viable alternative method of lifting the bonnet. This is because of a few fundamental disadvantages; due to the nature of being a gas it is affected by temperature changes and becomes less effective as the temperature is reduced (Pranay, 2014). However this could be overcome by the use of heating elements to control the temperature, but this not only increases complexity, it also increases the energy consumption and the mass of the overall system. The use of solenoid valves have also been investigated by (Luntz et al., 2007), who found that a large amount of actuation force is required to provide a sufficient opening of the valve, this is to overcome the pressure acting over a large surface area of the valve orifice to move the solenoid into the open position. As

a result many solenoids have difficulty meeting the time requirements needed. It is also very likely due to being a high pressure system that it may leak over time which will affect the performance and reliability. Although the cost of resetting is significantly reduced compared to pyrotechnic versions, after deployment the cartridge would still need to be renewed which cannot be done by the vehicle owner. And finally due to being a high pressure system there is also the inherit dangers associated with this. Overall even if CO_2 could provide the desired lifting time of the bonnet it would not be a viable replacement for the current pyrotechnic systems used.

5.1.2 Mechanical (Spring) Approach

Continuing the investigation the next stored energy approach is with the use of spring(s) to provide the lifting force for the bonnet.

Mercedes have developed an active bonnet system which is spring powered, fully resettable by the vehicle user and can raise the bonnet 50mm in a fraction of a second increasing the deformation area (Daimler AG, 2017).

Figure 36. Mercedes active bonnet deployed (Daimler AG, 2017)

Mercedes active bonnet raised 50mm after deployment where the rear portion is lifted; due to the bonnet being lifted this prevents a pedestrian head impact with the ridged wind-screen wiper shafts or engine components. The bonnets leading edge was also designed to yield due to tailored buckle characteristics of the inner panel. Also due to structural requirements it was still necessary to use a tubular brace for the bonnet, but this was repositioned to the front portion of the bonnet to insure that the rear of the bonnet offered the greatest

deformation potential. The joints between the bonnet and the front wings were regarded as too ridged, which were also altered by incorporating deformable grooves and perforations to further enhance the overall energy absorption characteristics (Daimler AG, 2017).

Testing Mercedes Active Bonnet hinge

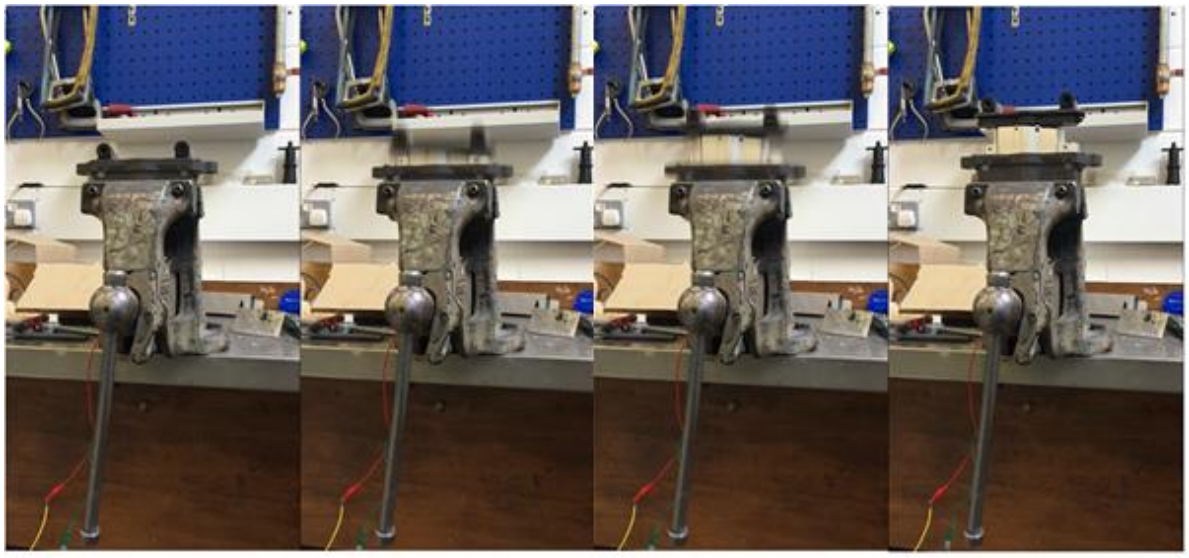

Figure 37. Mercedes active hinge in operation

The Mercedes system features a fully integrated bonnet hinge which is fixed to the top portion of the lifting mechanism but was removed for the tests.

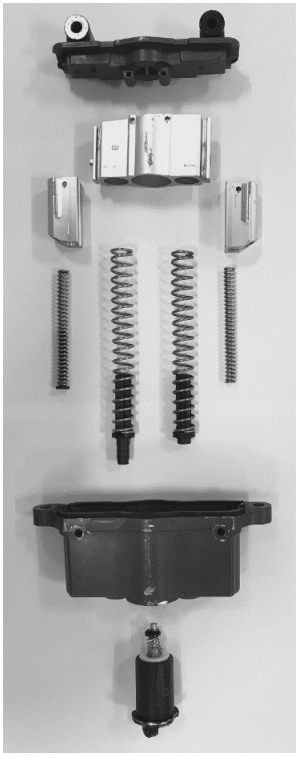

Figure 38. Mercedes active hinge disassembled during current research

A CAD model was prepared to study this system further

Operational characteristics of Mercedes active bonnet lifting system

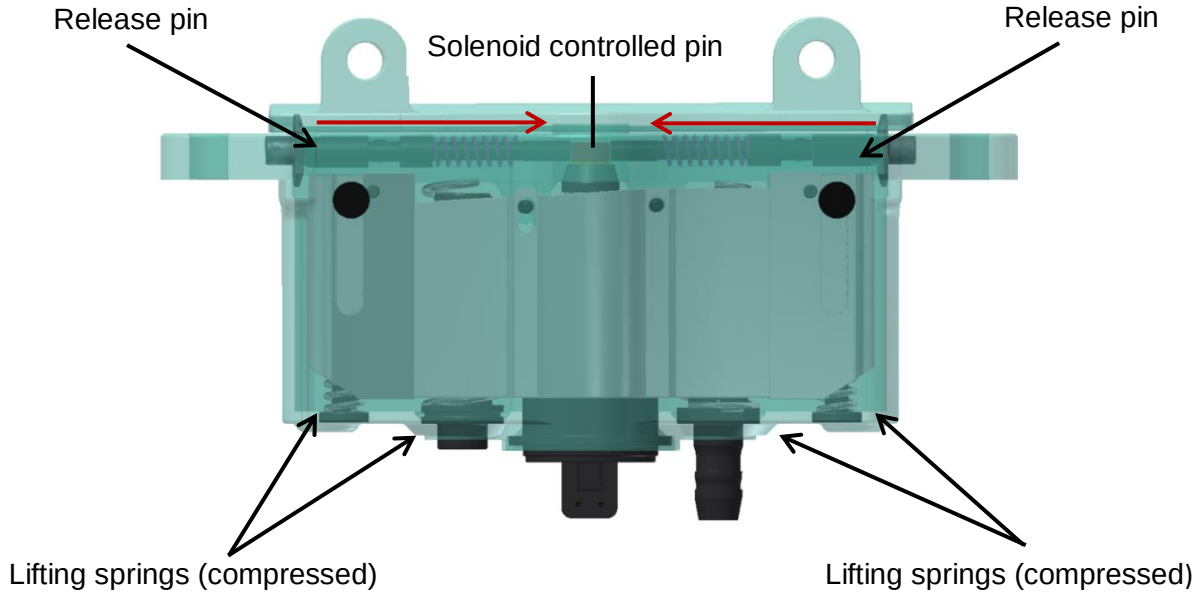

Figure 40. CAD of Mercedes Active Bonnet ready to fire state

The system consist of four springs which are compressed in parallel, where the outer two springs are much smaller, but with a much higher spring performance based on structural stiffness, these in conjunction with the middle two lifting springs provide necessary stored energy to lift the bonnet into position before the pedestrians head strikes the bonnet. The force of the springs is enough to overcome the release pins (arrowed), however to prevent this from happening an additional pin controlled by a linear solenoid is situated between the release pins.

To deploy the mechanism 12V DC signal is sent to the linear solenoid which retracts enough to allow the release pins to be pushed inwards, resulting in deployment initiation see Figure 41.

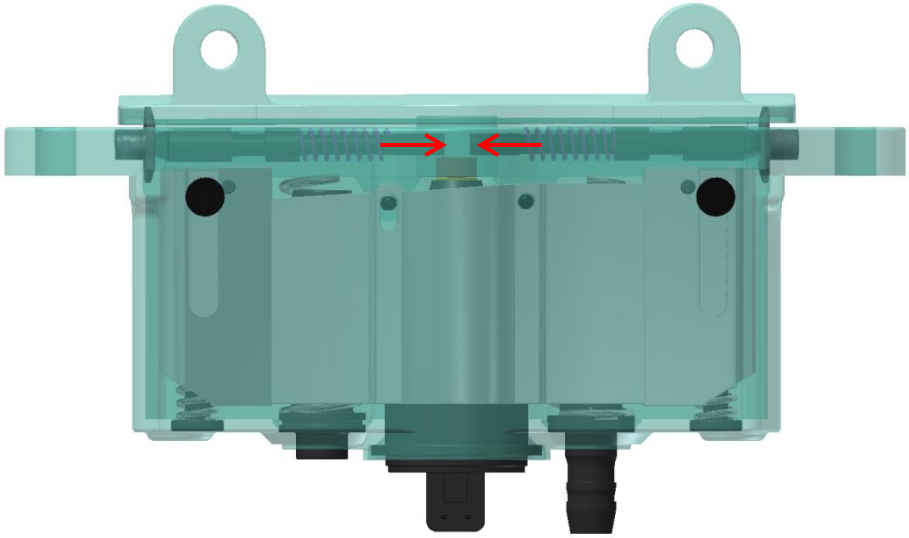

Figure 41. CAD of Mercedes Active Bonnet deployment initiated

Once fully deployed 4 locking pins stop the small spring housings close to half way, where the larger springs continue to lift till they are stopped by the second set of locking pins at this point the system is fully deployed and has reached the full lifting height.

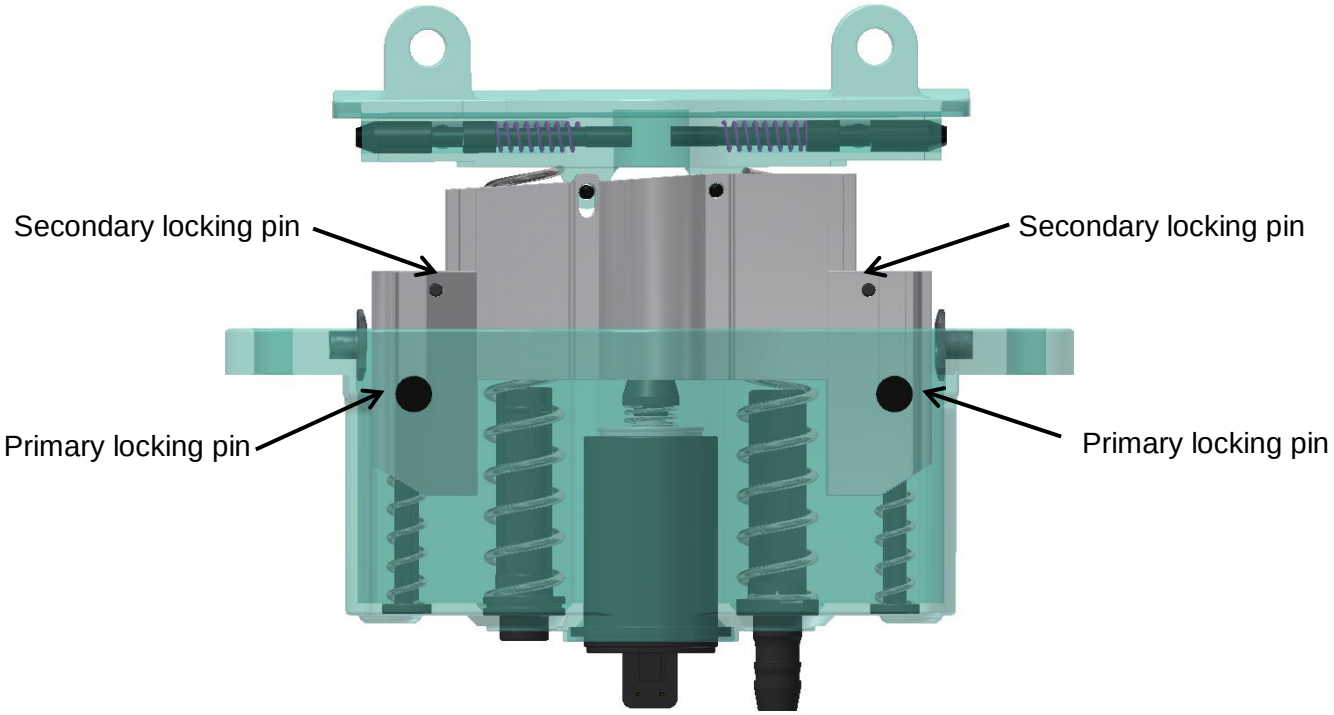

Figure 42. CAD of Mercedes Active Bonnet fully deployed

After testing the new Mercedes design with a total mass of 1.31 kg it was clear that this active hinge design was both reliable and very robust, the system was simple to reset and deployed very promptly. By reviewing Mercedes's design it was also clear that by using the stored energy approach with the use of springs, a bonnet system can be designed that both achieves the lift time required and can be re-set by the vehicle owner after deployment. This is a crucial advantage, because one of the main disadvantages with the current active systems is false deployment, which can cost the vehicle owner a tremendous amount of money to replace the pyrotechnic equivalents. However this system is resettable but, requires manual re-setting by the occupant, and also this system is designed that the whole bonnet hinge is lifted with the device, which reduces the flexibility of this system to be implemented onto other vehicles and the lifting mechanism cannot be used independently from the hinge as a result.

5.2 Proposal for New Design

5.2.1 Overview of the System

After investigating the stored energy approach the use of compressed gas was ruled out as an alternative and the use of stored spring energy was opted for. A new resettable spring powered lifting actuator will be designed.

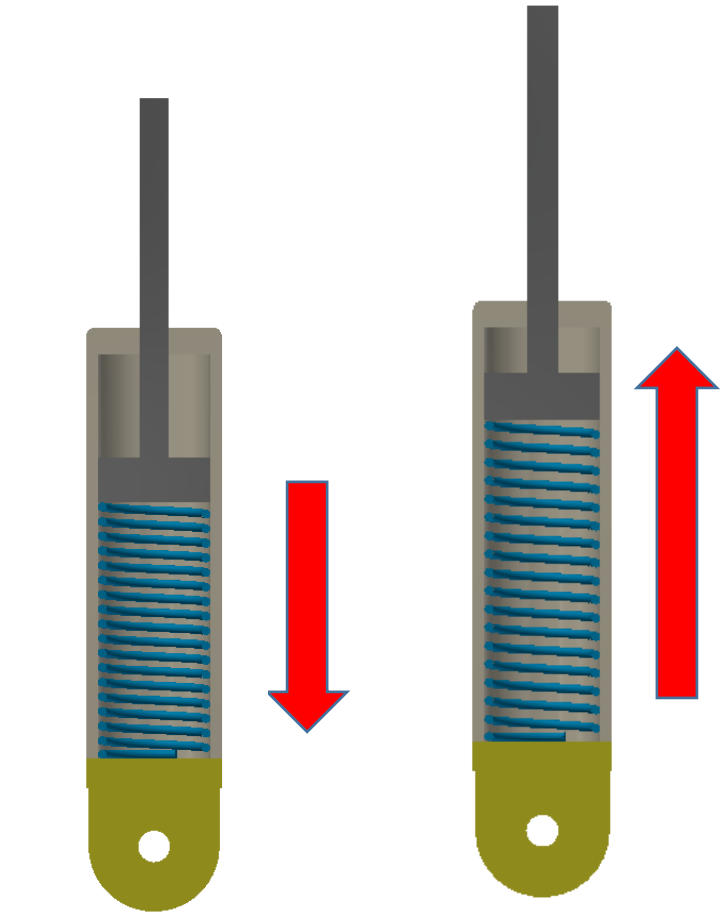

Figure 43. Illustration of spring design concept

The nominal state of the spring powered system is in the ready to fire state where the lift spring is compressed and held by a release mechanism, upon detection of a pedestrian impact a deployment signal releases the spring which in turn lifts the bonnet to the required distance within the selected time frame.

The first step to designing a spring powered system is spring selection; this is due to all other subsystems being affected by the lifting spring. The force created by the spring drives

all other design requirements, where the inner diameter of the spring must be large enough to house components for the release mechanism, while minimizing the overall exterior packaging size. The spring characteristics also determine the lift times and distance.

In order to calculate the required spring rate, a dynamic model of sprung mass oscillator Figure 44 has been derived by summing the moments from the spring force and weight of the bonnet and of the actuator around the pivot point. Using the dynamic displacement equation developed by (Luntz and Johnson, 2015)

Where I_h is half the rotational moment of inertia produced by the bonnet, α is the rotational acceleration, L is the distance between the pivot and lifting device mounting point, k is the spring stiffness, h is the required lift distance, m_h is half the mass of a bonnet, y is the current height of the rear portion of the bonnet, g is gravity, and m_a is the moving mass the actuator and associated mounting hardware. Half the inertia and bonnet mass was used because two devices would be used for the vehicle, therefore the requirements for each actuator can be halved. By solving the differential equation it produces the dynamic displacement relation (Luntz and Johnson, 2015).

$$y(t)=\frac{\left(2hk-gm_h-2gm_a-2hk\cos\left(\sqrt{k/I_h}Lt\right)+gm_h\cos\left(\sqrt{k/I_h}Lt\right)+2gm_a\cos\left(\sqrt{k/I_h}Lt\right)\right)}{2k} \quad \text{Equation 5}$$

Table 6. Bonnet dynamic modelling parameters modified from (Luntz and Johnson, 2015)

Parameter	Value
Half Bonnet Inertia (I_h)	2 kg m^2
Pivot Hinge Distance (L)	1 m
Bonnet Mass (m)	11 kg
Actuator Mass (m_a)	0.5 kg
Lift Distance (h)	50 mm
Lift Time (t)	25 ms

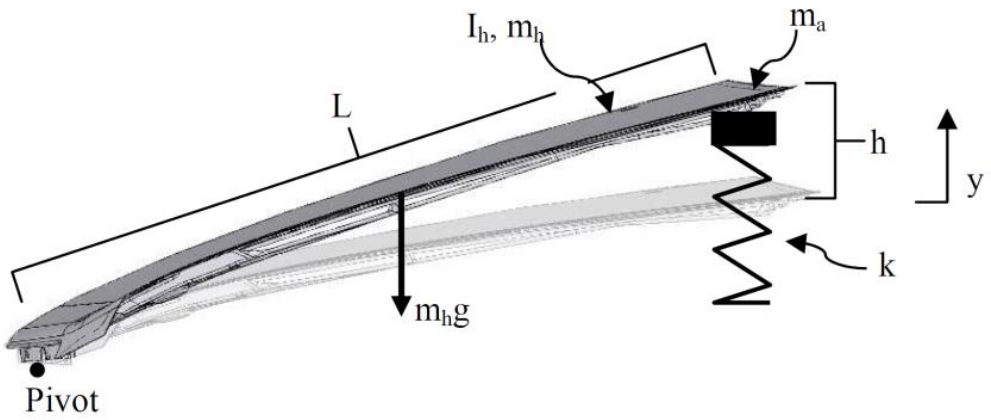

Figure 44. Dynamic bonnet model (Luntz and Johnson, 2015)

Using (Luntz & Johnson, 2015) dynamic displacement relation, Equation 5, to determine the required spring rate using the mid-sized sedan (Luntz & Johnson, 2015) case study in Table 6, where the lift distance was altered to 50 mm and the moving mass the actuator and associated mounting hardware was reduced to 0.5 kg. Solving Equation 3 iteratively to three significant figures, a value of 5.1 N/mm spring rate was found, however assuming losses from friction and other factors which reduce the spring rate by 10% as in the method used by (Luntz & Johnson, 2015), a spring rate of at least 5.60395 N/mm should be used. When compressed 50 mm the spring would produce a force of 280 N. This parameter was used to design and analyse the lifting mechanism.

In order to successfully utilise the stored energy generated from the spring a suitable release mechanism is required. The first design will incorporate the cylinder, where the two location holes allow the release pins to rest inside, resulting in the mechanism being in the ready to deploy state.

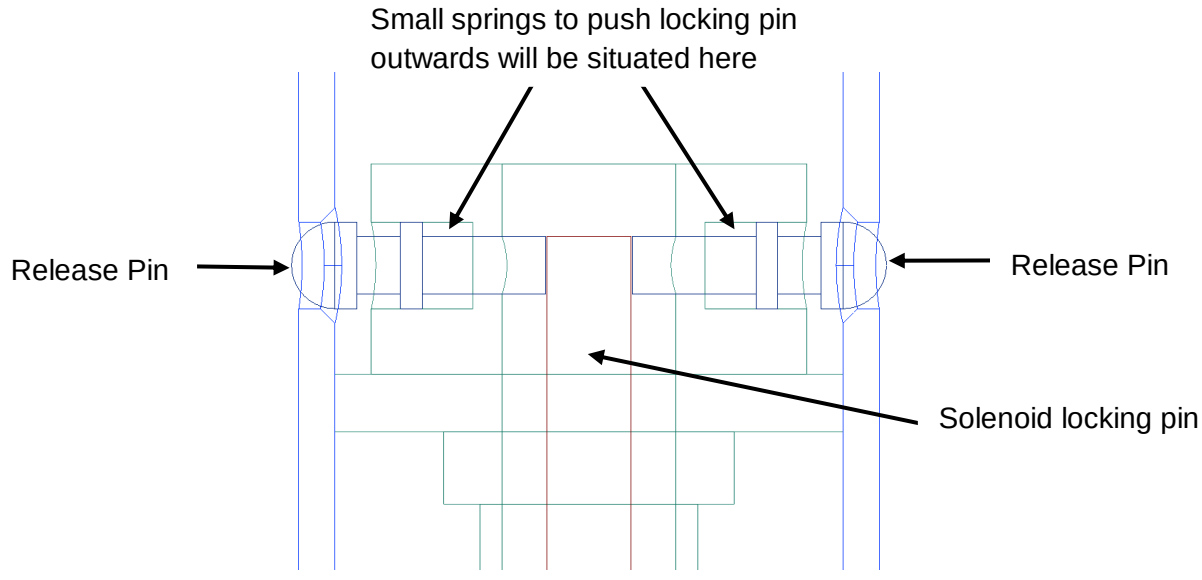

Figure 45A. Preliminary release mechanism design overview and deployment sequence

In order to keep the system in the ready to fire state a solenoid controlled pin is placed between the locking pins to prevent them from being pushed inwards by the overwhelming force generated by the spring.

Once the solenoid controlled pin is drawn downwards by a powerful electromagnet. The release pins are now as a result allowed to freely move into the centre. Resulting in deployment initiation illustrated in Figure 45B.

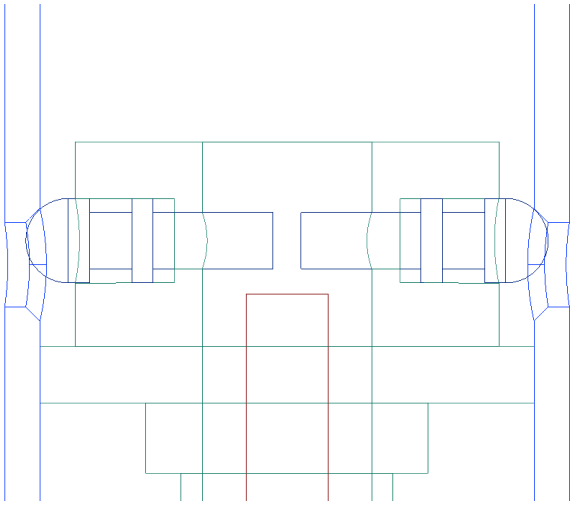

B. Preliminary release mechanism initiated

Finally, once the release pins have fully travelled to the centre, allowing the piston to move freely upwards thus deploying the system.

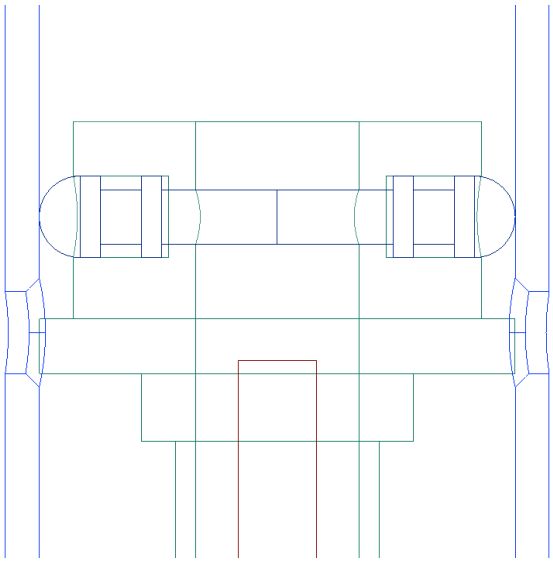

C. Preliminary release mechanism released

After reviewing the first design iteration it was clear from a conceptual perspective it could prove plausible. However further alterations/improvements are required, the areas which require further development include; the release pins and location holes.

Location Holes

If upon deployment any rotation of the piston which contains the release pins has occurred, resetting the system will be problematic.

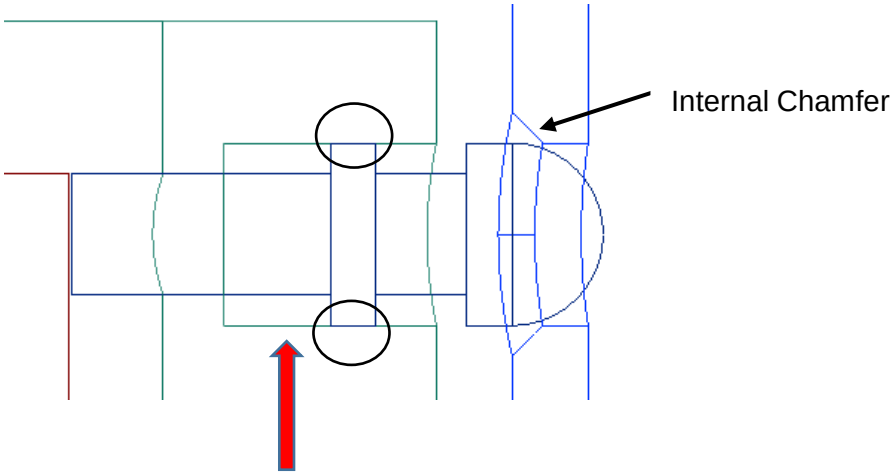

Figure 46. Preliminary release mechanism locking pin

5.2.2 Release System

The current configuration of the release pin requires further improvement the areas circled are likely to fail due to the potentially high stress concentration by having such a small surface area, upwards deflection of the release pin is a likely result.

In summary, in order to further develop the release mechanism the design must be amended to be none orientation specific so that in the event of rotation of the piston this does not affect the reset-ability of the lifting device. Also from a manufacturing perspective it will also be very difficult to create the internal chamfers on the location holes. The release pin configuration will also require further development to be more robust and prevent pin failure. Additionally, as the piston travels upwards the release pins faces will slide against the internal wall of the cylinder which may cause ware on the internal wall as well as the release pin head which not only can cause premature ware, the friction is also increased which can influence the performance and longevity of the device.

To address the issues experienced in the initial design, a new iteration of the release mechanism is created.

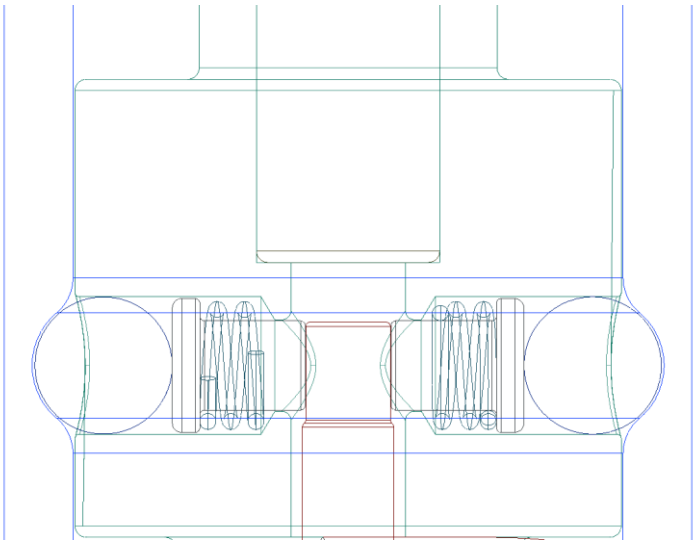

Figure 47. Final proposed design for release mechanism

The release pins were modified and a ball bearing is used instead, the advantage of using ball bearings is that they are very hard wearing, and as the piston travels upwards the ball bearings can rotate which reduces the friction generated as it passes over the cylinders internal wall, and the potential deflection experienced by the first release pin iteration is also mitigated.

In order to achieve none orientation specific reset-ability an internal fillet is created around the whole circumference of the cylinder to allow resetting in any orientation.

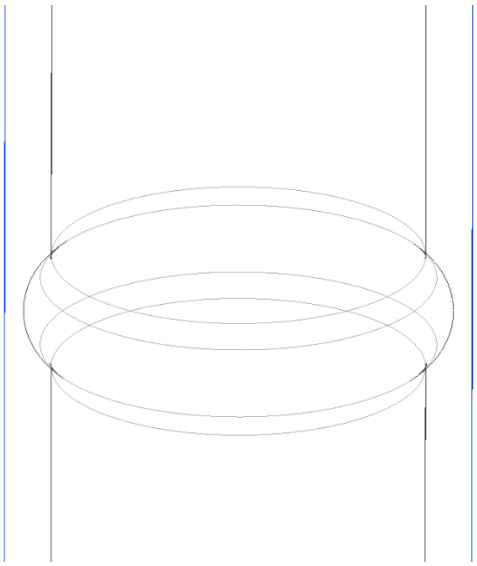

Figure 48. Internal fillet illustration

In order to assess the feasibility of the use of internal fillets a small sample was manufactured to illustrate it was possible to manufacture.

Figure 49. Internal fillet manufactured cross-sectional view

To release this system the linear solenoid pulls the release pin downwards allowing the secondary pins to be pushed inwards along with the ball bearings causing the piston to be forced upwards by the spring force.

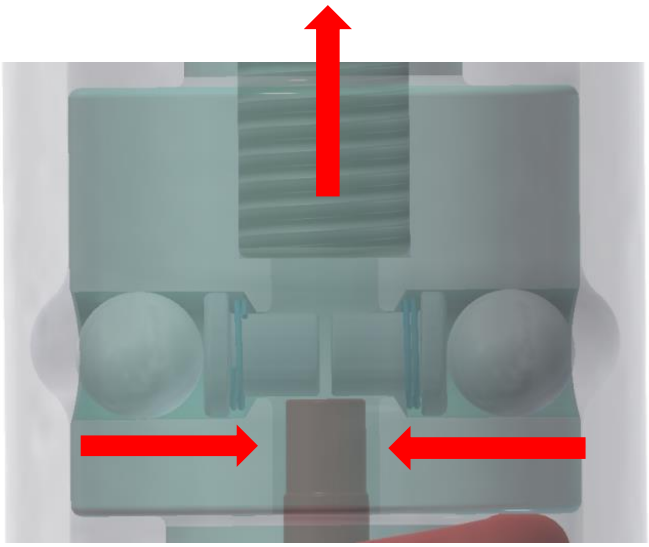

Figure 50. Close-up view of release mechanism following solenoid activation

To reset the device the spring is compressed 50 mm and the ball bearings will rest in the internal fillet which is located around the whole circumference of the cylinder's internal wall. This system is not orientation dependant, due to the fillet being around the whole circumference and being cylindrical is much more space friendly in design. Although the design cannot automatically be reset, it is intended to be incorporated into a bonnet hinge design where the bonnet provides enough leverage to be easily resettable.

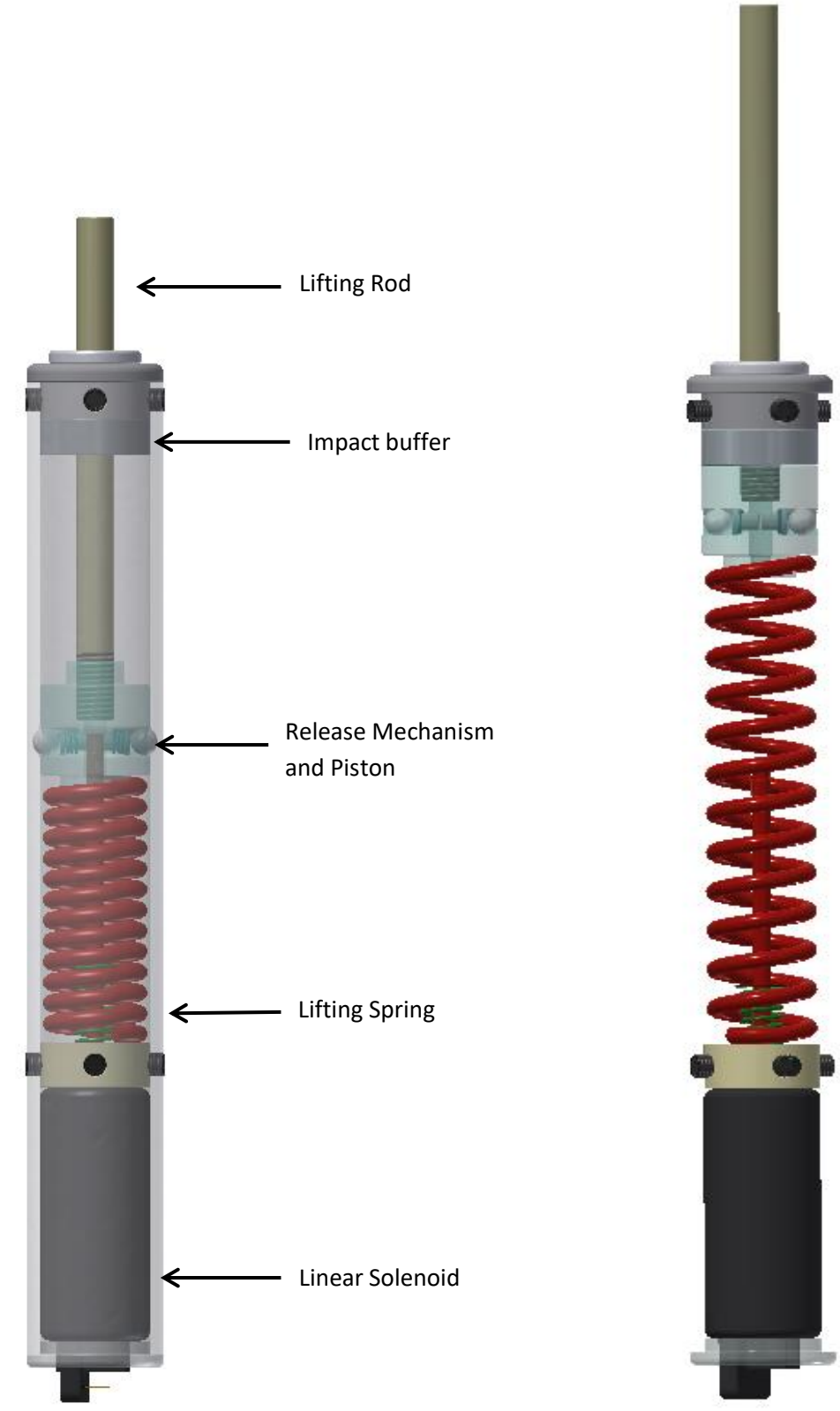

Figure 51. Proposed design for bonnet lifting mechanism

5.2.3 Advantage of new design compared to existing patents

In this section prior art will be reviewed to determine the key designs benefits when compared to the existing designs.

The presented inventions in Appendix C are all relate to lifting devices which can be fitted to a vehicle to raise the bonnet in the event of an accident involving a pedestrian.

In order to assess the designs five key areas will be reviewed: Performance, Resetability, Design Complexity, Placement Flexibility and Mass.

Performance – Although the performance of the prior art has not been published in the public domain, research by Luntz and Johnson 2015 suggests that the use of spring energy can in fact achieve the performance criteria, being further proven by the currently used Mercedes active hinge. Therefore all the inventions presented in Appendix C which are all spring powered, it can be assumed with a high degree of confidence that all these systems can or have the potential to fulfil the performance criteria of full bonnet deployments prior to the pedestrian head impact occurring.

Resetability – All designs features a mechanical locking device combined with an electromagnetic or solenoid component to activate the system by releasing the mechanical locking mechanism, but allows the system to be returned to its pre-deployed state due to the release mechanism having the ability to be retracted or reengaged resulting in a reusable system. Invention 1&2 have been designed in such a way that the bonnet hinge is fixed and fully incorporated onto the main body of the lifting system and the resetting link/mechanism is incorporated into the bonnet hinge. Whereas invention 3&4 and the proposed design all perform in a similar fashion but have been developed into a cylindrical format, and the actuator is placed independently form the hinge and all systems use the bonnet to provide enough leverage to allow the powerful spring(s) to be compressed with minimal effort.

Design complexity – From a visual evaluation invention 1&2 would appear to have the most complex release mechanisms, consisting of a number of levers to create the release system. Where invention 3&4 have far less moving components and have opted for a combination of (spherical objects) used in conjunction with a type of fillet where the sphere can plunge into resulting in the spring being allowed to move, thus releasing its stored energy. In the application of vehicles it would be advantageous to have a reduced number of moving components, which not only reduces the complexity, but can potentially result in a more robust design overall. The proposed design works in a very similar fashion to invention 4 seen in Figure 52, but the deployment mechanism has been approached differently and further simplified. Where it can be seen that the key difference being that the solenoid in Saab's design pushes part 27, 29 upwards by a solenoid controlled pin, this configuration therefore would require a powerful solenoid as it not only has to overcome the horizontal force component which is transition through part 27 by the main lifting spring, but also the vertical force generated by part 29. Whereas the proposed design only requires the solenoid to retract in order to deploy, this offers the added advantage of being able to use a lower powered solenoid. Additionally from a manufacturing perspective the proposed designs cylinder and internal fillet can be made in one section whereas invention 4 is made in two sections and the fillet has produced an external profile.

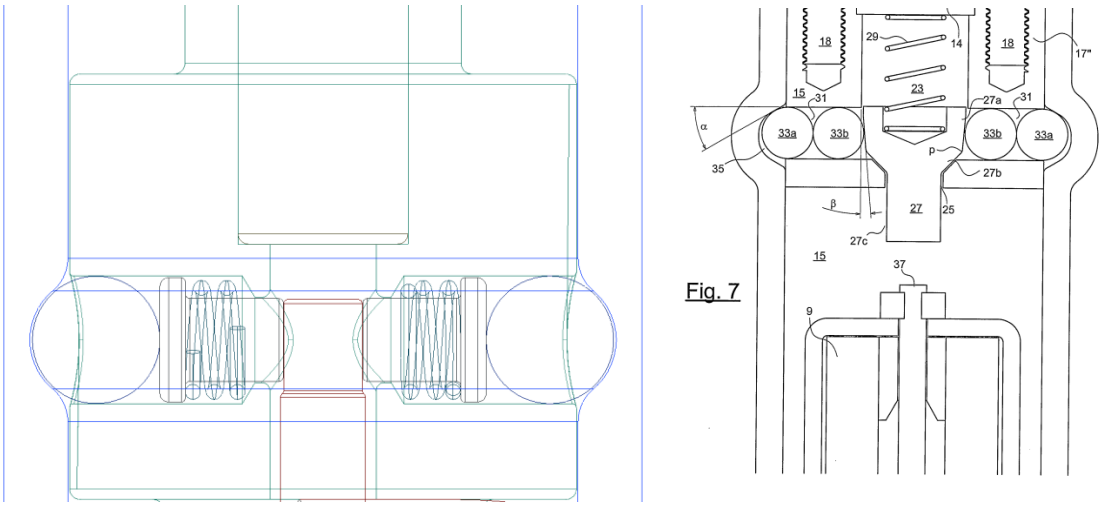

Figure 52. Comparison of proposed design (left) and Saab's release mechanism (right)

Placement Flexibility – Invention 1&2 and the Mercedes systems have been configured in such a way that the bonnet hinge is integrated onto the lifting actuator, this arrangement poses some restrictions on placement within the engine bay due to the primary function is to operate as a hinge to allow pivoting of the bonnet during opening and closing procedures.

Whereas invention 3&4 and the proposed offer a higher degree of flexibility when positioning the actuator as it can be either be incorporated into the bonnet hinge or be placed independently form the hinge offering less placement restrictions.

Mass – although the mass of the prior art is unknown due to limited information in the public domain a mass comparison of the currently used Mercedes active bonnet actuator and the proposed design can be made.

Proposed Models Mass based on CAD Model: 0.9885 kg

Mercedes actuator design: 1.31 kg

Percentage difference: 24.54 %

5.3 Finite Element Analysis of Proposed Design

Finite element Analysis (FEA) is generally implemented in most engineering disciplines. This technique is frequently used as a replacement for conventional experimental testing methods. The procedure is focused on the principle that an estimated solution to complicated engineering problem can be achieved by segmenting the components/structure into much smaller and easier managed (finite) elements. The Finite Element Model (FEM) is evaluated with fundamentally far more precision than that of conventional hand analysis. This is largely due to the fact the shape, loads applied, and constraints, along with material property characteristics can be defined with far more accuracy than of that used in conventional hand calculations (HERA Innovation in Metals, 2014).

The FEA method consists of three stages:

Pre-processing, this is where the finite element mesh of the geometry is created as well as boundary conditions, material properties and loads are applied to model.

Solution, the software obtains the governing matrix equations (displacement x stiffness = load), from the model and solves for strains, stresses and displacements in the case for implicit code applications. Otherwise, explicit codes can be implemented in high stain rate engineering problems.

Post-processing, this is where the results are obtained usually in the form of deformed shapes or contour plots etc. This is then used to assess the validity of the solution.

Firstly before any FEA simulation can be created, a suitable geometry must be generated for this investigation. A 3D CAD model was generated using Autodesk Inventor. In this investigation three models will be created and simplified in order to assess the final design's kinematics and identify high stress regions. In order to create a suitable FEA model the geometry must first be modified to avoid mesh penetration on areas where a "close fit" applies, this is because the mesh penetrations oppose parts sliding or moving between the two regions in contact, and also causes areas of high stress concentration at these penetrating points which produce none-supposed plastic/elastic deformations (Honarpardaz, 2011). Therefore, the geometry was reduced for this investigation and a spacing of 0.2 mm and appropriate boundary conditions were used to alleviate this issue. To solve these models ANSYS Explicit Dynamics will be used to determine the dynamic response and stress distribution of each model.

Here is an example where mesh penetration is likely to occur, for example the release mechanism. In this scenario the geometry was modified to allow for a 0.2 mm clearance to prevent penetration issues.

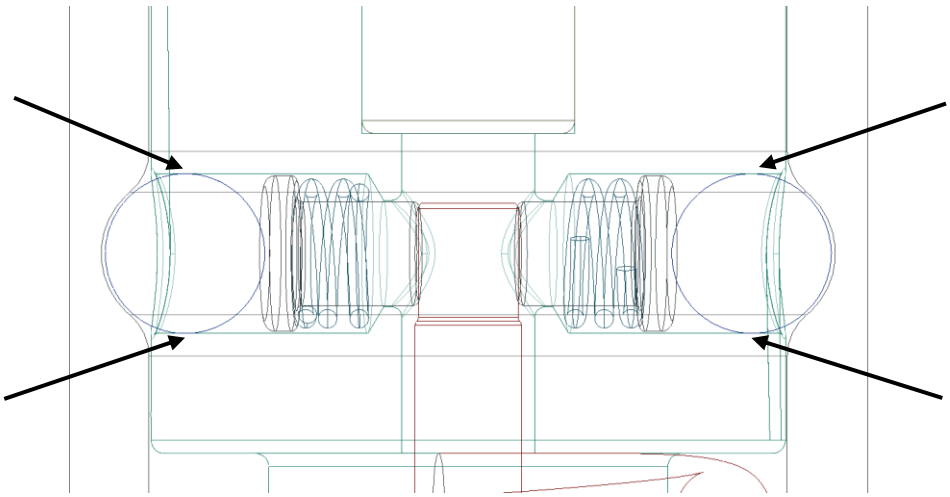

Figure 53. Illustration of release mechanism potential mesh penetration

In order to assess the structural integrity and performance of the proposed design three key areas will be assessed for this investigation. The Von-Mises stress is considered to assess the service stress acting on the specific components. By evaluating the stress distribution

this will identify areas of the model which are experiencing high stress levels. The stress distribution can be very important to optimise the design. By identifying areas with high stress this can be used to predict the locations where failure is a likely, to allow for preventative measures to increase the reliability and lifespan of the design (Syed, 2009).

The first area to be investigated is the release mechanism; a modified CAD model is generated to comply with possible mesh penetration. For this simulation the objective was to assess the kinematics and forces generated during the release of the mechanism. The solenoid controlled release pin was neglected, and the simulation was set-up to only capture the events following an assumed perfect operation of the solenoid controlled release pin.

Figure 54. Modified CAD of release mechanism design for FEA

After generating the final CAD design, the first step of pre-processing is to generate appropriate mesh and evaluate the mesh quality

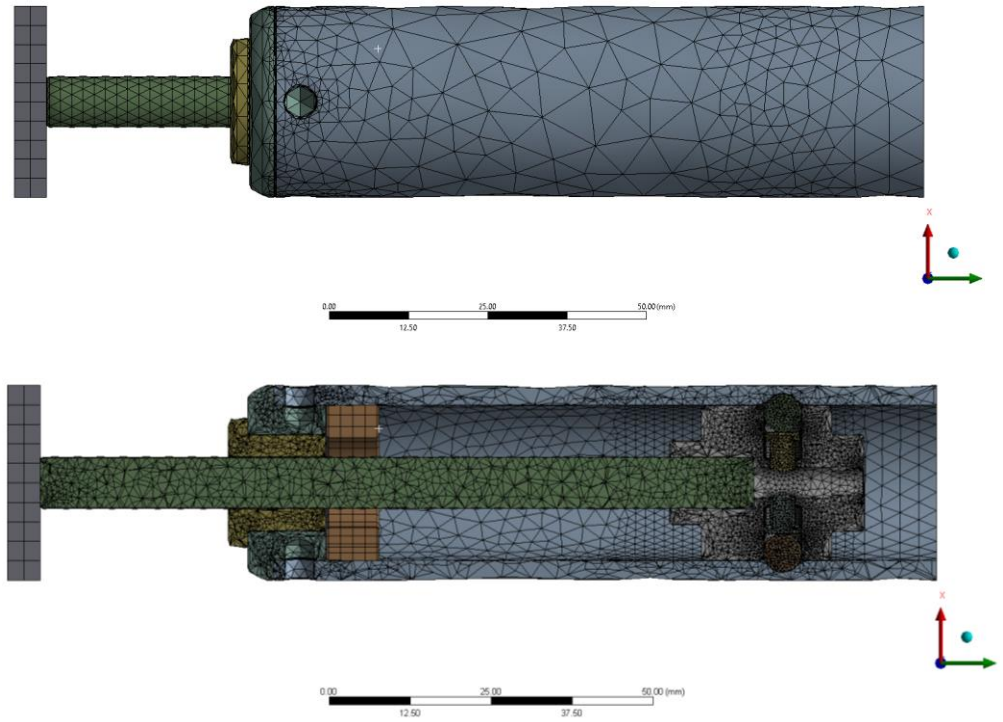

Figure 55. Side and Cross sectional view of release mechanism meshed

For Element Quality, Skewness, Aspect Ratio inspection tables prior to simulation: refer to Appendix 1 for release mechanism deployed.

To represent the active mass required to be lifted by the bonnet 2.75 kg was deemed appropriate to simulate the mass acting again the actuator. This value was derived from (Luntz and Johnson, 2015) where the total mass of the bonnet was 11kg.

Assignment	Stainless Steel
Bounding Box	
Properties	
Volume	4500. mm³
Mass	2.75 kg
Centroid X	2.6948e-016 mm
Centroid Y	96.112 mm
Centroid Z	2.7622e-015 mm
Moment of Inertia Ip1	211.98 kg·mm²
Moment of Inertia Ip2	412.5 kg·mm²
Moment of Inertia Ip3	211.98 kg·mm²

Figure 56 Mass addition to represent bonnet mass

The next pre-processing stages are to define specific boundary conditions to the model. The main type of loading used for FEA includes pressure, force and temperature. These are typically applied to edges, nodes or elements. The way in which the model is constrained can drastically affect the results outcome and requires special attention. Having under or over constrained models can give stress values which are inaccurate and make the data gathered inadequate (Value Design Consulting, 2016).

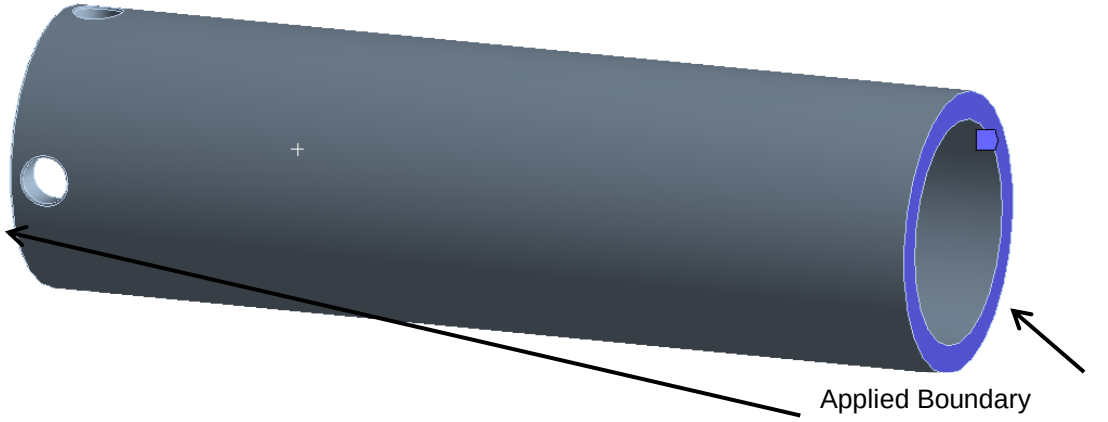

Figure 57. Outer cylinder with applied boundary condition i

The external cylinder was constrained on both faces (indicated in blue); this was to prevent the cylinder following the movement of the release mechanism during simulation. This boundary condition was deemed most appropriate because, the outer housing will be fixed to the vehicles chassis.

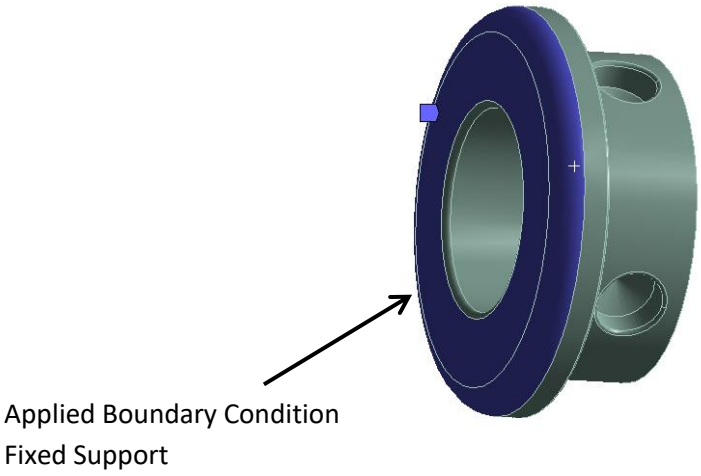

Figure 58 Top Cap with applied boundary condition

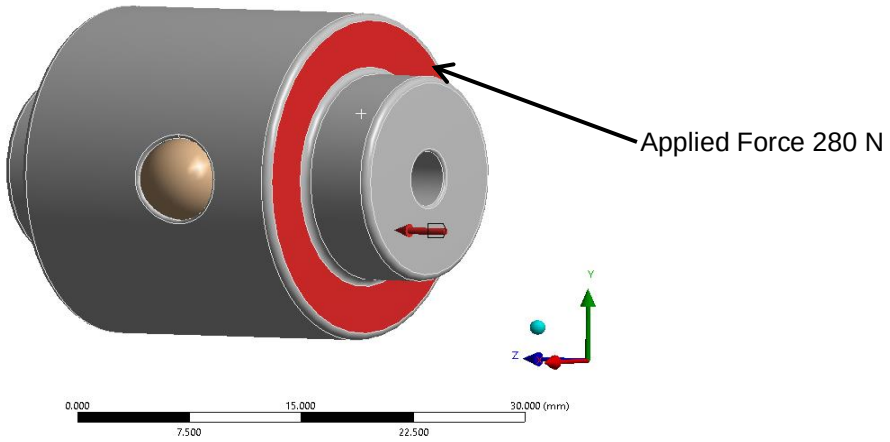

Figure 59. Applying 280 N spring force to the base of piston

A force of 280 N was applied simulating the force generated by the spring in accordance to the calculated value from Equation 3, and was applied to the pistons face (indicated in red) in the Z direction only.

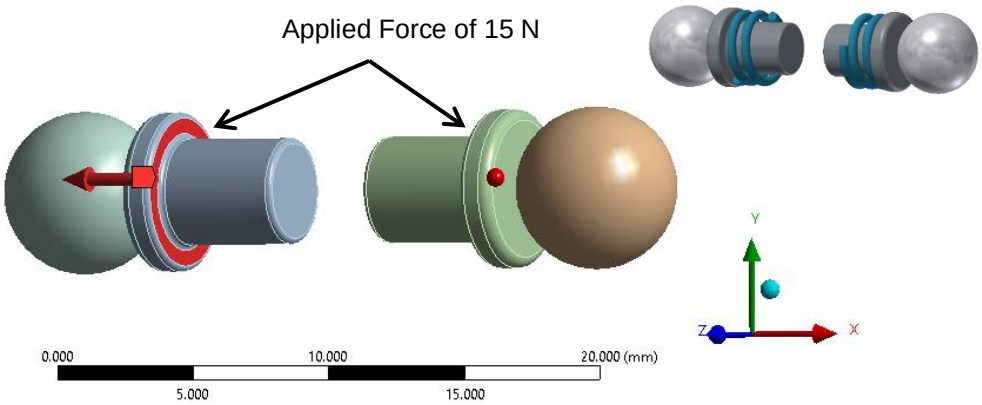

Figure 60. Release pins with 15 N applied to represent release pin springs

A force of 15 N was applied to each release pin in order to simulate the force exerted on the pins by the springs. A value of 15 N was deemed appropriate due to the function of the spring is only to insure that the ball bearings and the pins upon resetting are pushed into the internal filled to allow enough clearance for the solenoid controlled pin to fit between the pins.

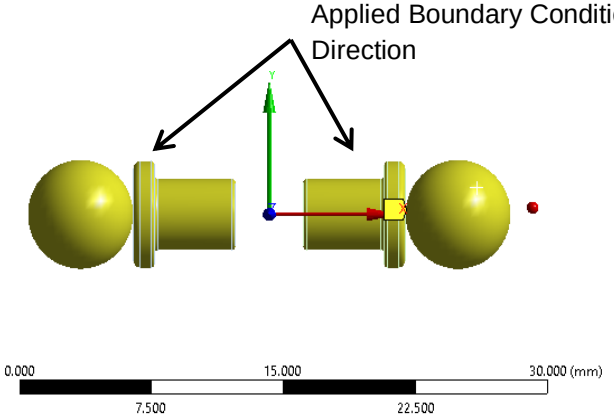

Figure 61. Displacement in the X and Y direction of release pins and ball bearings

In order to simulate the release mechanism, a pre described displacement was assigned to the release pins and the ball bearings. This was to allow movement in the X and Y plane to allow the pins and ball bearings to be pushed inwards as well as move upwards upon simulation once the force of the lifting spring over comes the resistance produced by the springs pushing the release pins outwards into the internal fillet.

The final phase of the model preparation was to assign body interactions between the various components to allow for representative body interactions during the dynamic simulation. In the initial simulation the body interactions will be frictionless followed with a simulation with added friction to more representatively model the true interactions to insure deployment time is maintained.

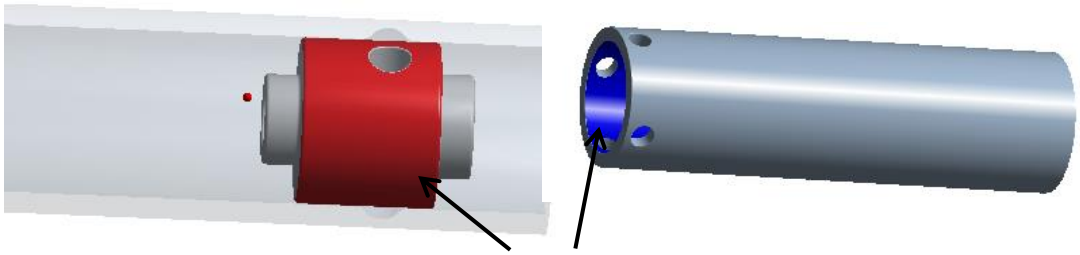

Figure 62 Assigned body interaction between piston and cylinder

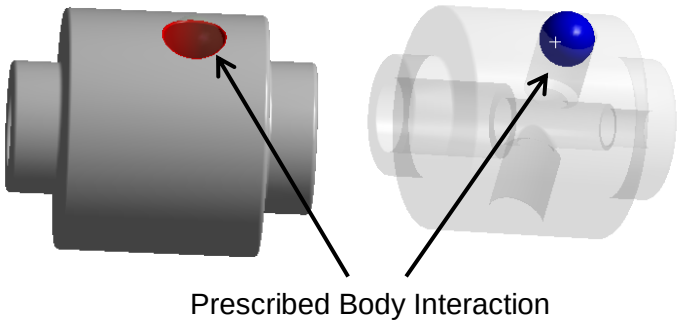

Figure 63 Assigned body interaction between piston and ball bearings

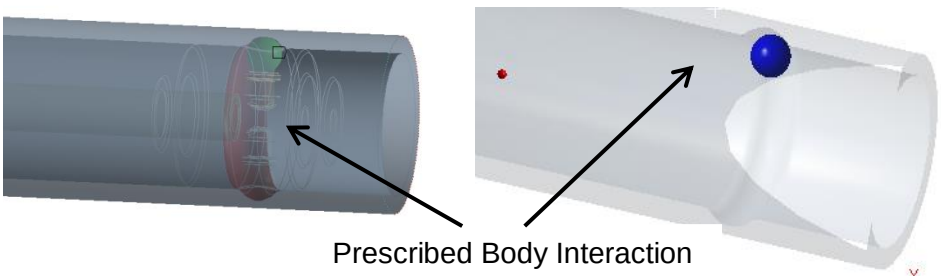

Figure 64 Assigned body interaction between internal fillet and ball bearing

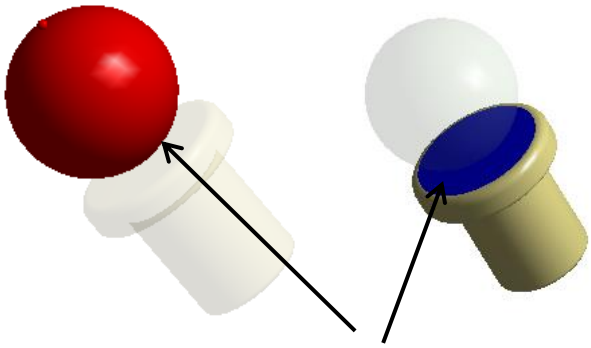

Figure 65 Assigned body interaction between release pin and ball bearing

Once all the boundary conditions were applied the model was simulated. The models cross-section is utilised to allow the internal interactions to be observed.

The first model with be simulated with no friction.

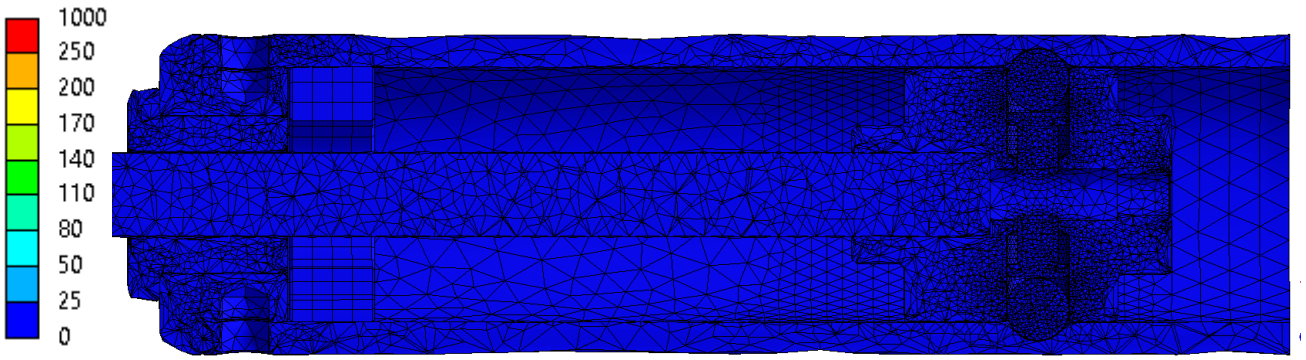

Figure 66. Simulated model of release mechanism deployed in initial state prior to loading

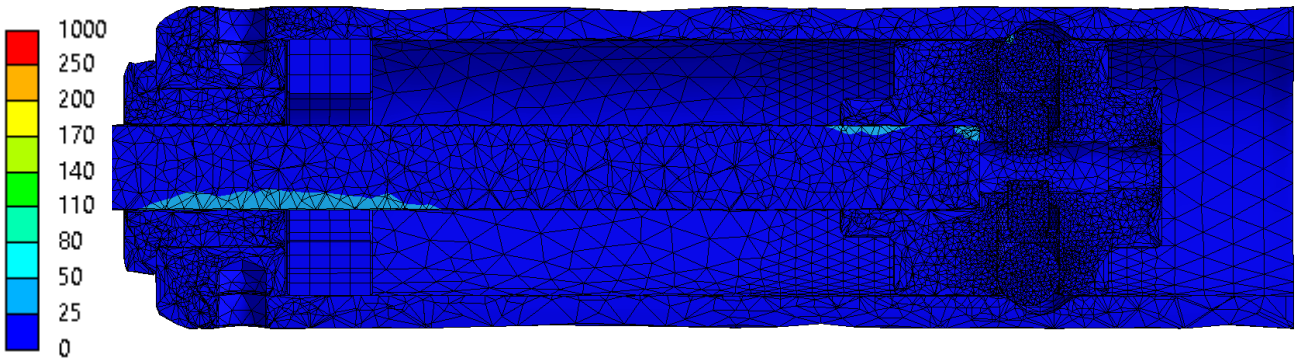

Figure 67 Von-Mises stress of release mechanism deployed at 0.0052 seconds

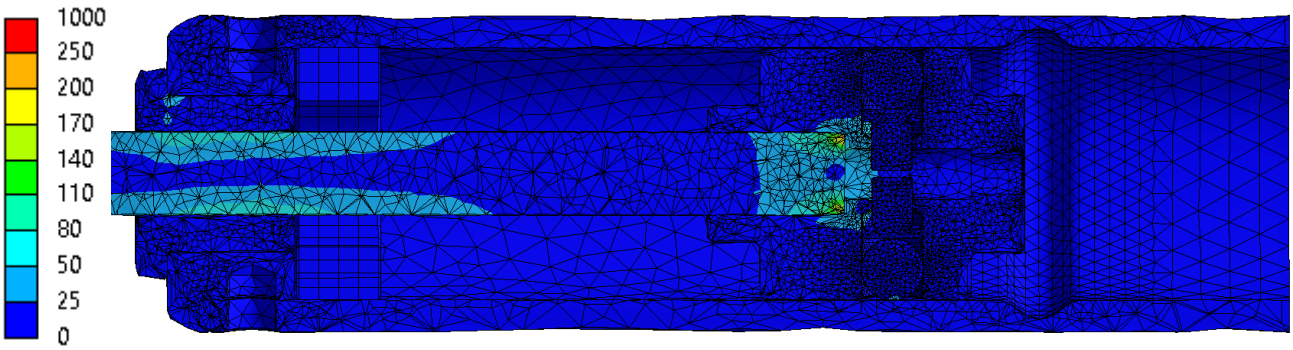

Figure 68 Von-Mises stress of release mechanism deployed at 0.018 seconds

To verify the deployment time has been achieved a stress probe was added to the impact buffer to identify peak stress as an indication of when full deployment has been reached.

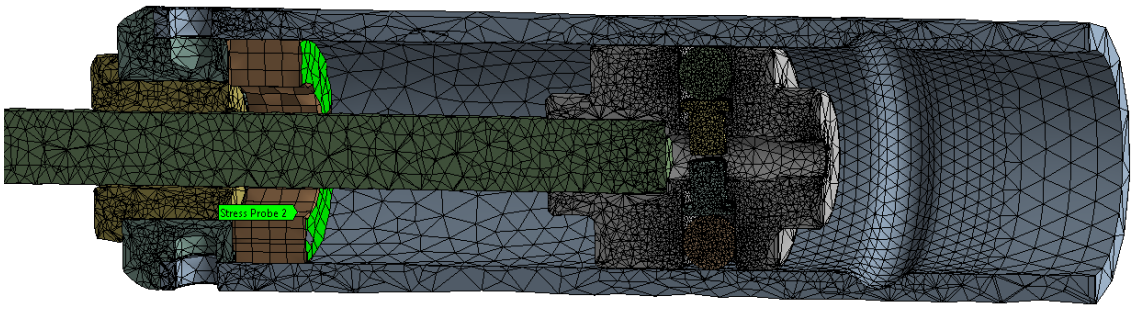

Figure 69 Stress probe for deployment verification

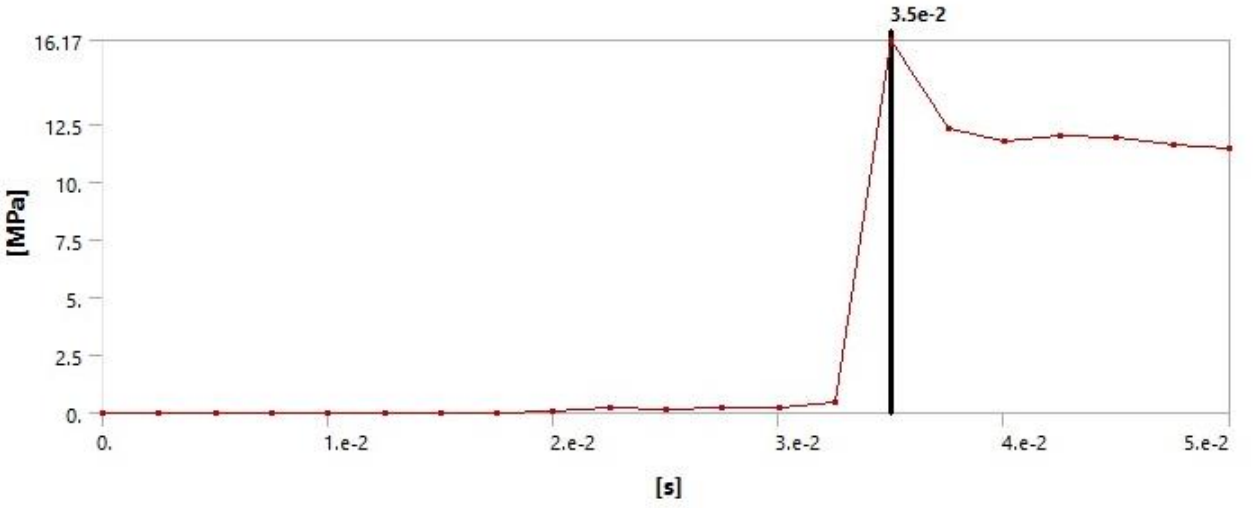

Graph 2 Zero friction deployment verified with stress probe

Investigation with the addition of 0.1 friction to verify deployment time, the following results presented have been produced following the same boundary conditions as the previous model.

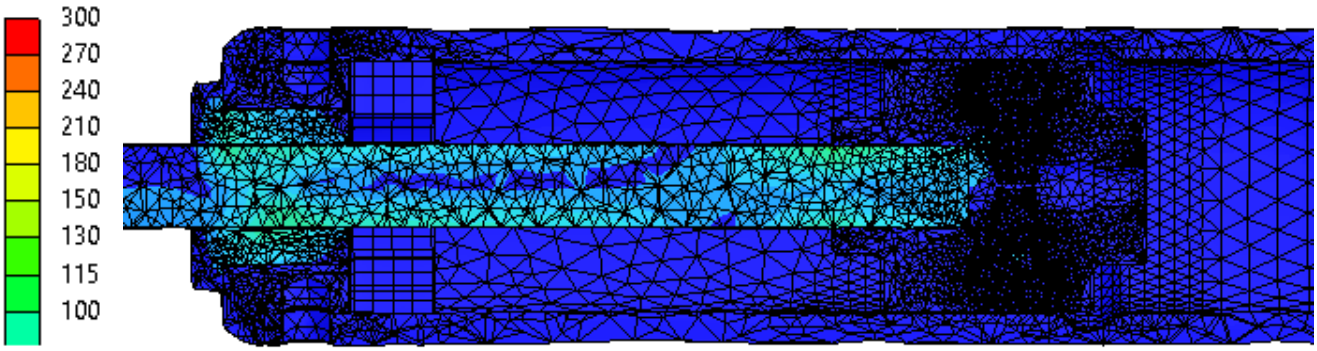

Figure 70 Von-Mises stress of release mechanism deployed at 0.0125 seconds

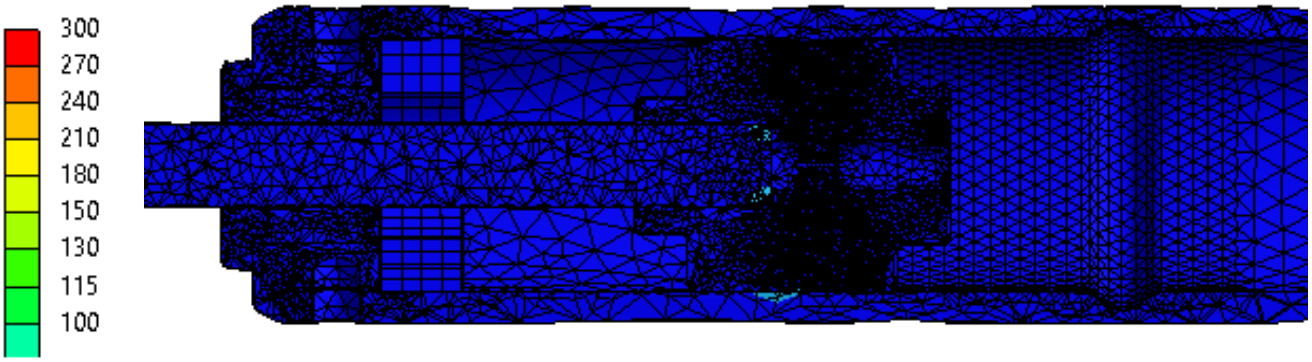

Figure 71 Von-Mises stress of release mechanism deployed at 0.025 seconds

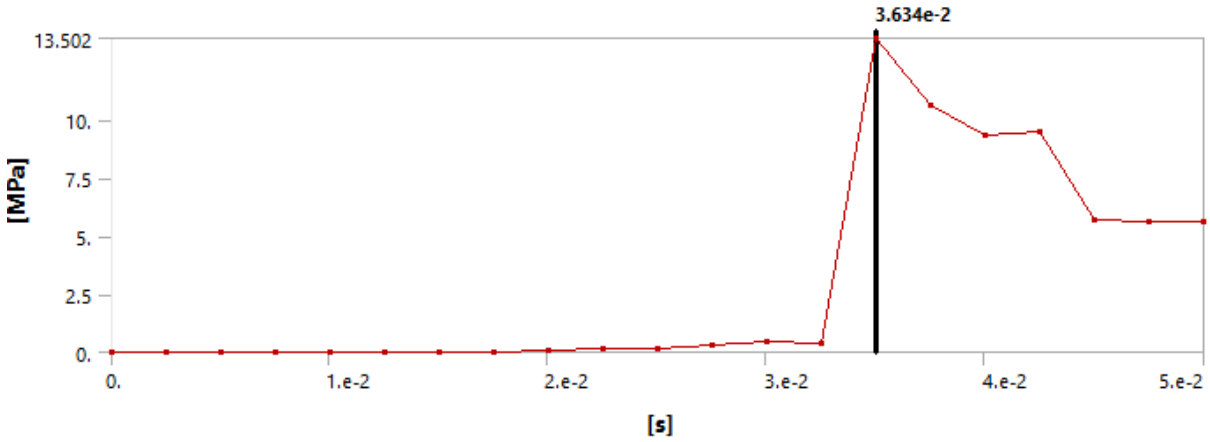

Graph 3 Friction 0.1 deployment verified with stress probe

The second model that has been investigated is the release mechanism in the ready to fire state, this model will be set-up to represent the spring being fully compressed and the solenoid controlled release pin will be engaged to simulate the armed (ready to deploy) state. The aim here was to assess forces generated by the spring on the various parts associated with the release mechanism.

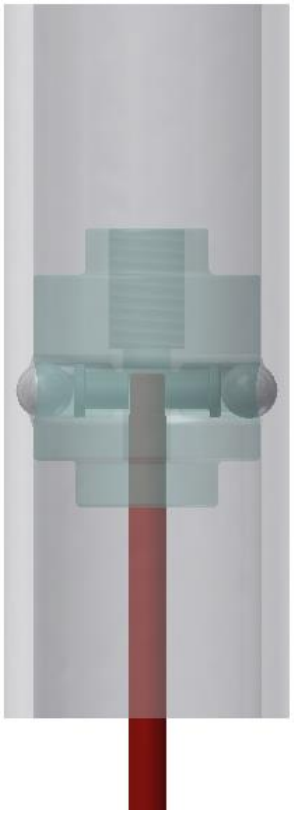

Figure 72. Modified CAD version with solenoid controlled release pin engaged

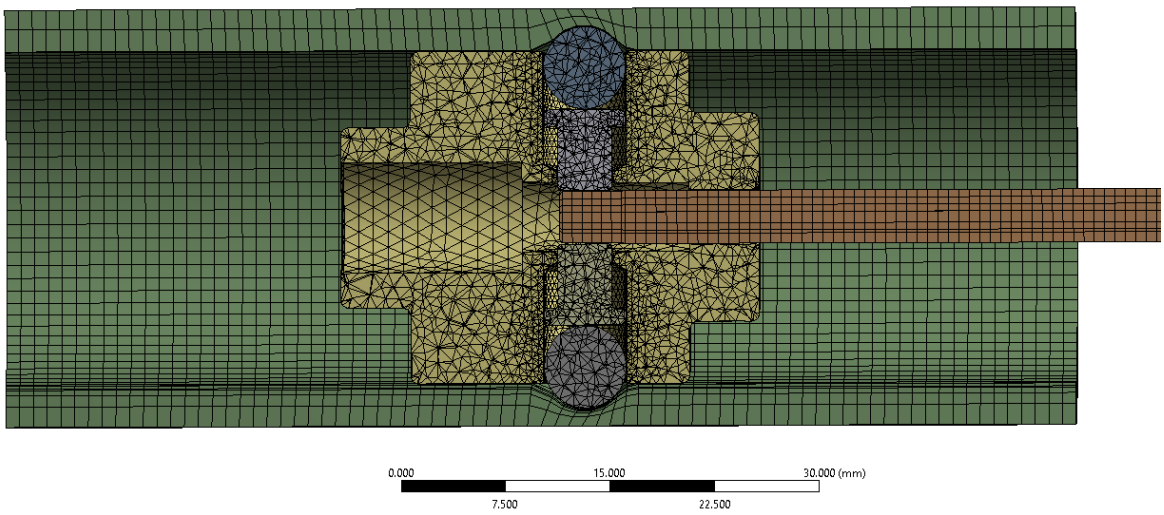

Figure 73. Cross sectional view of release mechanism ready to deploy state meshed

For Element Quality, Skewness, Aspect Ratio inspection tables prior to simulation: refer to Appendix 1 for release mechanism ready to deploy state.

The same boundary conditions were applied to this model as seen in figures 56 – 65 with the addition of the following.

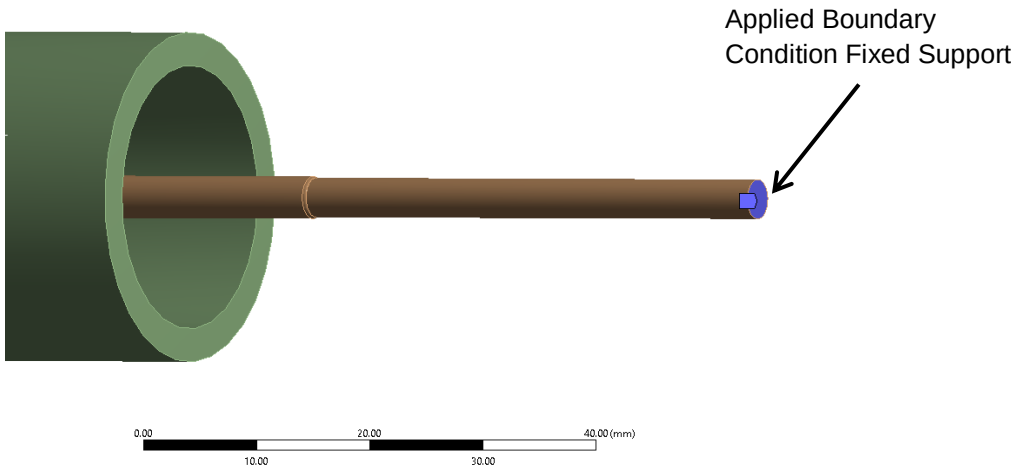

Figure 74. Boundary condition fixed support applied to solenoid controlled release pin

The fixed support boundary condition seen in Figure 80 (indicated in blue), this was used on the base of the release pin to illustrate the solenoid holding the release pin with zero degrees of freedom.

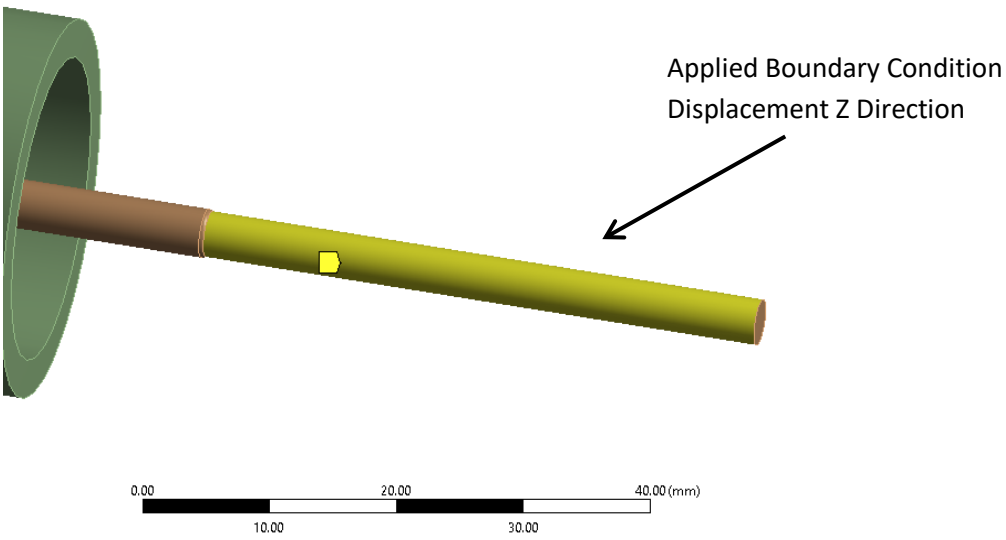

Figure 75. Release pin with added displacement in the Z direction

Displacement has been added to the release pin seen in Figure 81 (indicated in yellow), to allow movement in the Z direction only if any extension of the pin did occur under loading.

Simulated Results:

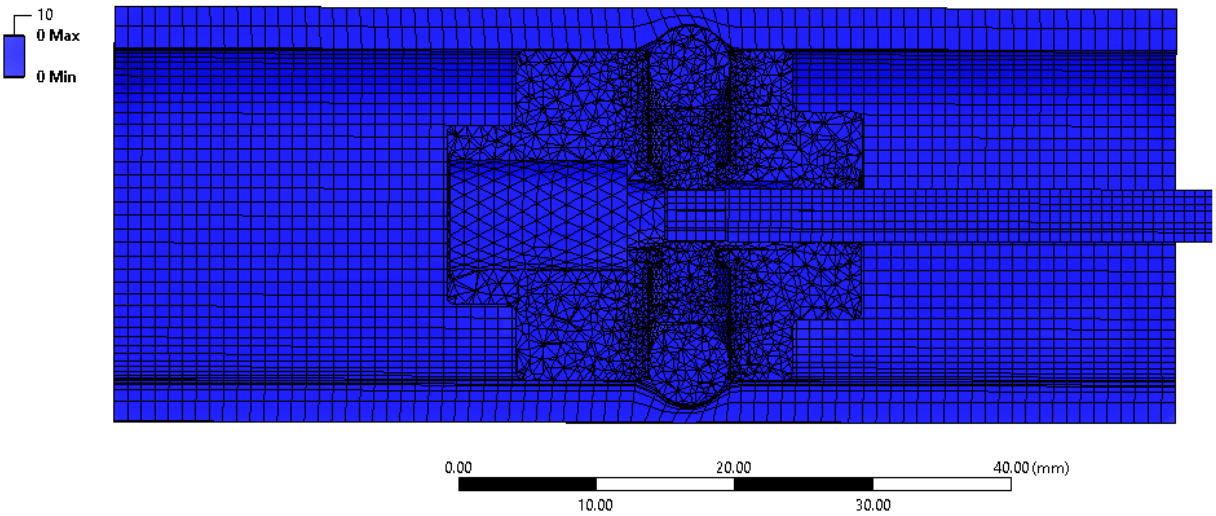

Figure 76. Release mechanism in ready to deploy state prior to loading

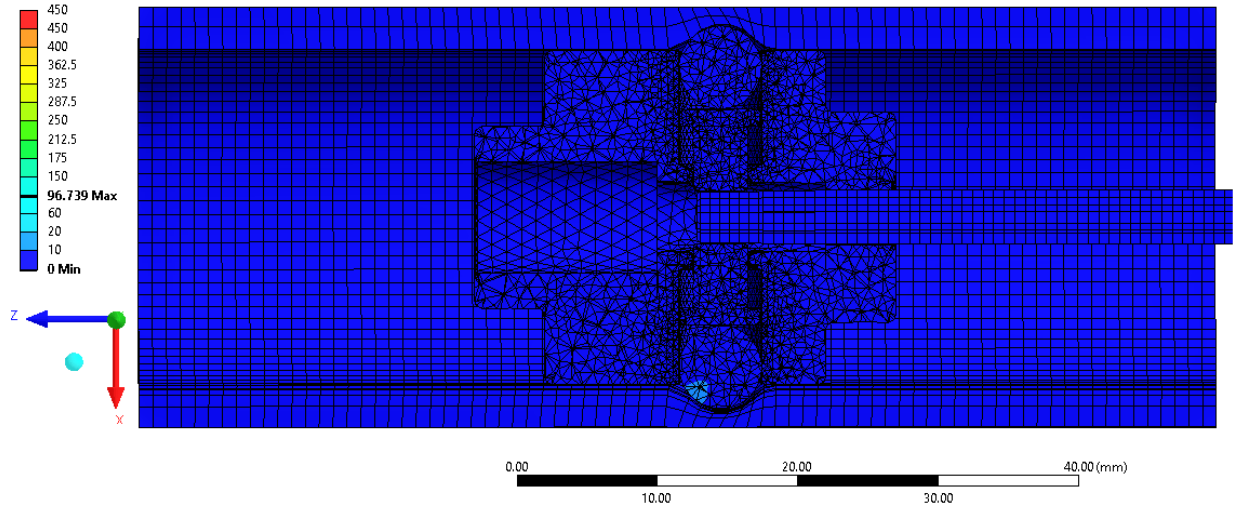

Figure 77. Von-Mises stress after loading at 0.0003 seconds

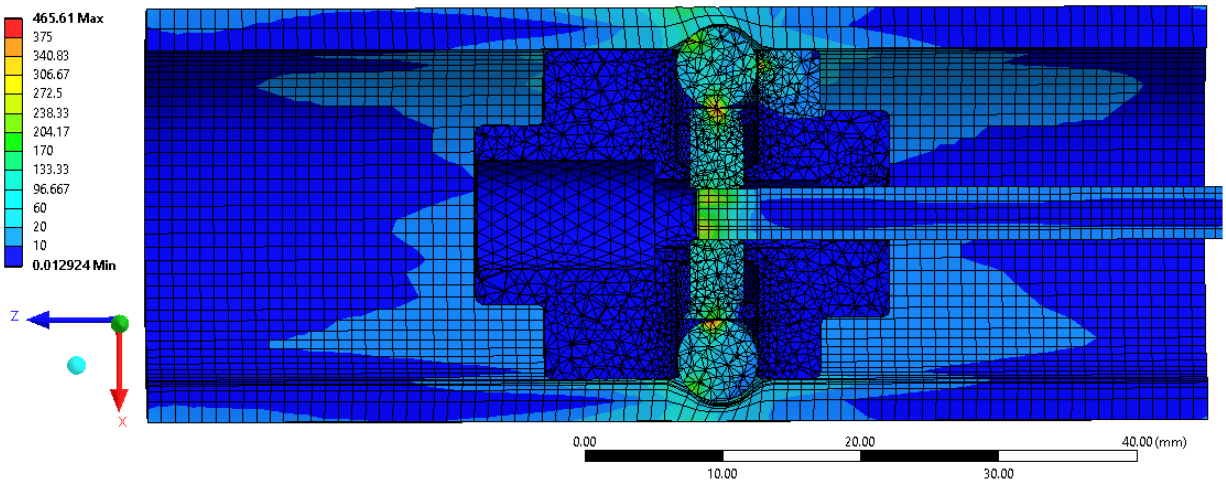

Figure 78. Von-Mises stress after loading at 0.00042 seconds

The third investigated model is the simulation to represent the impact of the piston on the impact buffer as the lifting mechanism reaches the maximum lift height. The aim was to evaluate the force experienced on the four bolt holes. The impact buffers role is to absorb some of the impact energy during the impact with the piston and prevent metal on metal contact; however most of the force will be transmitted through the buffer and will be exerted on the bolt holes.

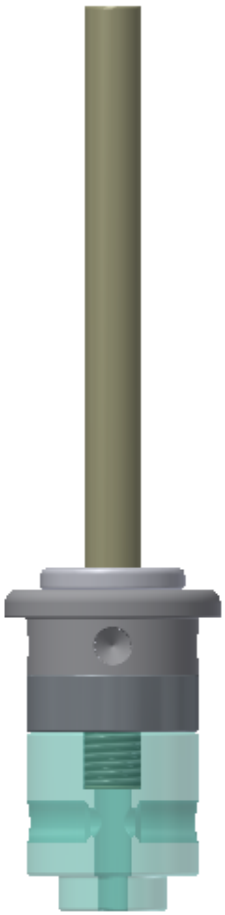

Figure 79. Modified CAD for piston impact buffer simulation

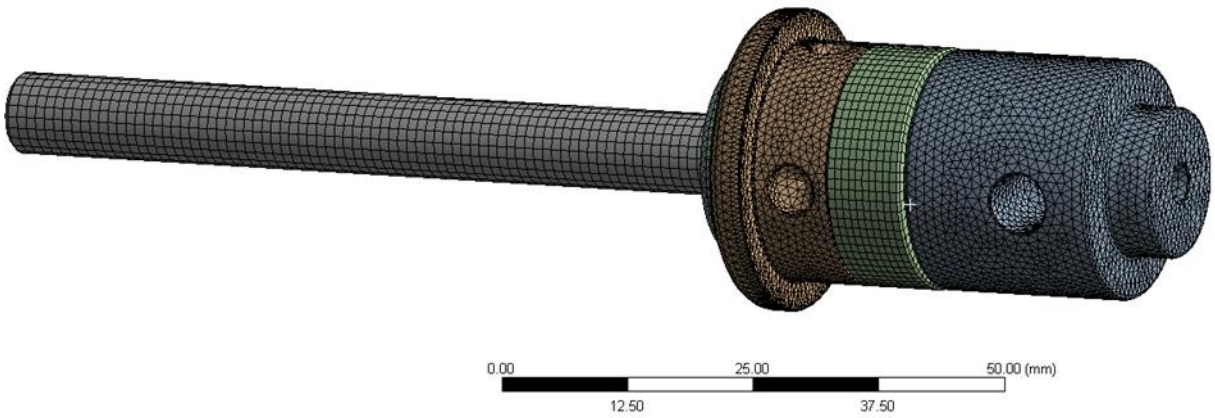

Figure 80. Piston and impact buffer meshed for simulation

Element Quality, Skewness, Aspect Ratio inspection tables prior to simulation: refer to Appendix 1 for piston and impact buffer.

In order to represent the conditions experienced during the release of the piston and the impact of the piston with the buffer and the force experienced by the bolts holding the top cap in place. Specific boundary conditions were used to replicate this.

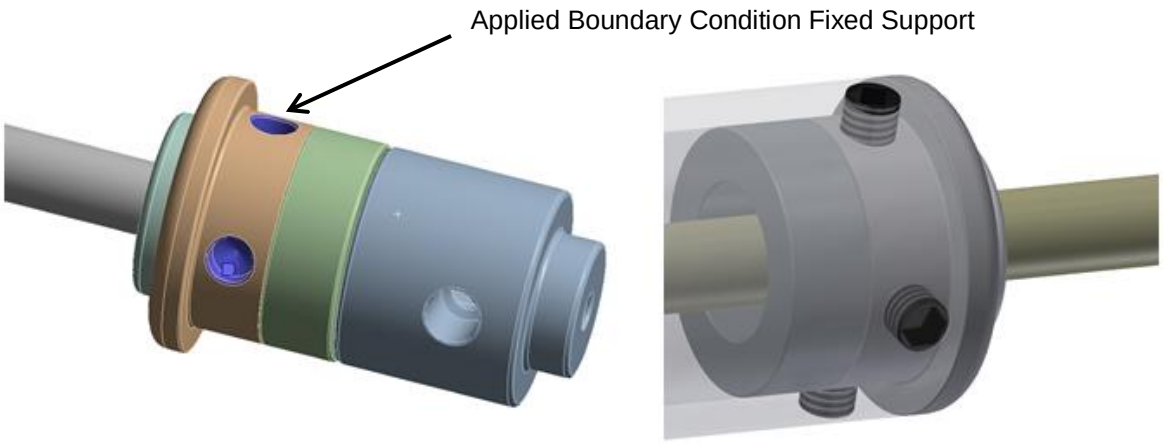

Figure 81. Boundary condition fixed support applied to top cap

Fixed support boundary condition was allocated (highlighted in purple) to represent the holding effect the grub screws have on the top cap.

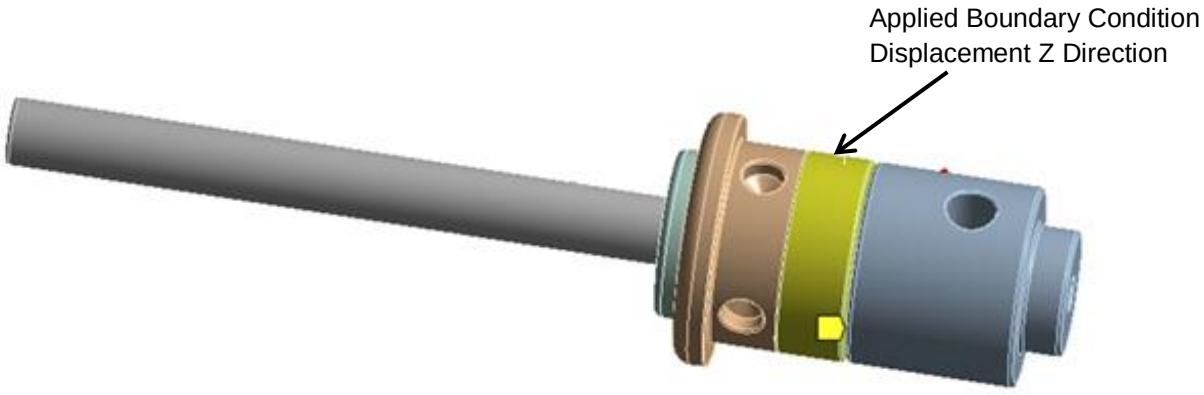

Figure 82. Impact buffer with added displacement in the Z direction

Displacement (highlighted in yellow) was added to allow movement and deformation of the energy absorber buffer after impact Z direction only.

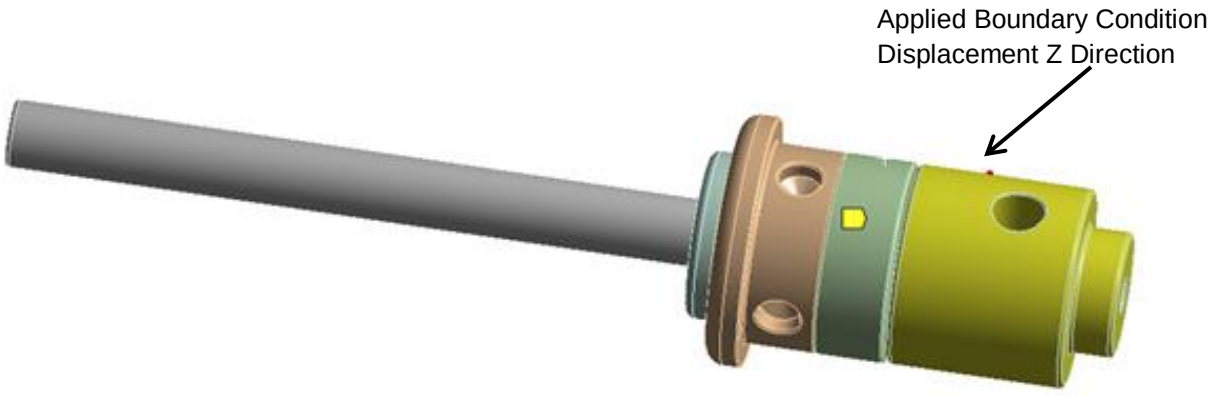

Figure 83. Piston with added displacement in the Z direction

Displacement was added to the piston in the Z direction to allow movement once the spring force is applied.

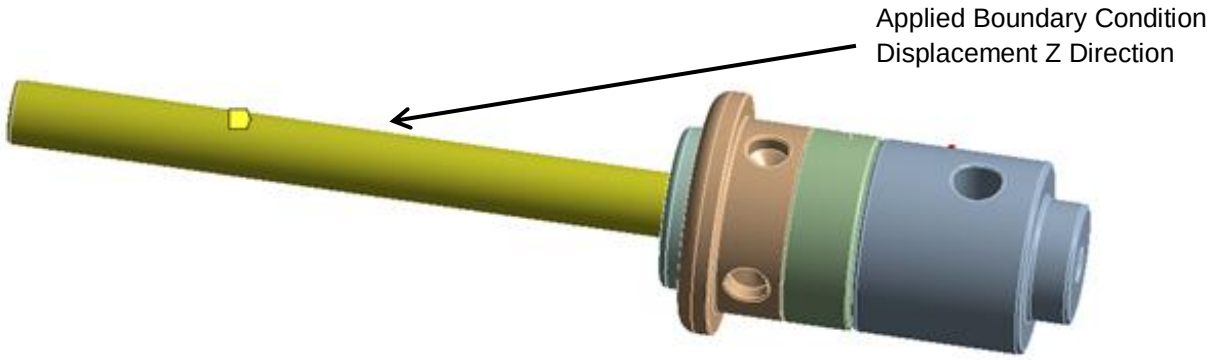

Figure 84. Lifting rod with added displacement in the Z direction

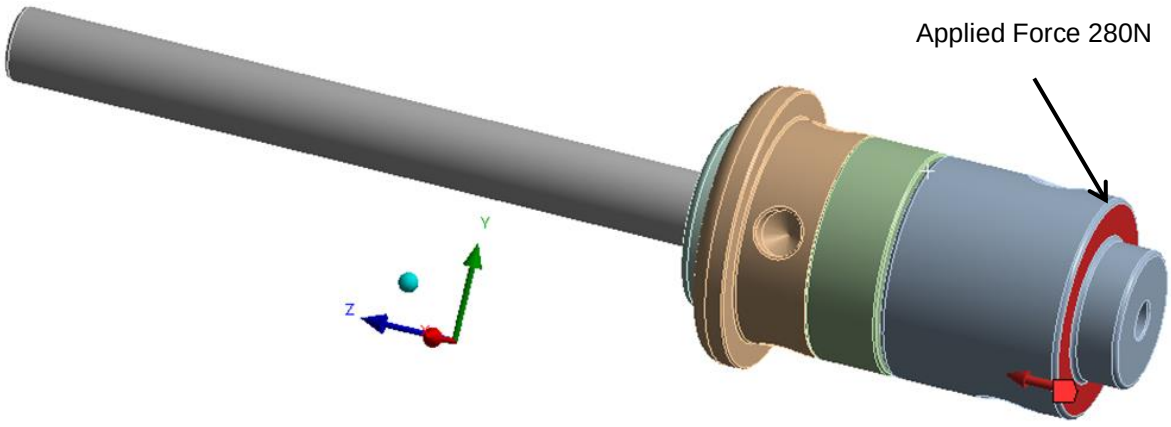

Figure 85. Applying 280 N to piston base in Z direction

A force of 280 N was applied simulating the force generated by the spring in accordance to the calculated value from Equation 5, and was applied to the pistons face (indicated in red) in the Z direction only.

Simulated Results:

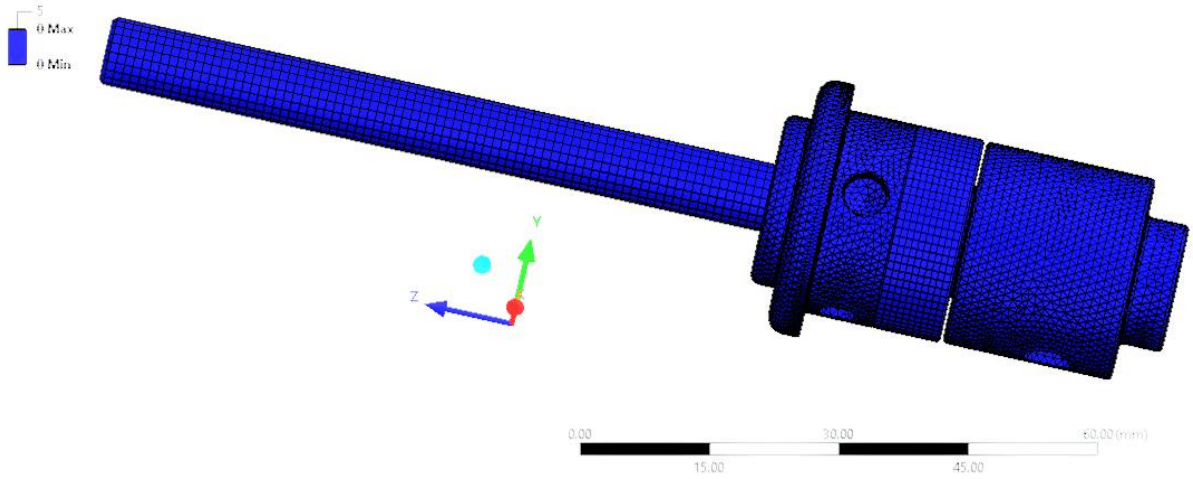

Figure 86. Piston impact buffer prior to loading

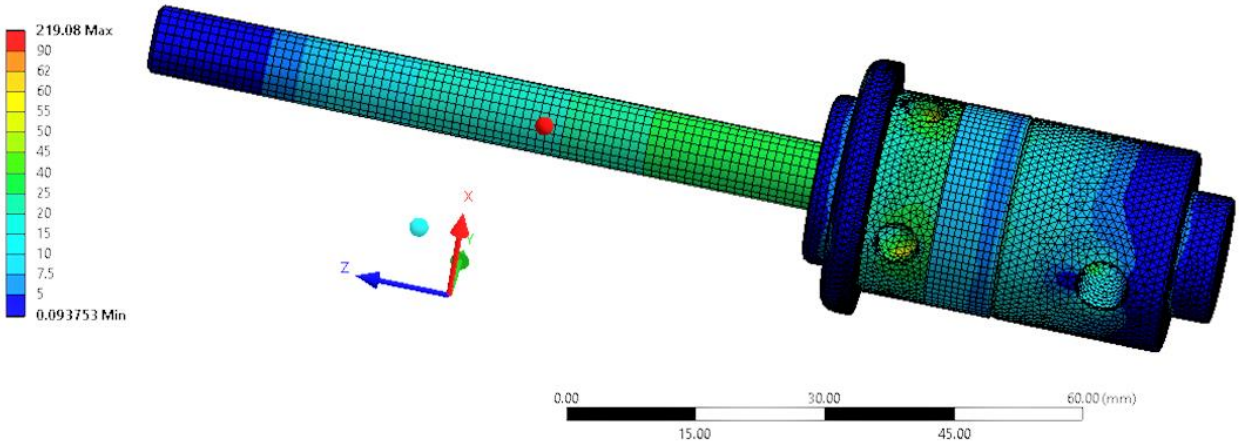

Figure 87. Von-Mises stress after loading at 0.0006 seconds

Ansys default Structural Steel material properties were assigned to all comports of these simulations. With the only exception being the impact buffer; this was changed to polyurethane. Polyurethane was selected because of the energy absorbing capacity of the local impact energy and works as a buffer, by easing the kinetic energy caused by the piston buffer impact.

Structural steel		
	Value	Unit
Density	7850	kg m^-3
Young's Modulus	200000	Mpa
Poisson's Ratio	0.3	
Bulk modulus	1.67E+11	Pa
Shear Modulus	7.69E+10	Pa

Table 7. Structural Steel material properties

Polyurethane		
	Value	Unit
Density	2365	kg m^-3
Shear Modulus	1500	Mpa
Gruneisen Coefficient	1.55	

Table 8. Polyurethane material properties

Evaluation of FEA Models

Deployed:

As observed during the initial deployment some stress was observed on the lifting rod, this is the result of the rod being subjected to a large amount of force during deployment. Followed by high stress between the lifting rod and the piston as this region is where most of the opposing force is acting. Although values as high as 1000 mPA (figure 68) were observed, this value occurs instantaneous and can therefore be neglected. The deployment time observed by the stress probe (graph 2) I identified that full deployment has occurred at 35 ms. With the addition of friction the model identified similar stress levels on the lifting rod and between the rod and piston. The deployment time was again verified by a stress probe and with the addition of 0.1 friction the deployment time increased to 36 ms graph 3). Overall the

kinematics observed throughout the simulation proves to be accurate and the behaved in accordance to the expected design specification and verified the deployment time.

Ready to Fire/Deploy:

As the force is applied to both the ball bearings and release pins, they both have a natural tendency to move towards the center; as observed in the previous simulation figure 66– 71. Instead of this occurring now the solenoid controlled release pin is placed between the release pins to prevent this from occurring. Subsequently the release pins and ball bearings are locked between the internal fillets and the solenoid controlled release pin. Figure 84 illustrates this effect and the resultant stress distribution between the internal fillets, ball bearings, release pins and the solenoid release pin. It is observed that the ball bearings are subject to a large amount of local stress on the surface which is also evident on the release pins surface. The high stress illustrated in (red), is to some extent ignored due to occurring only very locally, but instead the more general stress distribution is more important. At the areas where high stress levels are experienced levels reaching 340 MPa and tapering off to 204 MPa can be seen. Although no specific material properties have been defined for each component, this simulation has identified areas which are of particular concern and are the most prone to failure. As observed the ball bearing and release pins configuration are subject to a large amount of local stress on the surface. Correct material selection for these components, are of the highest priority, and a suitable material with a very hard surface is required.

Piston Buffer Impact:

As the impact between the buffer and the piston occur it can be observed that the buffer absorbs much of the energy, and the rest is transmitted through the bolt holes before coming to a stop. The stress experienced through the bolt holes is very minor and wouldn't result in excessive wear or deformation. Also in this scenario it was without the vehicles bonnet offering further dampening of the impact between the buffer and the impact.

In summary, although the FEA proves the kinematics and has identified particular areas which require special design consideration due to high stress levels, further development of the model is required to obtain more accurate results. As mentioned the boundary condition used was frictionless contact, due to this the forces generated form objects sliding were very low which with the addition of friction would be significantly higher. The force exerted on the piston was applied a generic force, instead spring elements should be incorporated to

accurately emulate the kinematics of the spring as intended by the design. Another model should be explored which investigates the forces required to disengage the solenoid controlled release pin, to examine the forces required to do so. Another parameter which requires examination is the lifting rod, due to the large lifting forces involved to deploy the bonnet a further analysis on the potential for buckling of the lifting rod should be conducted.

Conclusion and Future Work

This thesis presents the work to

- Study different proposed lifting methods and their feasibility to replace current systems.
- Propose a new lifting mechanism design which is resettable.
- Study new design capabilities using FEA techniques.

Based on this work, the resulting conclusions can be made.

- **The stored energy approach with the use of compressed gas was deemed not suitable as a viable replacement for current systems used. However, the use of a compressed spring to generate the lifting force was identified as suitable method.**

It has been identified conceptually that compressed gas could lift the vehicles bonnet through the review of previous studies. However, the main technical challenge was to release the compressed gas in a fast and controlled manner to allow quick lifting of the actuator. This was investigated by designing and testing two different types of gas discharging systems. The first iteration allowed for rapid discharge of the gas, but this was not in a controlled fashion, and the released gas couldn't easily be utilised to propel the actuator. The second design incorporated a solenoid valve; with this configuration the performance was significantly improved and the released gas was easily controllable, which would allow it to be incorporate into a lifting mechanism with ease. Although both systems had the potential to release gas, performances of both systems were significantly reduced due to freezing of the orifices; as a result of the sudden pressure drop within the system. This lead the investigation to the use of a spring powered system. To aid in research a commercially available system the Mercedes spring powered system active bonnet actuator was purchased. This was deconstructed to investigate the operational mechanics as well as its potential limitations were identified. The main drawback of this system was the size, and the bonnet hinge and the lifting mechanism were not independent from each other. However,

it was concluded that the stored energy approach with the use of spring(s) would be the most robust and reliable approach for the design of a new resettable lifting actuator.

- **A new cylindrical bonnet actuator can be designed which is resettable**

After identifying that the use of spring(s) would be the most suitable for this application. Conceptually the operating principles behind the use of are springs are very simple. However, the main challenge was to design a system which can contain the stored energy produced by the spring. This mechanism must also be able to release rapidly allowing the spring to release its energy, thus lifting the actuator and in turn the bonnet. The first design iteration did achieve a cylindrical design, but the release mechanism was not very robust and resetting of the system would be very problematic. To overcome the limitations of the initial design the release mechanism was redesigned to allow for easy resetting with the incorporation of ball bearings and a 360 degree fillet on the internal wall of the cylinder. These new features lead to the final design iteration which fulfilled all design specifications and potentially the performance requirements.

- **Finite element model identifies areas of high stress and verifies the kinematic response of proposed design.**

The investigation of the finite element model illustrated the intended design kinematics and the function of the release mechanism. Also during the simulation components were identified which were subject to high stress levels. By identifying the stress experienced by each component this allows for suitable material selection to further develop the mechanism. But overall proves the concept and verifies the deployment time.

Future Work

In order to fully verify the design further finite element analysis with additional boundary conditions to more accurately represent the factors and forces involved during operation. Further investigation of the forces and structural integrity of the lifting rod under deployed conditions lifting the mass of the bonnet to investigate the potential of buckling of the rod.

The next stage in the development process would be to manufacture the mechanism. Once manufactured a series of comparative tests with other spring lifting mechanisms should be conducted to evaluate the designs durability, repeatability and most importantly the performance compared to other systems, as well as validate the finite element model.

Finally once the concept is proven both through simulation and also practically, a final set of tests should be conducted with the system incorporated to a vehicles bonnet system, and the real word performance should be tested and verified from significantly lower HIC values during head impact tests.

Appendix A: Meshed Element Quality Checks

In order to review the quality of mesh the mesh elements skewness is evaluated. Skewness is one of the essential measures for mesh quality; the skewness defines how close to optimal the face of the element is https://www.sharcnet.ca/Software/Ansys/17.0/en-us/help/wb_msh/msh_skewness.html. Highly skewed cells can cause inaccuracy in the model and potentially destabilise the solution https://www.sharcnet.ca/Software/Ansys/17.0/en-us/help/flu_ug/flu_ug_mesh_quality.html. For example with the use in 3-dimensional analysis is will result in a perfect cube when using hexahedron and for in the case of tetrahedron will be a perfect equilateral tetrahedron https://ganeshvisavale.wordpress.com/tag/ansys-icem-cfd/.

For hexahedron elements, the skewness is obtained the following:

For each 6 faces the angle between face normal and vector which are characterised by the center of the hexahedron and the center of the face is also calculated.

Therefore the value obtained in therefore normalised so that value 0 represents a poor element and a value of 1 represents a perfect cube. This is the mathematical method used to calculate the skewness but in general means how closely the element represents a perfect cube. If the value deviates enough the value will be close to 0 https://ganeshvisavale.wordpress.com/tag/ansys-icem-cfd/.

For Triangular elements:

The skewness is defined by the area of the element and the area of a perfect equilateral triangle. For quadrilateral elements the skewness is obtained by connecting the mid points of each side to the midpoints of the opposite sides and calculating the angle between them https://ganeshvisavale.wordpress.com/tag/ansys-icem-cfd/.

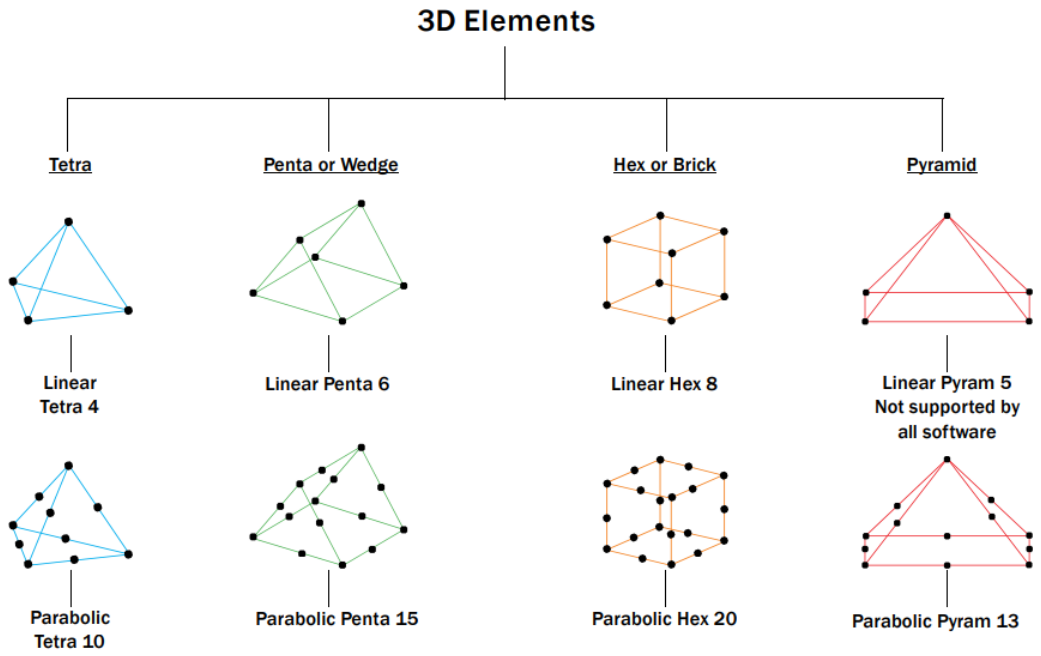

Example of 3D meshing elements https://altairuniversity.com/wp-content/uploads/2014/02/3DMeshing.pdf

The range of skewness values and the corresponding cell quality

Value of Skewness	Cell Quality
1	degenerate
0.9 — <1	bad (sliver)
0.75 — 0.9	poor
0.5 — 0.75	fair
0.25 — 0.5	good
>0 — 0.25	excellent
0	equilateral

https://www.sharcnet.ca/Software/Ansys/17.0/en-us/help/wb_msh/msh_skewness.html

Mesh statistics for each model

Mesh Inspection of Release Mechanism Deployed

Quality

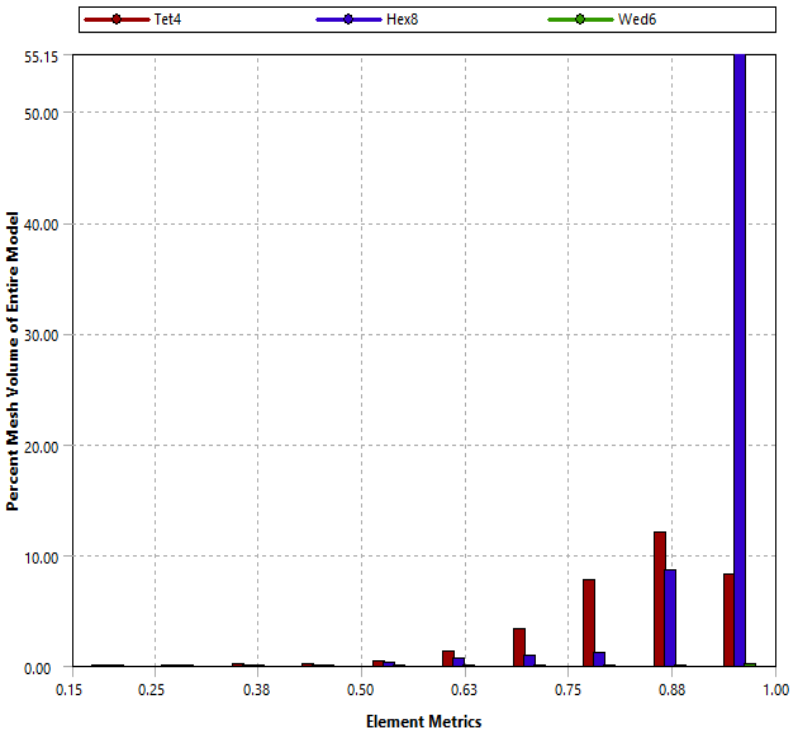

Skewness

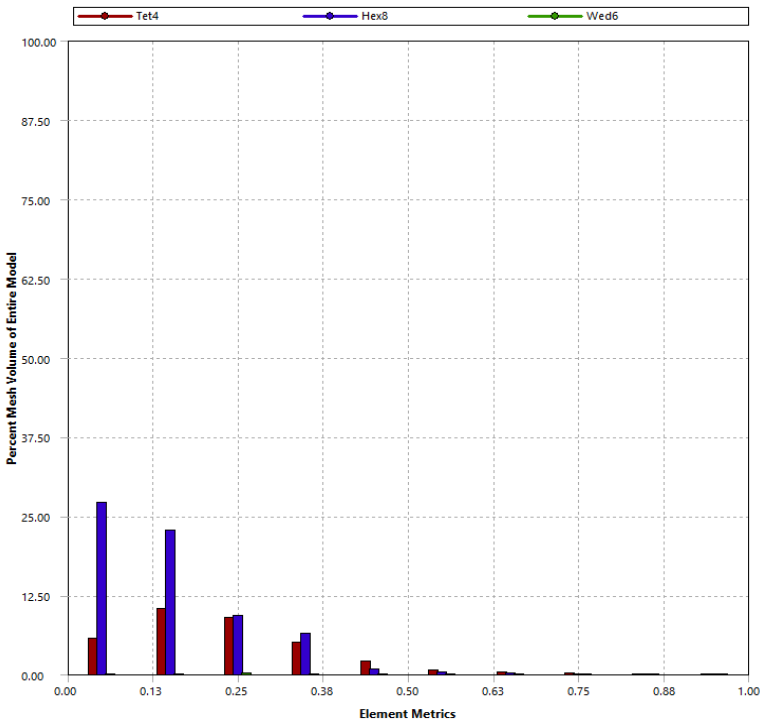

Aspect ratio

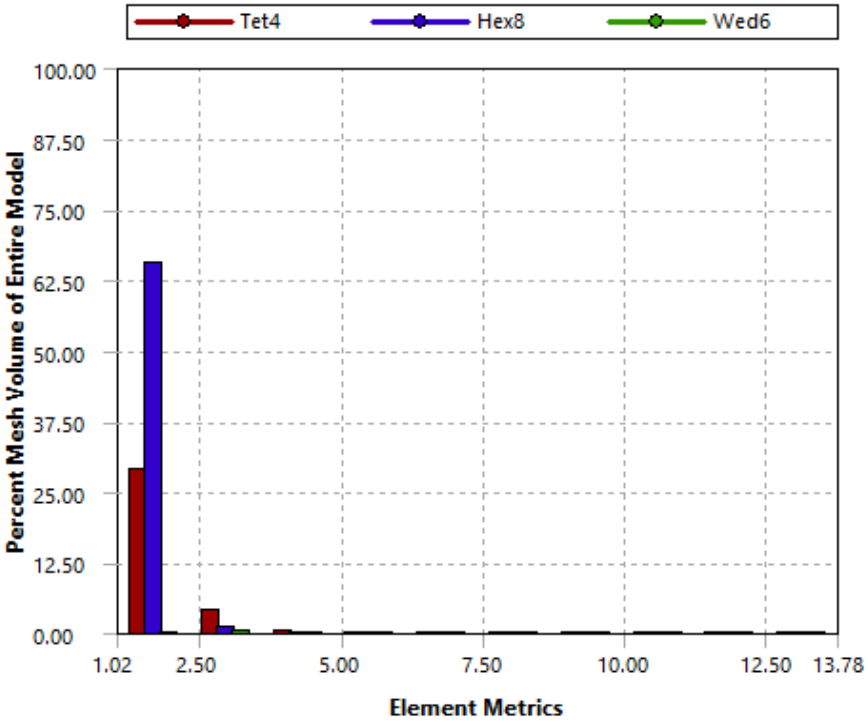

Mesh Inspection of Release Mechanism with Solenoid Pin

Quality

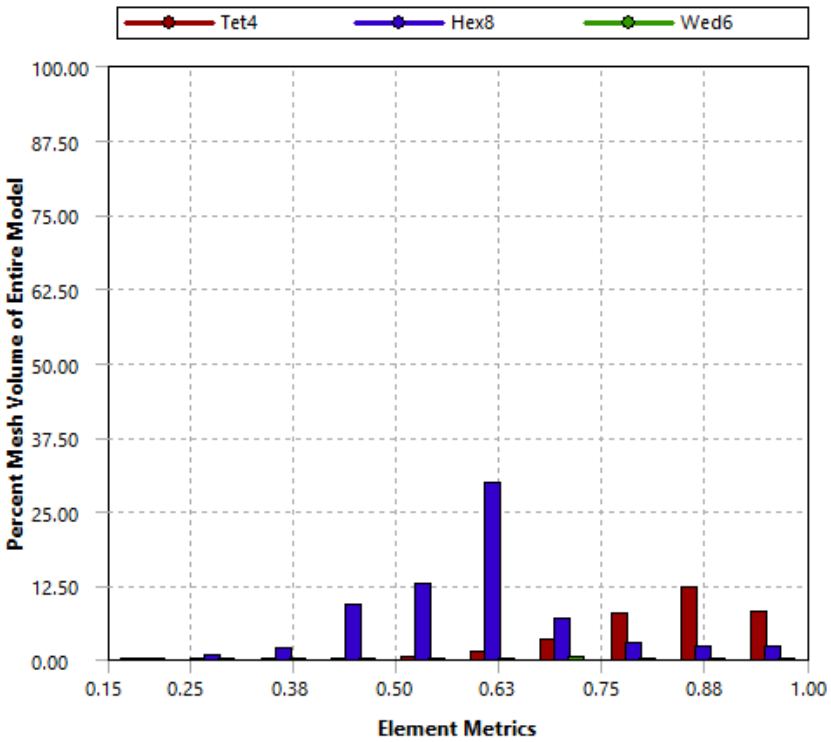

Skewness

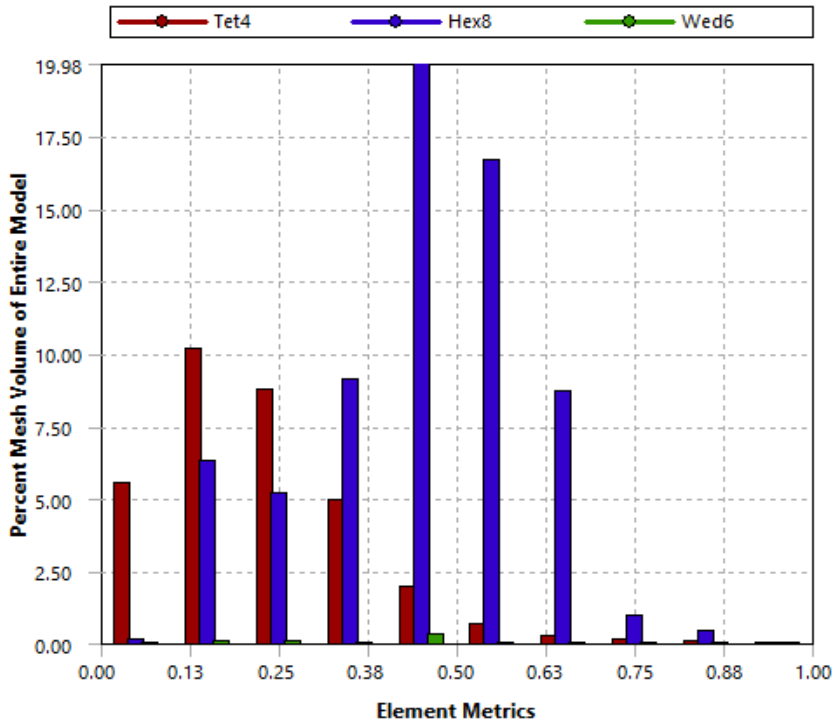

Aspect ratio

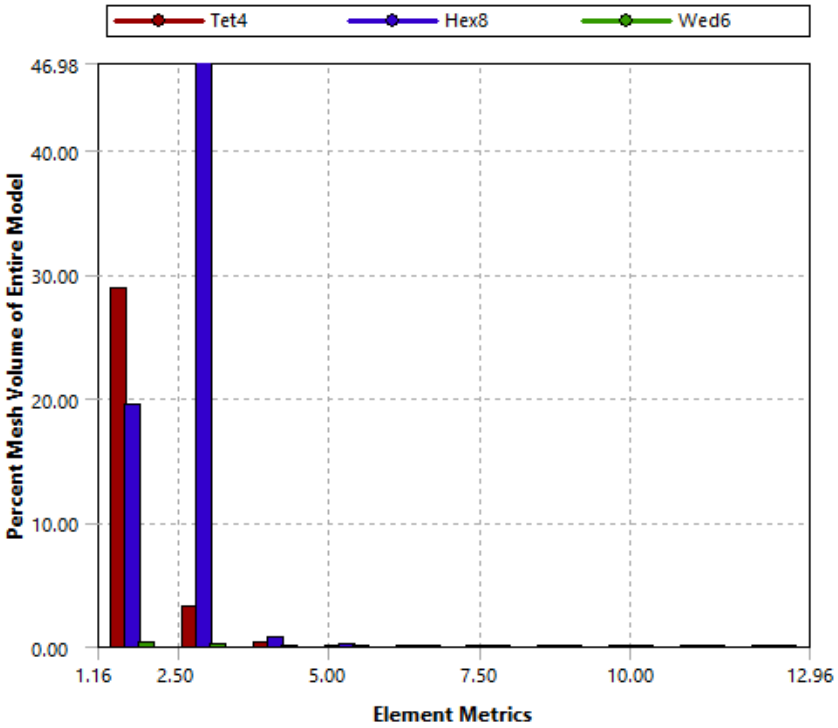

Mesh Inspection of Piston Buffer Impact

Quality

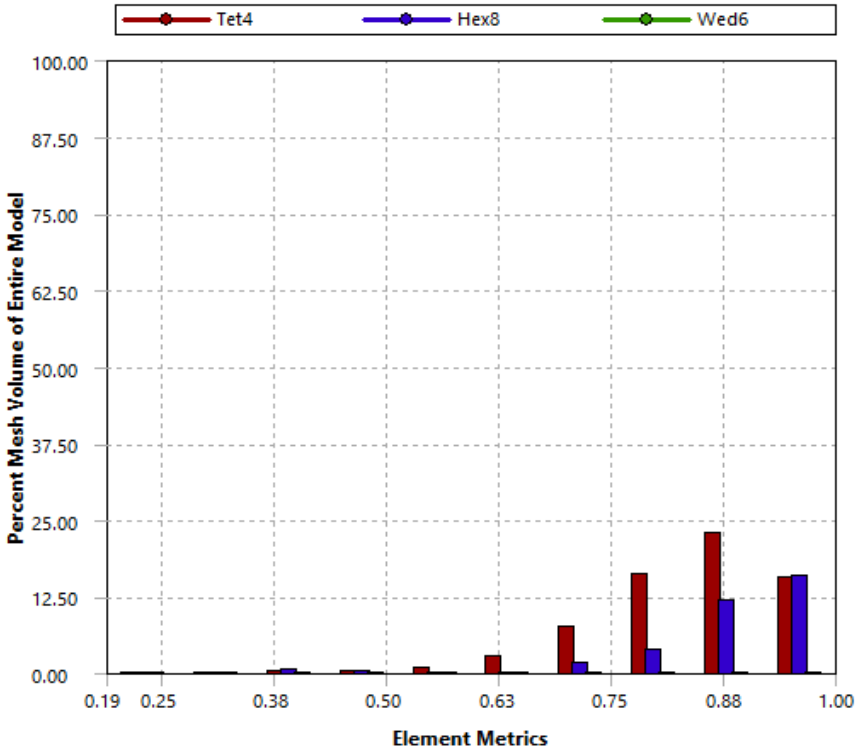

Skewness

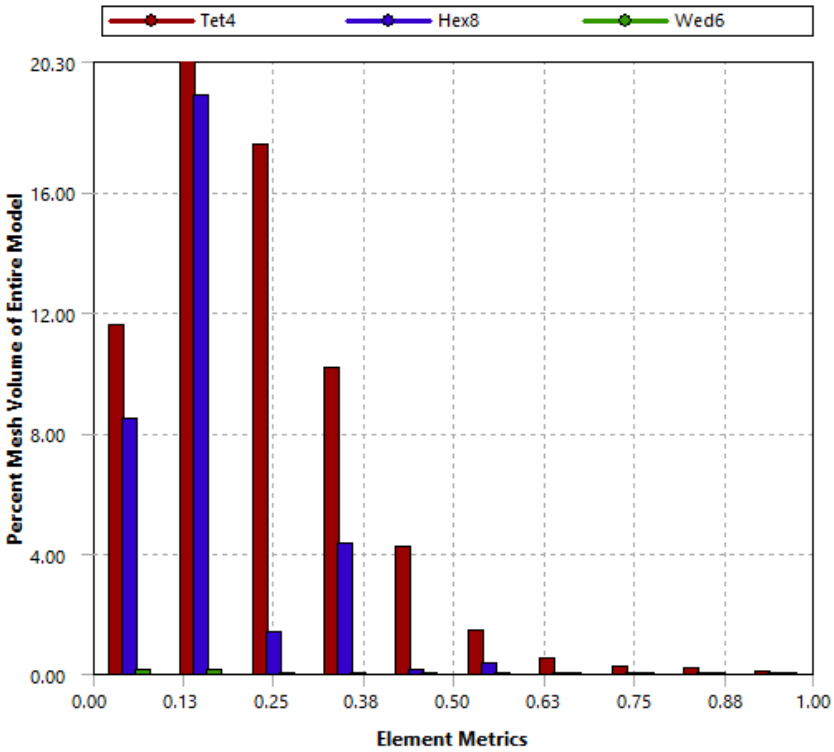

Aspect ratio

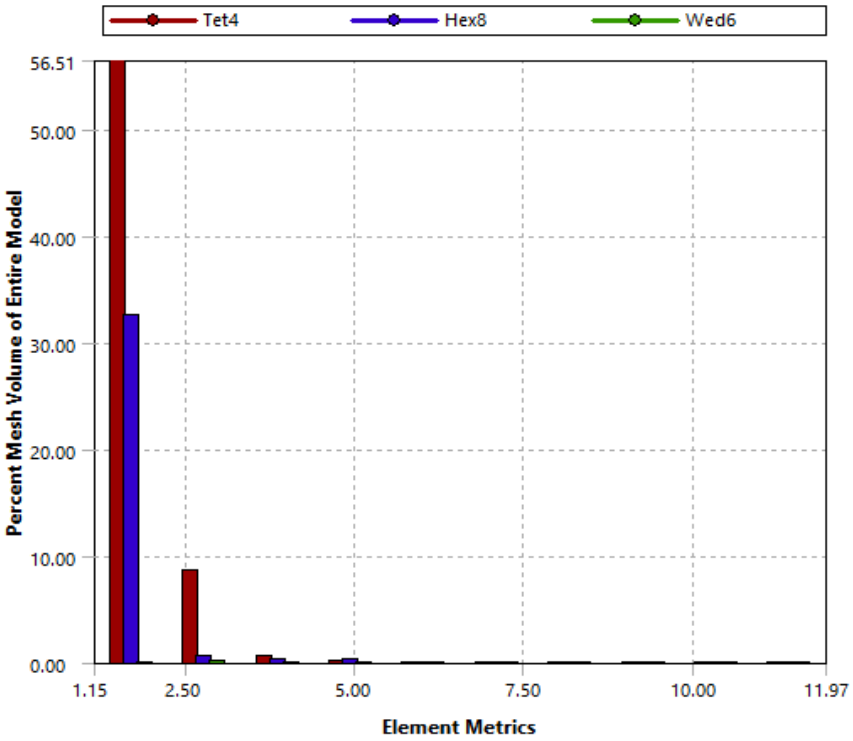

Appendix B – Mass Evaluation

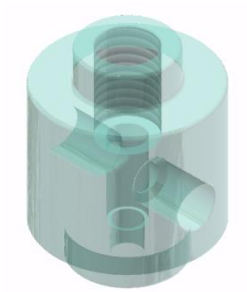

Material Type	Volume (mm^3)	Density (g/cm^3)	Mass (Kg)
Alloy Steel	8984.281	7.730	0.069
Mild Steel	8984.281	7.850	0.071
Stainless Steel	8984.281	8.000	0.072
Titanium	8984.281	4.510	0.041

Material Type	Volume (mm^3)	Density (g/cm^3)	Mass (Kg)
Alloy Steel	52932.102	7.730	0.409
Mild Steel	52932.102	7.850	0.416
Stainless Steel	52932.102	8.000	0.423
Titanium	52932.102	4.510	0.239

Material Type	Volume (mm^3)	Density (g/cm^3)	Mass (Kg)
High Strength Steel	107.536	7.850	0.001
Stainless Steel	107.536	8.000	0.001

Material Type	Volume (mm^3)	Density (g/cm^3)	Mass (Kg)
Alloy Steel	86.443	7.730	0.001
Mild Steel	86.443	7.850	0.001
Stainless Steel	86.443	8.000	0.001

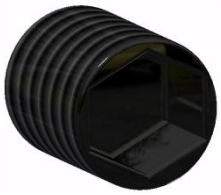

Material Type	Volume (mm^3)	Density (g/cm^3)	Mass (Kg)
Alloy Steel	77.728	7.730	0.001
Mild Steel	77.728	7.850	0.001
Stainless Steel	77.728	8.000	0.001

Material Type	Volume (mm^3)	Density (g/cm^3)	Mass (Kg)
Alloy Steel	5526.582	7.730	0.043
Mild Steel	5526.582	7.850	0.043
Stainless Steel	5526.582	8.000	0.044
Titanium	5526.582	4.510	0.025

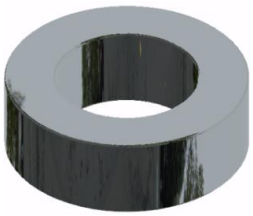

Material Type	Volume (mm^3)	Density (g/cm^3)	Mass (Kg)
Polyurethane	2384.408	2.365	0.018

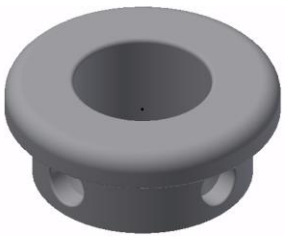

Material Type	Volume (mm^3)	Density (g/cm^3)	Mass (Kg)
Alloy Steel	4018.732	7.730	0.031
Mild Steel	4018.732	7.850	0.032
Stainless Steel	4018.732	8.000	0.032
Titanium	4018.732	4.510	0.018

Material Type	Volume (mm^3)	Density (g/cm^3)	Mass (Kg)
Nylon	2196.458	1.626	0.018

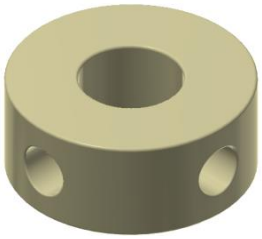

Material Type	Volume (mm^3)	Density (g/cm^3)	Mass (Kg)
Alloy Steel	3385.425	7.730	0.026
Mild Steel	3385.425	7.850	0.027
Stainless Steel	3385.425	8.000	0.027
Titanium	3385.425	4.510	0.015

Material Type	Volume (mm^3)	Density (g/cm^3)	Mass (Kg)
Alloy Steel	101.290	7.730	0.001
Mild Steel	101.290	7.850	0.001
Stainless Steel	101.290	8.000	0.001

Material Type	Volume (mm^3)	Density (g/cm^3)	Mass (Kg)
Alloy Steel	7640.495	7.730	0.059
Mild Steel	7640.495	7.850	0.060
Stainless Steel	7640.495	8.000	0.061

Material Type	Volume (mm^3)	Density (g/cm^3)	Mass (Kg)
Alloy Steel	2646.256	7.730	0.020
Mild Steel	2646.256	7.850	0.021
Stainless Steel	2646.256	8.000	0.021
Titanium	2646.256	4.510	0.012

Mercedes solenoid release system used for mass estimation of proposed design.

After using the CAD model to evaluate the parts geometry to a high degree of accuracy the total mass can be approximated.

Proposed Models Mass : 0.9885 kg

Mercedes Actuator : 1.31 kg

Percentage difference of 24.54 %

Appendix C - Prior Art

This section will summarize relevant prior art/inventions which were used to identify key limitations of existing resettable systems.

All four inventions presented act as a lifting apparatus by raising the bonnet to a pre-set height during a vehicle-pedestrian impact. The bonnet is therefore lifted to provide additional clearance to absorb the impact energy whilst avoiding collision with engine components.

Invention 1

Invented by: 이인제

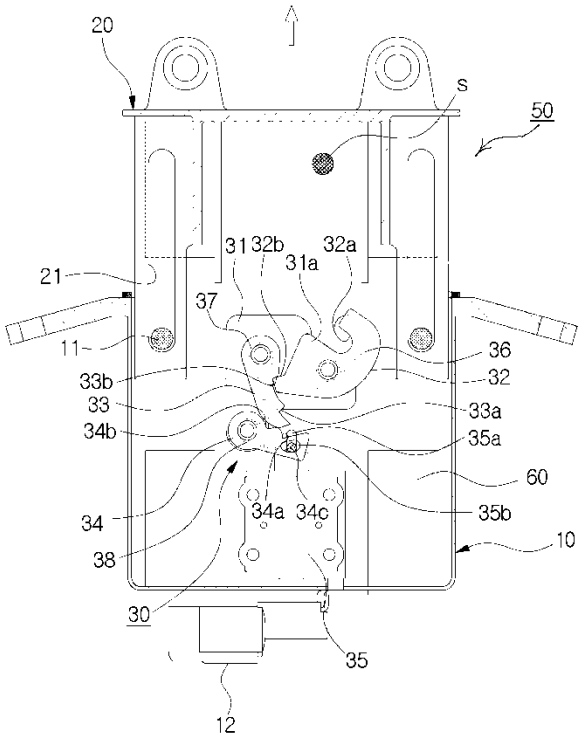

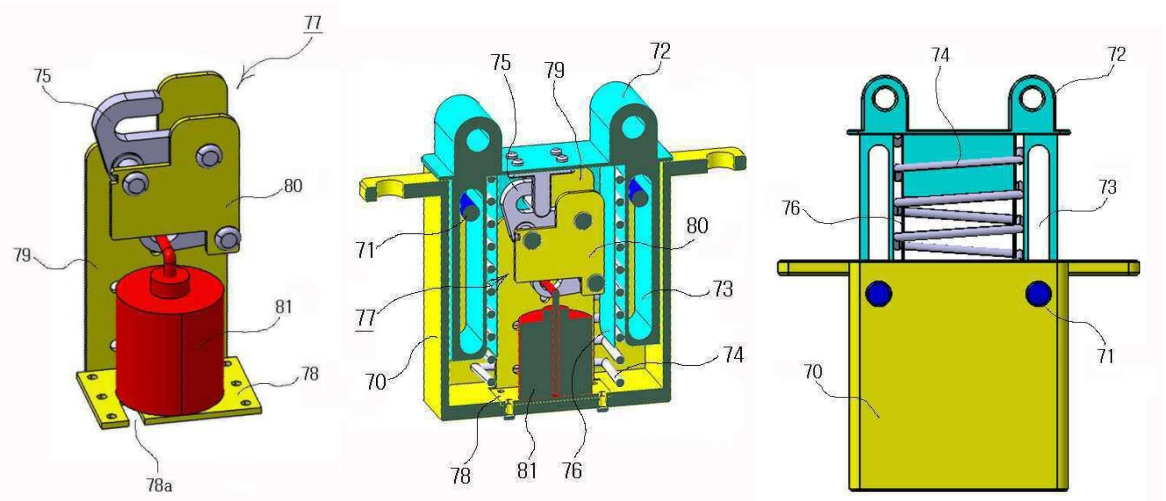

The inner body 20 is a striker (s) is securely fixed that as lifting element which is provided in a lower end portion with an opening box-like shape, disposed longitudinally in the horizontal between the rear panel and of the inner body front portion in the interior of the inner body (20) and the housing inner side with a latch mechanism (30) for a pedestrian collision accident locked state release (unlock) while keeping the striker (s) to the lock (lock) state in the lowered position of the inner body 10 and the inner body (20) and is installed, the electromagnet assembly 60 to lift the inner body 20 using a magnetic force generated when power is supplied the lower portion of the latch mechanism is provided.

Then, the solenoid 35 is in that the actuating rod (35a) under the power supply control of the controller is installed, enabling W, fall, slot-hole (34c) of the second pawl (34) to said actuating rod (35a) is a leading end the connecting pin (35b) is fitted to be assembled it consists of a fixed structure.

Accordingly, if the solenoid is driven operating rod (35a) to (35) lowered and rotated to the second pawl 34 is pulled downward the figure by the operation rod (35a) counter-clockwise, on the contrary the actuating rod (35a) if the rising while mm upward by the second pawl (34) is operating rod (35a) is rotated in a clockwise direction.

Thus in the first as the pawl 33 is rotated and release the fixed state of the latch 32, one after another, and eventually the latch as 32 is rotated in the clockwise direction by the elastic restoring force of the return spring 36, the striker (s) since thereby release the locking is raised rear end of the hood 44 by the restoring force of the coil spring 40 that was compressed as in Figure 2b.

More information can be found at:

https://patents.google.com/patent/KR20150082800A/en?q=active&q=hood&q=actuator&q=pedestrian+safety&q=solonoid&oq=active+hood+actuator+pedestrian+safety+solonoid&page=1

Invention 2

Invented by: Koo Hyun KIMSung Wook HongJi Young SongDae Yub Lee

The lift device 100 shown in FIG. 2 selectively lifts up the front of the hood 30. To this end, the lift device 100 includes a striker 110 placed under a bottom surface of the hood 30, a latch unit 120 placed in the engine compartment 40 for locking or unlocking the striker 110, and an elastic member 130 placed between the striker 110 and a portion of the engine compartment 40 for lifting up the hood 30, as shown in FIG. 2. The lift device 100 further includes a stopper unit 140 that limits the amount the hood 30 rises, that is, the lift height, and a hinge unit 150 installed between the hood 30 and the latch unit 120 for fixing the hood 30 in such a manner as to be pivotable (or rotatable) in the rear direction of the vehicle body. The striker 110 includes an upper panel 111 placed under the bottom surface of the hood 30, and a hanger 112 (or a suspension ring, a mount ring, or a stop-hook) installed substantially on the central region of the bottom surface of the upper panel 111.

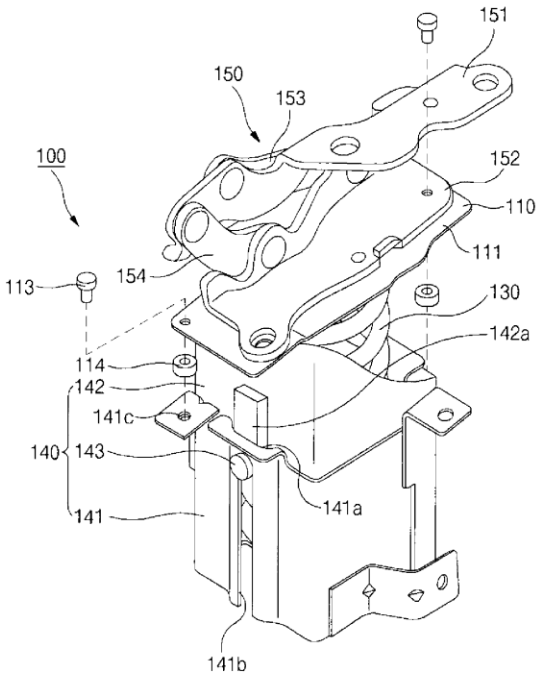

Fig.2

The latch unit 120 for locking or unlocking the striker 110 includes a base plate 121 placed on the upper surface of the engine compartment 40, and a latch 122 and first and second suspension levers (or stop levers or locking levers) 123 and 124 respectively installed pivotably (or rotatably) on the base plate 121. The latch unit 120 further includes a solenoid actuator 125 controlling a rotational direction of the second suspension lever 124 and springs 126, each engaged with the first and second suspension levers 123 and 124 and the latch 122 respectively to bring a restoring force. The base plate 121 has an insertion recess 121 a, which is formed in the top side (or portion) of the base plate 121. The insertion recess 121 a receives the hanger 112 of the striker 110. The latch 122 pivotally coupled to the base plate 121 locks or unlocks the hanger 112 of the striker 110, which is inserted into or released from the insertion recess 121 a. The first suspension lever 123 comprises a first trigger recess 123 a and a second trigger recess 123 b. The first trigger recess 123 a of the first suspension lever 123 pivotally engaged with a portion of the latch 122 performs a locking or unlocking combination with the latch 122 when the hanger 112 of the striker 110 is inserted into the insertion recess 121 a.

The second suspension lever 124 comprises a trigger arm 124 a and an activation arm 124 b. The trigger arm 124 a of the second suspension lever 124 is pivotally engaged with the second trigger recess 123 b of the first suspension lever 121. Accordingly the second

suspension lever 124 performs a locking or unlocking combination with the first suspension lever 123 when the latch 122 and the first suspension lever 123 are locked into each other via the first trigger recess 123 a.

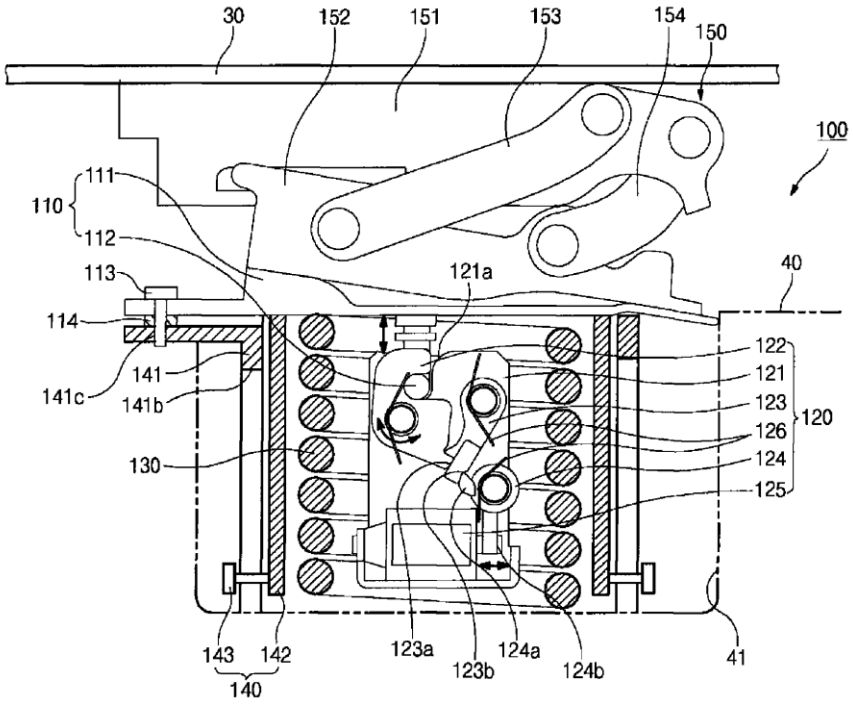

The solenoid actuator 125 controls the rotational direction of the activation arm 124 b of the second suspension lever 124 such that an electronic control device ECU supplies an electric power to the solenoid actuator 125 and thus releases the locked state of the first suspension lever 123 with the latch 122 when an electric power is applied to the solenoid actuator 125 and the second suspension lever 124 rotates counterclockwise as the electronic control device ECU senses a collision of the vehicle body with the pedestrian. The springs 126 apply elastic restoring force to the first and second suspension levers 123 and 124 and the latch 122, respectively.

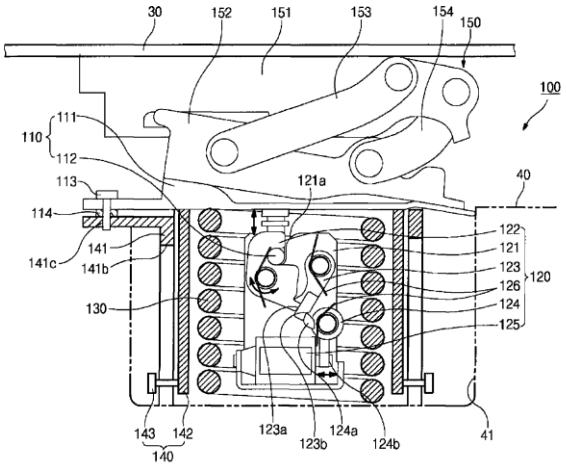

Fig.4

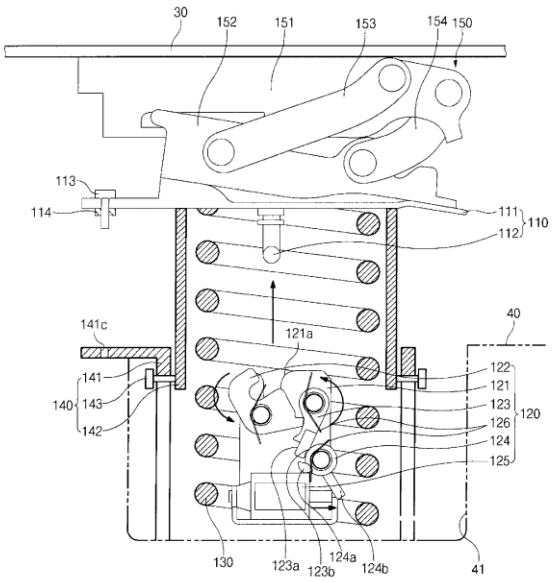

Fig.5

More information at: https://patents.google.com/patent/US7931111B2/en

In detail, in such a latch unit 120, the electronic control device controls the solenoid actuator 125 to move the second suspension lever 124. The solenoid actuator moving the second suspension lever 124 in counterclockwise direction as shown in FIG. 5 makes the trigger arm 124 a released from the second trigger recess 123 b of the second suspension lever 124 to allow the first suspension lever 123, which is locked to the second suspension lever 124, to be rotated by a release force, which the latch 122 itself generates using the suppressed elastic force of an elastic member 130 (which will be described later). Simultaneously, the latch 122, which is locked to the first trigger recess 123 a of the first suspension lever 123, is unlocked and the striker 110, which is locked by the latch 122, is also unlocked from the latch 122. The unlocked striker 110 is raised together with the hood 30 by the suppressed elastic restoring force of the elastic member 130, in the aforementioned state.

Invention 3

Invented by: Niall Caldwell, Fergus R McIntyre

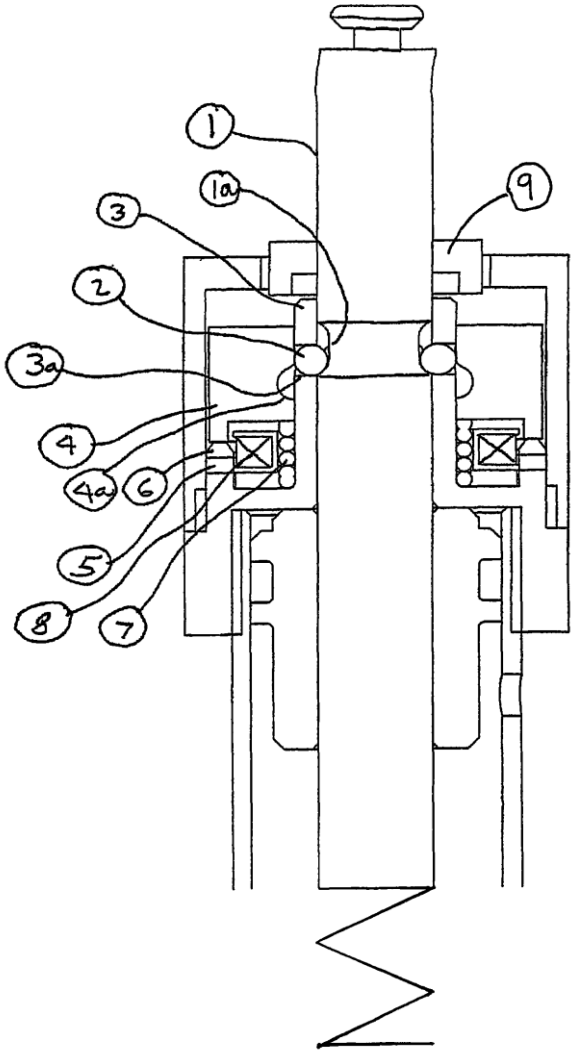

As shown in the drawing, a spring actuated rod 1 with an annular groove 1 a is held compressed position by a ball, or balls, 2 acting between the groove and a reaction tube 3, where the balls reside in transverse holes 3 a. The groove 1 a is profiled so that there is a net radial force on the balls which, in the locked position, is resisted by an annular release collar 4 a so that the balls are retained in such a position that they pass the axial load from the rod into the reaction tube.

The annular release collar has an internal profile 4 a which, once the collar moves axially, allows the balls to move radially outward and so disengage the groove 1 a and release the spring-operated rod.

In the locked position the annular collar is held by a magnetic circuit in which flux is driven by a permanent magnet 5, passes through the flux concentrator 6, the annular release collar 4 and the reaction tube 3, so that it returns to the other pole of the permanent magnet to complete the circuit. All of these parts are made of ferromagnetic material to reduce the reluctance. The force generated between the flux concentrator ring and the annular release collar is sufficient to retain the collar and keep the mechanism locked despite the influence of a mechanical spring 7 which is compressed and acting to push the collar into the release position.

By applying a current to the coil 8, the magnetic flux in the magnetic circuit is reduced to the point where the magnetically induced force between the collar and the flux concentrating ring is less than that of the charged spring 7. At this instant the annular release collar will accelerate and move to the release position. Once the release collar has completed its axial motion, the balls will be propelled radially outward by the radial component of force from the groove edge on the rod. The rod will then be able to translate under the influence of its spring energy.

The mechanism is reset by depressing the rod. A relatching collar 9, rigidly attached to the rod 1, moves the release collar 4 back to the locked position shown in the drawing, so that the balls 2 re-engage with the groove 1 a and so the release collar 4 compresses the spring 7 and once again is retained by the permanent magnet circuit.

A variant of this design is to use the rod spring to drive the release collar by means of using a more complex profile 4 a on the internal bore of the annular release collar so that in the locked position the balls exert a force on the spring collar opposing that of the permanent magnet. In this manner is possible to eliminate the spring 7 while also reducing the number of actions during the resetting. Information at:

https://patents.google.com/patent/US8083274?oq=resettable+active+bonnet

Invention 4

Invented by: Mikael Karlsson

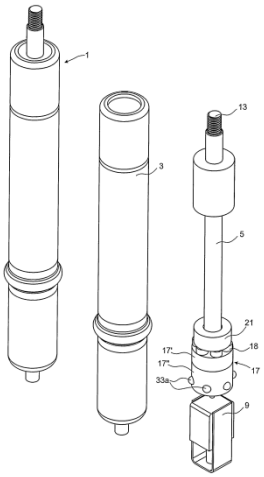

Fig. 1

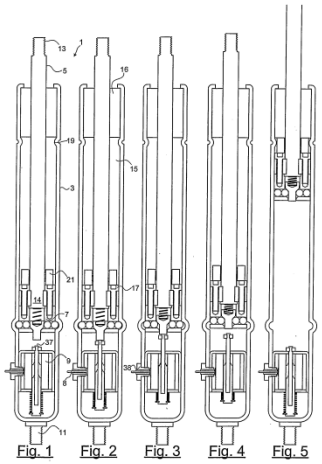

Fig. 2 Fig. 3 Fig. 4 Fig. 5

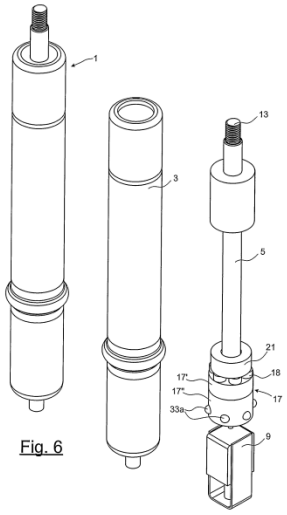

Fig. 6

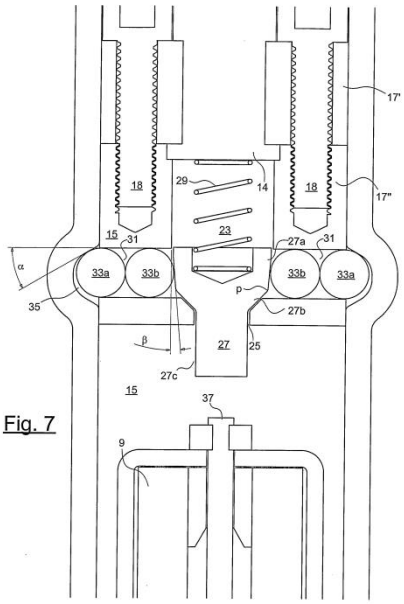

Fig. 7

In normal position, which is depicted in FIG. 7, the piston 17 is situated in a depressed bottom position, in which it is locked and not can be lifted in the lifting direction. The pin 27 is situated in a first, lower position, in which the lower part 27 c of the pin projects out from the underside of the piston, while the mantle of the upper part 27 a of the pin is in contact with the spherical elements 33 b and which are situated radially innermost. The innermost situated spherical elements 33 b are in turn in contact with the radially outermost, spherical elements 33 a, which partly are contained in a circumferentially extended cavity 35. This

cavity is substantially bowl-shaped with a diameter that is larger than the diameter of the spherical elements and with a defined angle with respect to the horizontal plane corresponding to the contact surface of the spherical elements with the housing. Since the upper part 27 a of the pin is slightly inclined, the pin 27 will hold a pressure in the radial direction outwardly and thus hold the spherical elements 33 a-b radially outwards in the direction of the cavity 35. At the same time, the piston 17 is subjected to a pressure in the lifting direction, due to the gas pressure that prevails in the housing 3 and the area difference between the upper and the lower part of the piston. Thus, the radially outermost spherical elements 33 a-b are pushed in the lifting direction of the piston stem 5 towards an upper portion of the cavity, whereby the spherical elements 33 a-b and the pin will be remained locked in this position as long as the pin is situated in this first position.

Below the piston, a release mechanism 9 in the shape of a low-resistant pressing solenoid is arranged. It is as mentioned before connected to a crash detector and can, when receiving an electrical pulse, be released. The solenoid comprises a striking element 37 in the shape of a spring biased plunger, where the spring constant is adapted so as not to put the plunger 37 in motion by the movements and vibrations of the vehicle, e.g. a strike-through of the spring-system. It is in the recessed position located on a small distance from the lower surface of the pin, usually a couple of mm.

Electrical contact occurs by means of a pressure resistant lead-through 38 (see FIG. 1-5) in the housing 3, or by isolating the housing 3 and the rod 5 by means of spherical elements of a ceramic material without any conducting properties and by contacting each end of the rod.

When activating the lifting device 1, the solenoid 9 will receive a signal from the crash detector which results in that the plunger 37 projects and hits the lower side of the pin 27. Since the plunger 37 is situated on a small distance from the lower side, prior to the commencement of the activation, it will reach a speed before the strike. This is of great importance since the plunger 37 only needs to accelerate its own mass, not the pin's 27, but also that the kinetic energy of the plunger 37 will be converted to a force during the impact, like a firing pin of a revolver. The sum of the kinetic energy and the compressive force of the plunger 37 during its movement overcome the static friction of the pin 27 against the spherical elements and put them in motion.

Due to this firing pin effect in combination with the compressive force of the solenoid, the pin 27 will start to move from the first, lower position in the direction of a second, upper position. When the position p, where the upper part 27 a of the pin transforms into the intermediate part, passes the centers of the spherical elements, the spherical elements 33 a-b will start to get pushed inwards in the radial direction. The reason is that the tangent in the point, where

the radially outermost positioned spherical elements 33 a are in contact with the cavity 35, forms a positive angle α (see FIG. 7) with respect to the horizontal plane, at the same time as the spring tension of the piston 17 pushes the radially outermost located spherical elements vertically upwards.

When the point p of the pin passes the centre of the spherical elements 33 a-b, the component force, which is directed radially inwards and which originate from the spring tension, will assist in the movement of the pin 17 so that the spherical elements are forced radially inwards until they not are in engagement with the cavity 35. At the same moment, the piston stem 5 will start to move upwards until it hits the stop element 16 which prevents further movement. In this suspended position, the piston will be springing and can absorb several impacts against the hood. The pin 27 is all the time situated in its second, upper position, in which the compression spring 29 is recessed, since the spherical elements 33 a-b locked by the diameter of the housing, prevent the tap from moving towards the first, lower position under the influence of the compression spring.

Accordingly, a large tightened force can be released with a relatively low release force due to the above mentioned construction, in which the geometry of the pin and of the cavity, the contact of the spherical elements with the latter during the load of the gas spring, is optimized so as to easily release the operating element, without sacrificing the locking of the lifting element.

Since the lifting device 1 is reversible, it is possible to restore the piston stem 5 to normal, locked position. This is accomplished by pressing the piston stem 5 downwards, and when the spherical elements 33 a-b are on the same level as the cavity 35, the outermost spherical elements 33 a will be pushed into it, so that the piston stem 5 is locked due to the spring-tensioned pin and the slightly inclined upper part of the pin 27 a, which secures that the spherical elements start to move in the direction of the radial outer position.

Instead of manually pushing the piston stem downwards, some form of automatic drawing-in device could be provided for restoring the piston stem to its normal position again.

The lifting device is of course not only restricted to lifting the rear edge of the hood, but it is also conceivable to use the lifting device in crash frames or in other respects where the demand for a rapid and efficient lifting exist.

More information at: https://patents.google.com/patent/US20080136140A1/en?q=active&q=hood&q=solonoid&q=

system&q=pedestrain&q=protection&oq=active+hood+solonoid+system++pedestrain+protection&page=3

Reference List

2-Chome, Y. & Chuo-ku, 2006. *White Paper on Traffic Safety in Japan 2006,* Tokyo: IATSS.

AAAM, 2005. *Abbreviated Injury Scale 2005,* Barrington,: Association for the Advancement of Automotive Medicine.

AAAM, 2017. *Abbreviated Injury Scale.* [Online]
Available at: https://www.aaam.org/abbreviated-injury-scale-ais/
[Accessed 8 August 2017].

Agrahari, S. K. et al., 2009. *Bumper System Redesign for Lower Leg Pedestrian Impact: A Simplified Parametric Spring Model Approach,* s.l.: Altairatc.

Ames, E. & Martin, P., 2015. *Pop-Up Hood Pedestrain Protection,* s.l.: National Highway Traffic Safety Administration.

Ames, E. & Peter, M., 2015. *Pop-up Hood Pedestrain Protection,* New Jersey Avenue: National Highway Traffic Safety Administration.

Anderson, R., Ponte, G. & Searson, D., 2008. *Benefits for Australia of the introduction of an ADR on pedestrian protection,* Adelaide: The University of Adelaide.

Baleki, D. d. M. & Ferreira, A. S., 2009. *Pedestrian protection Concepts With Focus on Head Impact,* Vargas: General Motors do Brazil.

Barnes, B. M. et al., 2008. *Shape Memory Alloy Resetable Spring Lift for Pedestrian Protection,* Michigan: Nancy L. Johnson.

Bhanage, A. S. et al., 2016. Finite Element Simulation of Oil Canning for Automotive Panel. *International Journal of Current Engineering and Technology,* 1(6), pp. 169-174.

Boggess, B. M. & Wong, J., 2003. *Development of Plastic Components for Pedestrian Head Injury Risk Reduction,* New Jersey Avenue: Honda R&D Americas.

CDPH Public Health , 2017. *Traffic Safety Reports: Pedestrian Injuries in California 2007-2013.* [Online]
Available at:
https://www.cdph.ca.gov/Programs/CCDPHP/DCDIC/SACB/CDPH%20Document%20Library/Crash%20Medical%20Outcomes%20Data%20(CMOD)%20Project/Pedestrian%20injuries%20Report_June%202017-ADA.pdf
[Accessed 8 August 2017].

Cheng, C.-S. & Wang, J. T., 2002. *An Analytical Study of Pedestrian Headform Impacts Using a Dual Asymmetrical Triangle Function.* Louisiana, ASME.

Chen, H., 2017. *Evaluating Pedestrian Head Sub-system Test Procedure against Full-scale Vehicle-Pedestrian Impact Using Numerical Models,* s.l.: School of Engineering and Applied Science, University of Virginia.

Crandall, J. R., Bhalla, K. S. & Madeley, N. J., 2002. Designing road vehicles for pedestrian protection. *British Medical Journal,* 324(1), pp. 1145-1148.

Daimler AG, 2017. *Pedestrian Protection at Mercedes-Benz.* [Online]
Available at: http://media.daimler.com/marsMediaSite/en/instance/ko/Pedestrian-protection-at-Mercedes-Benz-initiatives-measures-standpoints.xhtml?oid=9905173
[Accessed 17 October 2017].

Daimler AG, 2017. *Pedestrian Protection Offered by New E-Class.* [Online]
Available at:
http://media.daimler.com/marsMediaSite/instance/picture.xhtml?oid=start&ls=L2VuL2luc3RhbmNlL2tvLnhodG1sP29pZD05MzYxNTYzJnJlbElkPTEwMDEmZnJvbU9pZD05MzYxNTYzJmJvcmRlcnM9dHJ1ZSZyZXN1bHRJbmZvVHlwZUlkPTE3MiZ2aWV3VHlwZT10aHVtYnMmc29ydERlZmluaXRpb249bWFudWFsc29y
[Accessed 17 October 2017].

Department for Transport, 2017. *Reported road casualties in Great.* [Online]
Available at:
https://www.gov.uk/government/uploads/system/uploads/attachment_data/file/588773/quarterly-estimates-july-to-september-2016.pdf
[Accessed 8 August 2017].

Edmunds, 2009. *Protecting Pedestrians Through Vehicle Design.* [Online]
Available at: https://www.edmunds.com/car-safety/protecting-pedestrians-through-vehicle-design.html
[Accessed 18 September 2017].

EEVC, 1998. *Improved Test Methods to Evaluate Pedestrain Protection Afforded by Passanger Cars,* s.l.: EEVC Working Group 17.

EEVC, 2003. *EEVC Progress Report For GRSP,* s.l.: EEVC.

Eppinger, R. et al., 1999. *Development of Improved Injury Criteria for the Assessment of Advanced Automotive Restraint Systems - II,* s.l.: NHTSA.

Eur-Lex, 2009. Commission Regulation (EC) No 631/2009 of 22 July 2009. *Official Journal of the European Union,* 28(1), pp. 164-223.

Euro NCAP, 2014. *European New Car Assessment Programme (Euro NCAP),* s.l.: Euro NCAP.

Euro NCAP, 2015. *Assesment Protocol - Pedestrian Protection,* s.l.: Euro NCAP.

EURO NCAP, 2017. *Euro NCAP Launched.* [Online]
Available at: http://www.euroncap.com/en/about-euro-ncap/timeline/euro-ncap-launched/
[Accessed 05 May 2017].

Eurostat, 2016. *Road accident fatalities - statistics by type of vehicle.* [Online]
Available at: http://ec.europa.eu/eurostat/statistics-explained/index.php/Road_accident_fatalities_-

statistics_by_type_of_vehicle
[Accessed 8 August 2017].

Evrard, B., 2011. *Innovative Bonnet Active Actuator (B2A) for Pedestrian Protection,* Washington: 22nd International Technical Conference on the Enhanced Safety of Vehicles.

Fahlstedt, M., 2015. *Numerical Accident Reconstructions,* Huddinge: KTH Royal Institute of Technology.

Farkya, P. & Cheng, X., 2015. *Assessment of injuries to the lower leg and head of pedestrians in vehicle-to-pedestrian collisions through FE simulations,* Gothenburn: Chalmers University of Technology.

Forman, J. L. et al., 2015. *Biofidelity Corridors for Whole-Body Pedestrian Impact with a Generic Buck.* Virginia, University of Virginia.

Fredriksson, R., 2011. *Priorities and potential of Pedestrian Protection,* Stockholm: Karolinska Institutet.

Fredriksson, R., Boström, O., Zhang, L. & Yang, K., 2006. *Influnce of Pop-Up Hood System on Brain Injuries for Vulnerable Road Users,* s.l.: Autoliv Research.

Gadd, C. W., 1966. *Use of a Weighted-Impulse Criterion for Estimateing Hazard,* s.l.: Research Laboratories, General Motors Corp.

GHO, 2017. *Road Traffic Deaths.* [Online]
Available at: http://www.who.int/gho/road_safety/mortality/en/
[Accessed 8 August 2017].

Global technical regulation No. 9, 2009. *Agreement Concerning the Establishing of Global Technical Regulations for Wheeled Vehicles, Equipment and Parts Which can be Fitted And/Or Be Used On Wheeled Vehicles,* Geneva: United Nations.

GTR9-C-04, 2011. *History of Development of the Flexible Pedestrian Legform Impactor (Flex-PLI).* [Online]
Available at: https://www.unece.org/fileadmin/DAM/trans/main/wp29/GTR9-C-04.pdf
[Accessed 15 September 2017].

Gupta, V., 2014. *Pedestrian Head Protection During Car To Pedestrian Accidents: In The Event Of Primary Impact With Vehicle And Secondary Impact With Ground,* Detroit: Wayne State University,.

Gupta, V. & Yang, K. H., 2013. Effect of Vehicle Front End Profiles Leading to Pedestrian Secondary Head Impact to Ground. *Stapp Car Crash Journal,* 57(1), pp. 129-155.

Gurdjian, E., Roberts, V. & Thomad, L., 1966. Tolerance curves of acceleration and intracranial pressure and protective index in experimental head injury. *The Journal of Trauma,* 6(5), pp. 600-604.

Hamache, M., Eckstein, L. & Paas, R., 2012. *Vehicle Related Influence of Post-Car Impact Pedestrian Kinematics on Secondary Impact.* s.l., IRCOBI.

Harris Products Group, 2017. *Carbon Dioxide Regulator Freezing.* [Online]
Available at: http://www.harrisproductsgroup.com/en/Expert-Advice/tech-tips/carbon-dioxide-regulator-freezing.aspx
[Accessed 17 October 2017].

Helmer, T. et al., 2010. Injury risk to specific body regions of pedestrians in frontal vehicle crashes modeled by empirical, in-depth accident data. *Stapp Car Crash*, November, pp. 93-117.

HERA Innovation in Metals, 2014. *Finite Element Analysis,* Manukau City: HERA Innovation in Metals.

Honarpardaz, M. M., 2011. *Finite Element and Experimental Analysis of Function of Plastic Clips,* Karlskrona: Blekinge Institute of Technology.

Huang, S., 2010. *A Study of An Intergrated Safety System For the Protection of Adult Pedestrians From Car Collisions,* Göteborg: Chalmers University of Technology.

Hu, J. & Klinich, K. D., 2012. *Towards Designing Pedestrain-Friendly Vehicles,* Michigan: University of Michigan.

Ishikawa, H., Kajzer, J. & Schroeder, G., 1993. *Computer Simulation of Impact Response of the Human Body in Car-Pedestrian Accidents,* s.l.: SAE International.

Janssen, E., 1996. *EEVC test methods to evaluate pedestrain protection afforded by passenger cars,* Melbourne: EEVC.

Kalliske, I. & Friesen, F., 2001. *Improvements to Pedestrian Protection as Exemplified on Standard-Sized Car,* s.l.: Experimental Safety Vehicles Conference.

Karsch, H. M., Hedlund, J. H., Tison, J. & Leaf, W. A., 2012. *Review of Studies on Pedestrian and Bicyclist Safety,* Connecticut: Department of Transportation.

Kerkeling, C., Schäfer, J. & Thompson, D. G.-M., 2005. *Structural Hood and Hinge Concepts for Pedestrian Protection,* s.l.: GM Europe – Adam OPEL AG.

King, A. I., Yang, K. H., Zhang, L. & Hardy, W., 2003. *Is Head Injury Caused By Linear or Angular Acceleration ?.* Lisbon, Wayne State University.

Konosu, A., 2008. *Development of Flexible Pedestrain Legform Impactor (Flex-PLI) and Introduction of FLex-PLI Technical Evaluation Group (Flex-TEG) Activities.* [Online]
Available at: http://www.sae.org/events/gim/presentations/2008konosu1.pdf
[Accessed 15 September 15].

Krishnamoorthy, R., 2012. *Optimisation of Hood Panels of a Passenger Car for Pedestrian Protection,* s.l.: RMIT University.

Lawrence, G. J. L. et al., 2006. *A study on the feasibility of measures relating to the protection of pedestrians and other vulnerable road users,* Berkshire: TRL.

Lee, K. B., Jung, H. J. & Il, B. H., 2007. *The Study On Developing Active Hood Lift System for Decreasing Pedestrain Head Injury,* s.l.: Hyundail - KIA Motors.

Liu, Q., Xia, Y. & Zhou, Q., 2015. *Design Analysis of a Sandwich Hood Structure for Pedestrain Protection,* Warren: General Motors Research & Development.

Luntz, J. E. et al., 2007. *Feasibility Study of the Dual Chamber SMART (SMA ReseTtable) Lift Device.* Michigan, SPIE Proceedings.

Luntz, J. & Johnson, N. L., 2015. *Shape Memory Alloy Resetable Spring Lift for Pedestrain Protection,* Michigan: Proceedings of SPIE - The International Society for Optical Engineering.

Masoumi, A., Hassan, M. & Shojaeefard, A., 2011. Comparison of steel, aluminum and composite bonnet in terms of pedestrian head impact. *Science Direct,* 49(10), pp. 1371-1380.

Matsui, Y. et al., 2003. *Development of JAMA-JARI Pedestrian Child and Adult Head-Form Impactors,* s.l.: ESV.

Matsui, Y. et al., 2004. Development of JAMA-JARI Pedestrian Child and Adult Head-Form Impactors. *International Journal of Crashworthiness,* 9(2), pp. 129-139.

Mc Lean, A., 2005. *Vehicle design for pedestrian protection,* Adelaide: University of Adelaide.

McHenry, B. G., 2008. *Head Injury Criterion and the ATB,* s.l.: ATB Users Group.

Mellander, H., 1986. *HIC--the head injury criterion. Practical significance for the automotive industry,* s.l.: Acta Neurochirurgica Supplementum.

Mizuno, Y., 2003. *Summary of IHRA Pedestain Safety WG (2003) - Proposed Test Methods To Evaluate Pedestrain Protection Afforded by Passenger Cars,* s.l.: Japan Automobile Standards Intemationalization Center.

Mizuno, Y., 2003. *Summary of IHRA Safety WG Activities (2003) - Proposed Test Methods to Evaluate Pedestrian Protection Offered By Passenger Cars,* s.l.: Japan Automobile Standards Internationalization Centre (JASIC).

Mizuno, Y., 2005. *Summary of IHRA Pedestain Safety WG (2005) - Proposed Test Methods To Evaluate Pedestrain Protection Afforded by Passenger Cars,* s.l.: Japan Automobile Standards Internationalization.

Nagatomi, K. et al., 2005. *Development and Full-Scale Dummy Tests of A Pop-Up Hood System for Pedestrian Protection,* s.l.: Honda R&D Co.

Namjoshi, D. et al., 2013. Towards clinical management of traumatic brain injury: a review of models and mechanisms from a biomechanical perspective.. *Pub Med*, 6 Novemeber, pp. 1325-1338.

New York State Law, 2017. *Vehicle and Traffic Law.* [Online]
Available at: http://ypdcrime.com/vt/article1.htm#t130.
[Accessed 24 April 2017].

NHTSA, 2017. *Traffic Safety Facts,* Washington: National Highway Traffic Safety Administration.

Nissan Motor Corporation, n.d. *Pop Up Engine Hood For Pedestrain Protection.* [Online]
Available at: http://www.nissan-global.com/EN/TECHNOLOGY/OVERVIEW/puehfpp.html
[Accessed 19 September 2017].

Otte, D. & Haasper, C., 2005. *Technical Parameters and Mechanisms for the Injury Risk of the Knee Joint of Vulnerable Road Users Impacted By cars in Road Traffic Accidents,* Hanover: Hanover Medical School.

Paas, R., 2015. *Head kinematics in car–pedestrian crashes,* Gothenburg: Chalmers University of Technology.

Paas, R., 2015. *The influence of sliding, spine bending, elbow and shoulder impacts,* Gothenburg: Chalmers University of Technology.

Paas, R. et al., 2012. *Pedestrian Shoulder and Spine Kinematics in Full-Scale PMHS Tests for Human Body Model Evaluation.* Gothenburg, IRCOBI.

Pappully, R. N., Mandava, H., Abhishek, M. & Kumar, S., 2017. Design and Fabrication of Active Hood Lift System. *International Research Journal of Engineering and Technology (IRJET),* 4(4), pp. 2370-2375.

Parsons, F. G., 1929. The Thickness of the Living Scalp. *Journal of Anatomy*, July, pp. 427-429.

Pia, L.-B., 2010. *Road accidents to be 5th leading cause of death by 2030 - WHO.* [Online]
Available at: http://www.philstar.com/headlines/604688/road-accidents-be-5th-leading-cause-death-2030-who
[Accessed 19 September 2017].

Pranay, P., 2014. *Liquification of gases.* [Online]
Available at: http://chemistrynotmystery.blogspot.co.uk/2014/11/liquification-of-gases.html
[Accessed 17 October 2017].

Ramesh, C. K., S, D. S. & M. L. J., S., 2012. *Design of Hood Stiffener of a Sedan Car for Pedestrain Safety,* Bangalore: Ramaiah School of Advanced Studies.

Ratingen, M. v. et al., 2016. The European New Car Assessment Programme: A historical review. *Chinese Journal of Traumatology,* 19(2), pp. 63-69.

ROSPA, 2015. *About Pedestrian Protection.* [Online]
Available at: https://www.rospa.com/road-safety/advice/vehicles/pedestrian-protection/about/
[Accessed 18 September 2017].

Scherf, O., 2007. *Development and Performance of Contact Sensors For Active Pedestrain Protection Systems.* SE Washington, 19th International Technical Conference on the Enhanced Safety of Vehicles (ESV).

Schmitt, K., Niederer, P. & Muser, M. W. F., 2010. *Trauma Biomechanics - Accidental Injury in Traffic and Sport.* 3 ed. Berlin: Springer-Verlag.

Ševčik, L. et al., 2013. *Modern Methods of Construction Design: Proceedings of ICMD 2013 (Lecture Notes in Mechanical Engineering).* 2014 ed. s.l.:Springer.

Shape Corp, 2017. *Testing.* [Online]
Available at: http://pedestrianprotection.shapecorp.com/testing-2/
[Accessed 15 September 2017].

Shin, M.-K., Park, K.-T. & Park, G.-J., 2007. *Design of the active hood lift system using orthogonal arrays,* Seoul: Hanyang University.

Simms, C. & Wood, D., 2009. *Pedestrain and Cyclist Impact.* Dublin: Springer.

Simms, C. & Wood, D., 2009. *Pedestrian and Cyclist Impact.* Dublin: Springer.

Stevenson, T. J., 2006. *Simulation of Vehicle-Pedestrain Interaction,* Canterbury: University of Canterbury.

Syed, M. J., 2009. *Finite Element Analysis of Prosthetic Finger Implants,* Toronto: University of Toronto.

T.J., H. et al., 1999. *Development of a Boifidelic Dummy for Car-Pedestrain Accident Studies,* s.l.: Tochigi R&D Center.

Takahashi, H. et al., 2013. *Development of Pop-Up Hood System for Pedestrain Protection,* s.l.: Toyota Motor Corporation.

Tefft , B., 2011. *Impact Speed and a Pedestrian's Risk of Severe Injury or Death,* Washington: AAA Foundation for Traffic Safety .

Traumatic Brain Injury, 2001. *Car Accident TBI.* [Online]
Available at: http://www.traumaticbraininjury.com/understanding-tbi/car-accident-tbi/
[Accessed 15 September 2017].

Tur, F. J. M., 2013. *Pedestrain,* Barcelona: Universitat Autonoma.

Value Design Consulting, 2016. *Boundary Conditions.* [Online]
Available at: http://www.value-design-consulting.co.uk/boundary-conditions.html
[Accessed 23 November 2017].

Ward, D., 2014. *Pedestrian Safety - Developments in Crash Worthiness and Crash Avoidance.* [Online]
Available at: http://www.who.int/roadsafety/events/2014/Appendix_6.pdf
[Accessed 18 September 2017].

World Health Organization, 2004. *World report on road traffic injury prevention,* Geneva: World Health Organization.

Xu, D. et al., 2010. *The Research of Reversible Pop-up Hood for Pedestrian Protection,* Shanghai: Tongji University.

Ye, H., Hu, P., Jie Che, C. & Lu, F., 2011. Multidisciplinary Optimization Method about the Thickness of Engine Hood Based on Pedestrian Protection. *Applied Mechanics and Materials,* Volume 54, pp. 1958-1963.

Ye, H., Zhu, M. & Hu, P., 2011. Design Optimization Method about the Spring Stiffness used in Active Engine Hoof of Pedestrian Protection. *Applied Mechanics and Materials,* 1(1), pp. 110-116.

Zander, O., 2017. *Prerequisites for Testing of Deployable Bonnets Systems in deployed State,* s.l.: Federal Highway Research Institute.

Zanella, A., Butera, F., Gobetto, E. & Ricerche, C., 2002. *Smart Bumper for Pedestrian Protection,* s.l.: Fiat.